

LINKS BETWEEN THREE-DIMENSIONAL PATELLAR KINEMATICS,
CARTILAGE MORPHOLOGY AND VARUS/VALGUS ALIGNMENT
IN EARLY KNEE OSTEOARTHRITIS

by

Emily Jane McWalter

B.Sc., Queen's University, 2002

A THESIS SUBMITTED IN PARTIAL FULFILLMENT OF
THE REQUIREMENTS FOR THE DEGREE OF

MASTER OF APPLIED SCIENCE

in

THE FACULTY OF GRADUATE STUDIES

(DEPARTMENT OF MECHANICAL ENGINEERING)

THE UNIVERSITY OF BRITISH COLUMBIA

December 2004

© Emily Jane McWalter, 2004

Abstract

In this pilot study, we assessed the relationship between three-dimensional patellar kinematics and patellofemoral cartilage morphology in 10 individuals with varus or valgus alignment and early knee osteoarthritis (OA). We used a novel, validated, non-invasive magnetic resonance imaging (MRI)-based technique to assess three-dimensional patellar kinematics and a validated quantitative MRI (qMRI) technique to assess cartilage morphology at the patellofemoral joint. Varus and valgus alignment was assessed from a standing anteriorposterior radiograph.

Differences in three-dimensional patellar kinematics between the varus and valgus groups were assessed using a random effects model. We found that the varus group displayed constant medial tilt, constant external spin and decreasing anterior translation with increasing tibiofemoral flexion. We found that the valgus group displayed increasing medial tilt, constant internal spin, a greater proximal position and a constant anterior position with increasing tibiofemoral flexion. No difference was seen in lateral translation between the varus and valgus groups and the patella was centred in the trochlear groove.

Medial and lateral compartment cartilage morphology was compared to varus and valgus alignment using a two-way analysis of variance (ANOVA). No difference was found between the varus and valgus groups. A power analysis revealed that 30 subjects are required in each group to detect a significant difference.

The relationship between three-dimensional patellar kinematics and the ratio of medial to lateral compartment cartilage morphology was assessed using a regression model. We found that the rate of medial tilt increased with decreasing ratio of medial to lateral compartment bone/cartilage interface area. Results suggested a relationship between lateral patellar translation and proportion of medial to lateral cartilage normalized volume, mean thickness and percentage cartilage coverage. This finding was greatly influenced by two data points and therefore this result is not conclusive.

Cartilage degeneration at the patellofemoral joint cannot be completely explained by the presence of varus or valgus malalignment. Other local biomechanical factors, such as kinematics, are likely involved. A better understanding of the relationship between three-dimensional patellar kinematics and cartilage degeneration allows for the development of improved treatment strategies to arrest the onset and progression of patellofemoral OA.

Table of Contents

Abstract.....	ii
Table of Contents.....	iii
List of Tables.....	viii
List of Figures.....	x
Acknowledgements.....	xiii
CHAPTER 1: Introduction.....	1
CHAPTER 2: Literature Review.....	5
2.1 Introduction.....	5
2.2 The Patellofemoral Joint.....	6
2.2.1 Anatomy.....	6
2.2.2 Mechanics.....	7
2.2.2.1 Articular Cartilage.....	7
2.2.2.2 Loads on the Patella.....	7
2.2.2.3 Kinematics.....	9
2.2.2.4 Contact Areas and Stresses.....	10
2.2.3 Summary.....	11
2.3 Knee Osteoarthritis.....	12
2.3.1 Characteristics of Knee OA.....	13
2.3.2 Clinical and Radiographic Assessment of Knee OA.....	15
2.3.2.1 Clinical OA.....	16
2.3.2.2 Radiographic OA.....	17
2.3.3 Treatment.....	20
2.3.4 Economics.....	22
2.3.5 Risk Factors.....	22
2.3.6 Lower Limb Alignment and Knee OA.....	24
2.4 Methods of Assessing Articular Cartilage Morphology.....	29
2.4.1 MRI Methods.....	29

2.4.2	Biochemical Methods.....	35
2.5	Three-dimensional <i>in vivo</i> Patellar Tracking.....	36
2.5.1	Invasive Methods.....	37
2.5.2	Non-invasive Imaging Methods.....	38
2.5.3	Non-invasive Methods using MRI.....	39
2.5.4	Summary of MRI-based Methods.....	45
2.6	Summary.....	47
Chapter 3: Methods A: Patellofemoral Cartilage Morphology.....		49
3.1	Introduction.....	49
3.2	Input Device Study.....	50
3.2.1	Subjects and Imaging.....	50
3.2.2	Image Analysis.....	51
3.2.3	Statistical Analysis.....	53
3.3	Cartilage Morphology of Individuals with Varus/Valgus Alignment.....	55
3.3.1	Image Acquisition.....	55
3.3.2	Cartilage Segmentation.....	56
3.3.3	Assessment of Morphological Parameters.....	59
3.3.3.1	Volume.....	59
3.3.3.2	Thickness.....	60
3.3.3.3	Surface Area.....	61
3.3.4	Measured Parameters.....	62
3.3.5	Accuracy and Precision.....	63
CHAPTER 4: Methods B: Three-dimensional Patellar Kinematics.....		65
4.1	Introduction.....	65
4.2	High-resolution Scan.....	67
4.3	Loading Rig Design.....	69
4.4	Low-resolution Scan.....	71
4.5	Anatomical Axes Assignment.....	73
4.6	Shape-matching.....	74

4.6.1	Iterative Closest Points Algorithm.....	75
4.6.2	Pre-computation.....	76
4.6.3	Shape-match.....	77
4.7	Kinematics.....	78
4.8	Accuracy and Precision.....	80
 CHAPTER 5: Methods C: Study Design.....		81
5.1	Study Population.....	81
5.2	Measurements.....	81
5.2.1	Assessment of Varus/Valgus Knee Alignment.....	82
5.2.2	Assessment of Patellofemoral Cartilage Morphology.....	83
5.2.3	Assessment of Three-dimensional Patellar Kinematics.....	84
5.2.4	WOMAC Questionnaire.....	85
5.2.5	Height and Weight Measurement.....	86
5.3	Statistical Analysis.....	86
5.3.1	Varus/Valgus Alignment Groups.....	86
5.3.2	Varus/Valgus Alignment vs Cartilage Morphology.....	87
5.3.3	Varus/Valgus Alignment vs Three-dimensional Patellar Kinematics.....	87
5.3.4	Three-dimensional Patellar Kinematics vs Cartilage Morphology...	89
 CHAPTER 6: Results.....		91
6.1	Introduction.....	91
6.2	Varus/Valgus Alignment.....	92
6.3	WOMAC.....	93
6.4	Input Device Study.....	94
6.5	Varus/Valgus Alignment vs Cartilage Morphology.....	96
6.5.1	Patellar Cartilage.....	96
6.5.2	Patellar Cartilage vs Varus/Valgus Alignment.....	97
6.5.3	Femoral Cartilage.....	98
6.5.4	Femoral Cartilage vs Varus/Valgus Alignment.....	99

6.6	Varus/Valgus Alignment vs Patellar Kinematics.....	100
6.6.1	Patellar Flexion.....	101
6.6.2	Patellar Spin.....	102
6.6.3	Patellar Tilt.....	103
6.6.4	Proximal Patellar Translation.....	104
6.6.5	Lateral Patellar Translation.....	105
6.6.6	Anterior Patellar Translation.....	106
6.6.7	Summary of Significant Differences.....	107
6.7	Patellar Kinematics vs Patellar Cartilage Morphology.....	108
6.7.1	Bone/Cartilag Interface.....	108
6.7.2	Surface Area.....	110
6.7.3	Normalized Volume.....	112
6.7.4	Mean Thickness.....	113
6.7.5	Percentage Cartilage Coverage.....	115
6.8	Summary.....	117
CHAPTER 7: Discussion.....		119
7.1	Introduction.....	119
7.2	Synthesis- A Comparison to the Literature.....	120
7.2.1	Alignment.....	120
7.2.2	BMI.....	120
7.2.3	WOMAC.....	121
7.2.4	Cartilage Morphology and Alignment.....	121
7.2.4.1	Comparison to Normal Cartilage.....	121
7.2.4.2	Compartment Specific Progression of OA.....	122
7.2.5	Kinematics and Alignment.....	123
7.2.5.1	Lateral Translation.....	124
7.2.5.2	Tilt.....	125
7.2.5.3	Spin.....	126
7.2.5.4	Patellar Flexion, Proximal Translation and Anterior Translation.....	127

7.2.5.5	Patellar Kinematics and OA.....	127
7.3	Analysis of Results.....	129
7.3.1	Input Device Study.....	129
7.3.2	Cartilage Morphology and Varus/Valgus Alignment.....	129
7.3.3	Three-dimensional Patellar Kinematics and Varus/Valgus Alignment.....	130
7.3.4	Three-dimensional Patellar Kinematics and Cartilage Morphology..	132
7.4	Strengths and Limitations.....	135
7.4.1	Strengths.....	135
7.4.2	Limitations.....	136
7.4.2.1	Group Differences.....	136
7.4.2.2	Three-dimensional Patellar Kinematics.....	137
7.4.2.3	qMRI.....	138
7.4.2.4	Statistics.....	139
7.4.2.3	Study Design.....	140
7.5	Contributions and Future Work.....	141
7.5.1	Relevance of Work.....	141
7.5.2	Future Work.....	142
 CHAPTER 8: Conclusion		145
 References.....		149
 APPENDIX A: WOMAC Questionnaire.....		162
APPENDIX B: Anatomical Axes Assignment.....		169
APPENDIX C: Participant consent form.....		179
APPENDIX D: Higher order regression results for cartilage surface area, normalized volume, mean thickness and percentage coverage		185

List of Tables

Table 2.1: The Kellgran-Lawrence osteoarthritis grading scale.....	18
Table 2.2: Results of distribution of tibiofemoral (TF) and patellofemoral (PF) OA progression from Cahue et al. 2004.....	28
Table 2.3: Summary of <i>in vivo</i> MRI based techniques for assessing patellar kinematics.....	46
Table 3.1: Investigator schedule for cartilage segmentation.....	52
Table 3.2: qMRI imaging parameters.....	56
Table 3.3: Units of measurement for cartilage morphologic parameters.....	63
Table 4.1: High-resolution imaging parameters.....	67
Table 4.2: Low-resolution imaging parameters.....	72
Table 6.1: Angles of lower limb alignment for 12 study participants.....	92
Table 6.2: Mean and standard deviation () of the pain, stiffness and difficulty performing activities of daily living for the WOMAC questionnaire.....	93
Table 6.3: Mean and standard deviation of time for each segmentation input device.....	94
Table 6.4: Systematic difference and standard deviation in cartilage volume, surface area and mean thickness.....	95
Table 6.5: Precision (reproducibility) expressed as CV% and mean and standard deviation.....	95
Table 6.6: Difference in total patellar cartilage morphology between the varus and valgus groups.....	96
Table 6.7: Mean and standard deviation () values for patellar cartilage morphologic parameters in the medial and lateral compartments.....	97
Table 6.8: P-values for 2-way ANOVA of patellar cartilage morphology and varus/valgus alignment.....	97
Table 6.9: Difference in total femoral cartilage morphology between the varus and valgus groups.....	98
Table 6.10: Mean and standard deviation () values for femoral cartilage morphologic parameters in the medial and lateral compartments.....	99
Table 6.11: P-values for 2-way ANOVA of femoral cartilage morphology and varus/valgus alignment.....	99
Table 6.12: Summary of significant p- and z- values for the linear random effects model parameters.....	107
Table 6.13: Results of linear regression for bone/cartilage interface and patellar kinematic parameters.....	108
Table 6.14: First and second order regression fit for bone/cartilage interface to tilt.....	109
Table 6.15: Results of linear regression for surface area and patellar kinematic parameters.....	111

Table 6.16: 1 st , 2 nd and 3 rd order regression fit for surface area to lateral translation.....	111
Table 6.17: Results of linear regression for normalized volume and patellar kinematic parameters.....	112
Table 6.18: 1 st , 2 nd , 3 rd and 4 th order regression fit for surface area to lateral translation.....	112
Table 6.19: Results of linear regression for mean thickness and patellar kinematic parameters.....	114
Table 6.20: 1 st , 2 nd and 3 rd order regression fit for mean thickness to lateral translation.....	114
Table 6.21: Results of linear regression for percentage cartilage coverage and patellar kinematic parameters.....	115
Table 6.22: 1 st , 2 nd and 3 rd order regression fit for percentage cartilage coverage to lateral translation.....	115

List of Figures

Figure 1.1: The relationship between research questions 1,2 and 3.....	4
Figure 2.1: The Knee Joint.....	6
Figure 2.2: Measurement of Q-angle.....	6
Figure 2.3: Resultant forces action on the patella.....	8
Figure 2.4: Distribution of knee osteoarthritis in the Framingham cohort knee pain group (n=608).....	13
Figure 2.5: Left-Anteroposterior radiograph of the tibiofemoral joint. Right-Skyline radiograph of the patellofemoral joint.....	14
Figure 2.6: Left: The OARSI protocol for skyline view radiographs of the patellofemoral joint. Right: An example of a skyline radiograph.....	20
Figure 2.7: Varus alignment or bow-legs (left) and valgus alignment or knock knees (right).....	24
Figure 2.8: Results from Cahue et al. 2004. Number of varus and valgus knees undergoing medial and lateral patellofemoral OA progression.....	27
Figure 2.9: The distribution of gadolinium in the patellofemoral joint measured using the dGEMRIC protocol.....	35
Figure 2.10: Hyper-pressure syndrome of the patella as described by Ficat et al.....	36
Figure 2.11: Patellar kinematics, 3 translation and 3 rotations.....	37
Figure 2.12: Coordinate System used by von Eisenhart-Rothe et al., 2004.....	42
Figure 2.13: Anatomical coordinate system assignment, Sheehan et al. 1998.....	44
Figure 3.1: MRI image of patellofemoral joint cartilage.....	56
Figure 3.2: The Cintiq 18SX by Wacom, a touch sensitive screen.....	57
Figure 3.3: Manual cartilage segmentation.....	58
Figure 3.4: Three-dimensional representation of a patellar cartilage plate.....	60
Figure 4.1: Flow chart of three-dimensional patellar kinematics method.....	66
Figure 4.2: Segmentation of the femur (red), the tibia (green) and the patella (yellow).....	68
Figure 4.3: Three-dimensional point cloud model of the femur, tibia and patella.....	69
Figure 4.4: MR compatible loading rig.....	70
Figure 4.5: An example of loading a participant's knee.....	70
Figure 4.6: Low-resolution contours.....	73
Figure 4.7: A manual trial and error translation and rotation of the geometric model.....	77
Figure 4.8: Left: Final shape match. Middle: Motion of the patella. Right: Motion of the femur and tibia.....	78
Figure 4.9: Patellofemoral kinematics positive directions.....	79
Figure 5.1: The measurement of femorotibial angle.....	82
Figure 5.2: Articular surface of the femur with the patella.....	83
Figure 5.3: Segmented patellar (pink) and femoral cartilage (blue).....	83
Figure 5.4: The medial and lateral division of patellar and femoral cartilage.....	84

Figure 6.1: Linear random effects model of mean patellar flexion.....	101
Figure 6.2: Linear random effects model of mean patellar spin.....	102
Figure 6.3: Linear random effects model of mean patellar tilt.....	103
Figure 6.4: Linear random effects model of mean proximal patellar translation.....	104
Figure 6.5: Linear random effects model of mean lateral patellar translation.....	105
Figure 6.6: Linear random effects model of mean anterior patellar translation.....	106
Figure 6.7: Linear regression fit of the ratio of medial to lateral bone/cartilage interface to the slope of patellar tilt.....	109
Figure 6.8: 2 nd order regression fit of the ratio of medial to lateral bone/cartilage interface to the slope of patellar tilt.....	110
Figure 6.9: 1 st order polynomial (linear) regression fit of the ratio of medial to lateral surface area and the slope of lateral patellar translation.....	111
Figure 6.10: 1 st order polynomial (linear) regression fit of the ratio of medial to lateral normalized volume and the slope of lateral patellar translation.....	113
Figure 6.11: 1 st order polynomial (linear) regression fit of the ratio of medial to lateral mean thickness and the slope of lateral patellar translation.....	114
Figure 6.12: 1 st order polynomial (linear) regression fit of the ratio of medial to lateral percentage cartilage coverage and the slope of lateral patellar translation.	116
Figure 7.1: <i>In vivo</i> assessment of lateral patellar translation.....	125
Figure 7.2: <i>In vivo</i> assessment of patellar tilt.....	126
Figure 7.3: <i>In vivo</i> and <i>in vitro</i> assessment of patellar spin.....	127
Figure B.1: The lower arrow indicates the lateral posterior femoral point (f1) and the upper arrow indicates the medial posterior point of the femur (f2).....	169
Figure B.2: Point f3 identifies the most distal point on the femur.....	170
Figure B.3: Femoral coordinate system.....	171
Figure B.4: Point t1 is the most superior point of the fibula identified on a sagittal slice.....	172
Figure B.5: The axial slice containing the most superior point of the fibula.....	173
Figure B.6: Most superior point of the medial tibial eminence found on a sagittal slice.....	173
Figure B.7: Tibial coordinate system.....	175
Figure B.8: The most posterior point (p1) and lateral point (p2) on the axial midslice of the patella.....	176
Figure B.9: The superior (p3) and inferior (p4) points on the sagittal midslice of the patella.....	177
Figure B.10: Patellar coordinate system.....	178
Figure D.1: 2 nd order polynomial regression fit of the ratio of medial to lateral surface area to the slope of lateral patellar translation.....	185
Figure D.2: 3 rd order polynomial regression fit of the ratio of medial to lateral surface area to the slope of lateral patellar translation.....	185
Figure D.3: 2 nd order polynomial regression fit of the ratio of medial to lateral mean thickness to the slope of lateral patellar translation.....	186

Figure D.4: 3 rd order polynomial regression fit of the ratio of medial to lateral mean thickness to the slope of lateral patellar translation.....	186
Figure D.5: 2 nd order polynomial regression fit of the ratio of medial to lateral normalized volume to the slope of lateral patellar translation.....	187
Figure D.6: 3 rd order polynomial regression fit of the ratio of medial to lateral normalized volume to the slope of lateral patellar translation.....	188
Figure D.7: 4 th order polynomial regression fit of the ratio of medial to lateral normalized volume to the slope of lateral patellar translation.....	188
Figure D.8: 2 nd order polynomial regression fit of the ratio of medial to lateral percentage cartilage coverage to the slope of lateral patellar translation.....	189
Figure D.9: 3 rd order polynomial regression fit of the ratio of medial to lateral percentage cartilage coverage to the slope of lateral patellar translation.....	189

Acknowledgements

- I would like to thank Dr. David Wilson for giving me the opportunity to work in such enriching multidisciplinary environment. You have given me the freedom to really make this project my own! Your guidance was invaluable.
- I would like to thank Dr. Felix Eckstein welcoming me into your lab and allowing me to learn your qMRI technique. My experience in Munich, working with your group, will be one I always remember. Your enthusiastic approach to your work really inspired me to continue a career in research.
- I would like to thank Dr. Jolanda Cibere and Dr. Savaas Nicolaou for providing your expertise. The project would not have developed so well without your input.
- To Derek, Agnes, Amy and Mike for your input at our weekly lab meetings.
- To the girls in the lab, Saija, Heather, Katie, Carolyne, Sarah, Miranda, Christina, and of course Tim too, thank you so much for all the moral support! The lab wouldn't be the same without you all!
- To Steve, thanks for helping me get through the past few months of writing by making me lots of coffee!
- And last but not least to my family, for supporting me in everything I do. I wouldn't have achieved this without you.

Chapter 1: Introduction

Osteoarthritis (OA) of the knee is a disease characterized by pain, reduced mobility and joint dysfunction that becomes prevalent in individuals over the age of 50. The knee is made up of the tibiofemoral joint and the patellofemoral joint. OA can be found in one of these two joints or in both. Articular cartilage degeneration at the joint is one indication of OA. The Framingham Osteoarthritis Study, a subsection of the Framingham cohort cardiovascular study which began in 1948 with 5209 participants, was conducted at the 22nd biennial examination (1992-3). Approximately 50% of the 608 surviving members (mean age 80.7) who experienced knee pain had some form of knee OA¹²³. 5.3% had isolated patellofemoral OA and 19.7% combined tibiofemoral and patellofemoral OA. At this time there is no known cure for knee OA.

Biomechanical factors almost certainly play a role in the initiation and progression of knee OA, although it is not clear which ones are most important. These factors may be different for the tibiofemoral and patellofemoral joints. Various studies have related obesity^{37,68}, varus-valgus laxity^{30,60,158} and patella position⁷⁴ to patellofemoral OA. In particular, valgus malalignment is associated with the progression of lateral patellofemoral OA and varus malalignment is associated with the progression of medial patellofemoral OA^{30,60}. However many subjects in this study did not follow this pattern of progression. Of the individuals with medial progression 30% had valgus malalignment and of the individuals with lateral progression 45% had varus alignment. This suggests that alignment alone is not sufficient to explain patellofemoral OA progression. Ultimately we would like to identify local biomechanical factors to design effective prevention and treatment strategies.

A key limitation of recent studies of the mechanics of patellofemoral OA progression is that they assess mechanics with tibiofemoral alignment. Tibiofemoral alignment provides little information about the local biomechanical environment at the patellofemoral joint in activity. Patellar kinematics and contact areas play a role in the transference of force through the joint. Relative positions of articular surfaces, lines of actions of muscles and soft tissues influence patellar kinematics and contact areas. OA may be caused by altered magnitudes and patterns of loading. Ideally, we would measure force at the joint to better understand the local environment and its relationship to OA but at this time we are not able to do so *in vivo*. We can, however, measure three-dimensional patellar kinematics *in vivo*. Our group has developed a novel, non-invasive, magnetic resonance imaging (MRI)-based technique to assess three-dimensional patellar kinematics both accurately and precisely *in vivo*⁶⁷.

A second key limitation is that joint space narrowing, the measure of distance between bones from a radiograph, is widely used as an indicator of OA. Radiographic OA is defined by the presence of joint space narrowing and osteophytes (bony protrusions through the cartilage surface). But OA also has a clinical or symptomatic definition which focuses on pain and reduced mobility of the patients. One study found that radiographic evidence of OA does not correlate well with clinical/symptomatic OA¹⁰³. This suggests there are limitations to the radiographic definition of OA. MRI has many advantages over conventional radiology, in particular the ability to visualize soft tissues, such as articular cartilage. Several groups have developed quantitative MRI (qMRI) methods of measuring cartilage morphology *in vivo*^{27,32}. By examining the

articular cartilage with MRI, rather than measuring the space it should fill with radiography, specific regions of cartilage degeneration can be identified.

It is not clear how tibiofemoral alignment affects patellar kinematics, and ultimately load transmission, through the patellofemoral joint. Understanding this relationship is important as abnormal loading conditions likely contribute to the onset and progression of knee OA. It is not clear how tibiofemoral alignment relates to cartilage morphology. If compartmental cartilage degeneration is associated with alignment, corrections to alignment can be made in order to minimize cartilage degeneration. It is not clear whether there is a relationship between patellar kinematics and cartilage morphology. If this is the case, treatment strategies should focus on correcting patterns of patellar kinematics rather than malalignment.

There are three objectives in this pilot study. The first objective was to examine the relationship between varus and valgus alignment and patellar kinematic parameters and to determine the effect size required to observe statistically and clinically significant differences. The second objective was to determine if medial and lateral compartmental cartilage morphology was associated with varus and valgus alignment and to determine the effect size for observing possible differences. Finally, the third was to study the relationship between patellar kinematic parameters and cartilage morphology in order to identify which relationships should be examined in more detail in future studies.

To examine the three objectives we asked three particular research questions (Figure 1.1):

1. Which features of three-dimensional patellar kinematics are associated with valgus alignment and which features are associated with varus alignment?
2. Is local, compartmental patellofemoral cartilage morphology associated with varus or valgus alignment?
3. Are specific patterns of three-dimensional patellar kinematics associated with local, compartmental patellar cartilage morphology?

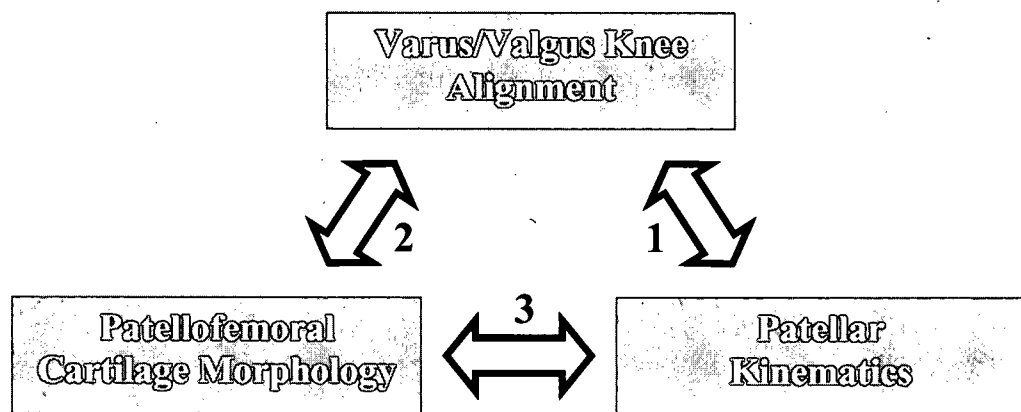


Figure 1.1: The relationship between research questions 1, 2 and 3.

Chapter 2: Literature Review

2.1 Introduction

The local biomechanical environment at the patellofemoral joint is thought to play a key role in the onset and progression of patellofemoral osteoarthritis (OA). This chapter begins by providing an overview of the anatomy and biomechanics at the patellofemoral joint. It then defines OA and examines its economical impact, the risk factors associated with it and the treatment options available to individuals suffering from it. Finally, new imaging based technologies which allow us to gain insight into cartilage health and biomechanics at the patellofemoral joint are discussed. In particular, new and novel techniques for assessing cartilage morphology and three-dimensional patellar kinematics *in vivo* will be discussed.

2.2 The Patellofemoral Joint

2.2.1 Anatomy

The knee joint consists of two distinct joints, the tibiofemoral joint and the patellofemoral joint. The tibiofemoral joint facilitates the flexion and extension of the leg while the patellofemoral joint plays an important role in guiding the line of action of extensor muscles in the leg (Figure 2.1). The patella is a large sesamoid bone which articulates in the trochlear groove on the anterior side of the distal femur. The patella is an insertion site for the quadriceps tendon and an origin site for the patellar ligament which then inserts into the tibial tuberosity on the anterior side of the tibia. The patellar ligament is often considered an extension of the quadriceps tendon which passes through the patella.

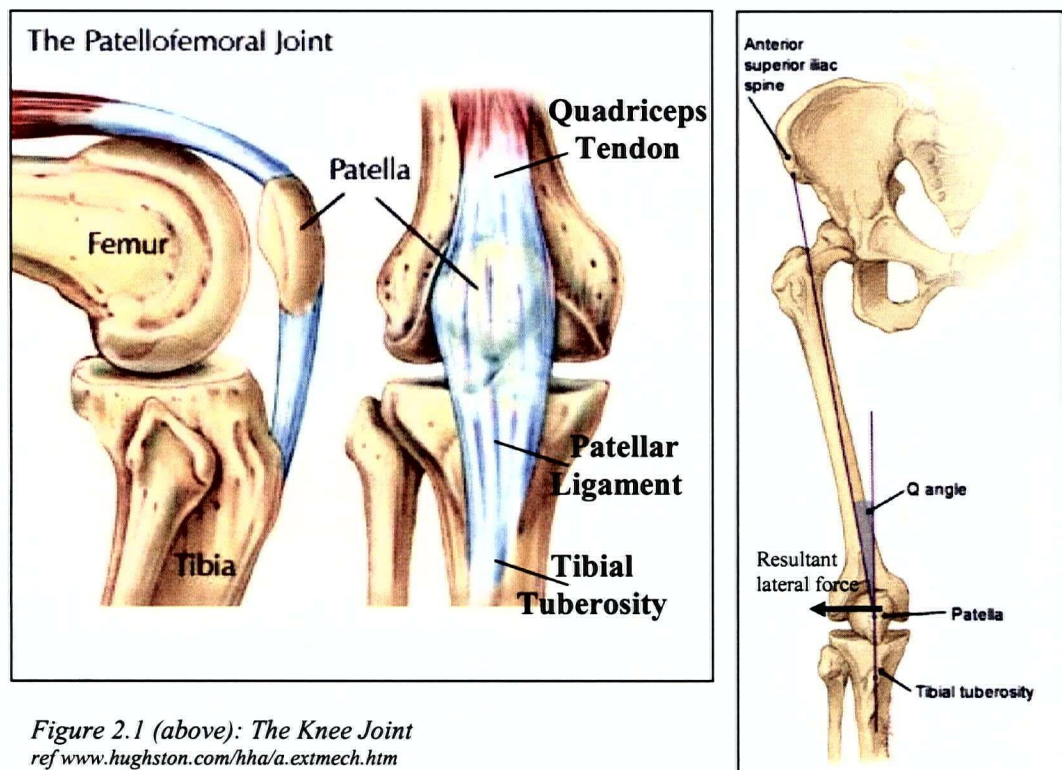


Figure 2.1 (above): The Knee Joint
ref www.hughston.com/hha/a.extmech.htm

Figure 2.2 (right): Measurement of Q-angle ref 1999 Floyd E. Hosmer
<http://www.aafp.org/afp/20030901/907.html>

2.2.2 Mechanics

2.2.2.1 Articular cartilage

Both the posterior surface of the patella and the trochlear groove of the femur are covered in articular cartilage (hyaline cartilage) which provides a smooth, low-friction surface for the patella to travel along as the knee flexes and extends. The patellar articular cartilage is very thick when compared to cartilage in other compartments of the knee and other joints⁸⁶. It has also been suggested that the patellar cartilage is more permeable than other articular cartilage as well as having a greater compressive aggregate modulus^{96,133}, even in comparison to its mating cartilage in the trochlear groove. This likely makes it more susceptible to damage⁸⁶. It has been suggested that cartilage damage increases the frictional force on the bearing surface².

2.2.2.2 Loads on the Patella

A posteriorly directed resultant force acts on the patella. The patella acts as the fulcrum of a lever as the knee flexes and extends, increasing the moment arm of the quadriceps muscle as it travels along the trochlear groove². The quadriceps are strong as they are used in all activities involving knee flexion, such as walking, climbing stairs, sitting down etc. Tension in the quadriceps tendon and patellar ligament, measured in the sagittal plane, produces a resultant posteriorly directed force that acts on the patella (Figure 2.3). It has been found that the ratio of tension in the patellar ligament to the quadriceps tendon decreases from angles of tibiofemoral flexion of 30° and above³. This increase in resultant force is also due to the increasing distance of the joint from to the body's centre of gravity. Through cadaver studies, the maximum force has been found to

be half of body weight during walking and over eight times body weight during deep knee bends⁹⁸.

There is also a lateral force component acting on the patella. The q-angle, measured in the frontal plane, is measured as the angle between the line from the origin of the quadriceps muscle (the anterior superior iliac spine) to the centre of the patella and the line from the tibial tuberosity to the centre of the patella (Figure 2.2). The resultant force vector of the tension applied by the quadriceps tendon and the patellar ligament is directed laterally (Figure 2.3). In knee extension the patella tends to sit in a lateral position because the trochlear groove is shallower at its superior end and allows for lateral displacement. As the knee flexes to 20° and greater, the patella is confined by the lateral side of the trochlear groove.

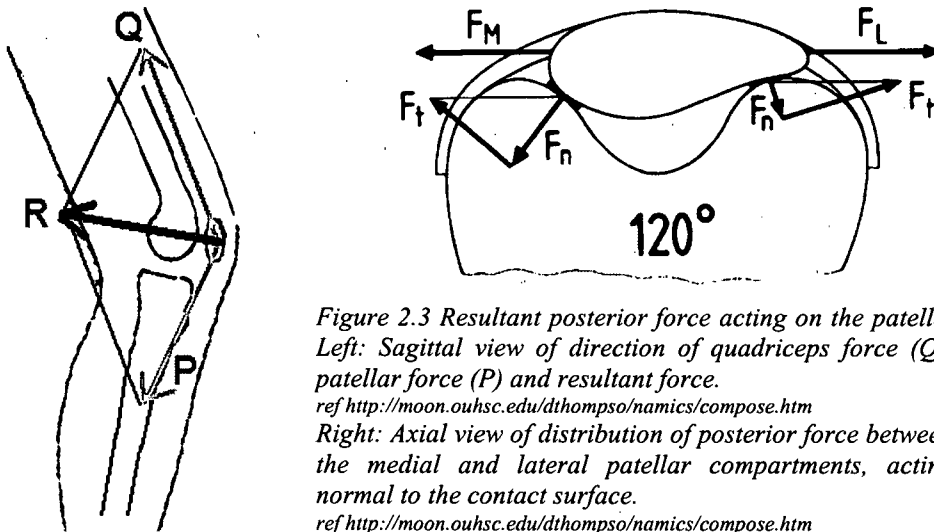


Figure 2.3 Resultant posterior force acting on the patella. Left: Sagittal view of direction of quadriceps force (Q), patellar force (P) and resultant force.

ref <http://moon.ouhsc.edu/dthomps/namics/compose.htm>

Right: Axial view of distribution of posterior force between the medial and lateral patellar compartments, acting normal to the contact surface.

ref <http://moon.ouhsc.edu/dthomps/namics/compose.htm>

2.2.2.3 Kinematics

The forces acting upon the patella and the geometry of the patellofemoral joint define the three-dimensional kinematics of the patella. For example, as just mentioned the lateral side of the trochlear groove constrains the motion of the patella in angles of knee flexion above approximately 20° . Although a great deal of research on the topic of three-dimensional patellar tracking has been carried out (mostly *in vitro* but some *in vivo*) there lacks consensus as to what normal patellar tracking is. This is likely due to the large variations in muscle strength and bone geometry between individuals. In *in vitro* studies loading conditions must be simulated, and therefore the loading conditions are likely not exactly what is seen *in vivo*. *In vivo* studies have been, until recently, invasive in nature however new imaging technologies have allowed for non-invasive techniques for measuring kinematics *in vivo*. The non-invasive, *in vivo* studies are however limited by imaging bore sizes (limiting the range of tibiofemoral flexion that can be studied), the supine orientation of the study participants, the simulation of erect loading conditions, and the great expense involved with imaging. *In vivo* study is essential to understanding three-dimensional kinematics.

Consensus about patterns of patellar tracking has emerged in the literature. One review article studied difference in patellar tracking parameters in *in vitro* and *in vivo* studies¹⁰⁵. Most *in vitro* studies have found that as the tibiofemoral joint flexes the patella shifts medially and then tends to shift laterally after approximately 30° of flexion¹⁰⁵. Patterns in *in vivo* studies are not as consistent however there seems to be a consistent medial shift up to 30° ¹⁰⁵. For medial/lateral patellar tilt, *in vitro* studies have found a medial tilt in early stages of tibiofemoral flexion and then a lateral tilt later, while

in vivo studies have found both increasing medial tilt and increasing lateral tilt¹⁰⁵. No consistency has been seen in patterns of internal/external rotation of the patella in either *in vitro* or *in vivo* studies¹⁰⁵. Other kinematic parameters such as anterior and superior patellar translation and patellar flexion are not as commonly measured. As the knee flexes the patella flexes about the femur and shifts inferiorly until about 90°. Anterior translation is likely related to patellar flexion, the morphology of the patellar and trochlear cartilage and bone geometry. Further study is required in order to understand the range of normal three-dimensional patellar kinematics.

2.2.2.4 Contact Areas and Stresses

The magnitude of load and three-dimensional patellar kinematics both contribute to defining contact areas and stresses at the patellofemoral joint. Since the patella has a relatively small area for potential contact when compared to other joints, large contact pressures are found. *In vitro* studies have shown that the contact area is located at the distal end of the patella near extension, shift proximally up to 90 degrees of flexion and then returns towards the middle after 90 degrees of flexion⁸¹. The size of this contact area appears to increase from 0 to 60 degrees² but after that there is no consensus about the size of the contact area. Some groups report that it increases^{81,98}, others that it decrease⁴⁵ and others that it stays the same³. New MRI-based methods of measuring contact area *in vivo* are being developed. However, as with patellar kinematics, the range of tibiofemoral flexion that can be studied is limited by the size and geometry of the imaging bore and the methods have not been rigorously validated as of yet^{92,135}. It is

difficult to calculate the actual magnitude of contact stresses at the joint *in vivo* as both the resultant forces and the areas of contact change as the knee flexes and extends.

2.2.3 Summary

The local biomechanical environment at the patellofemoral joint is a very complex interaction between geometry, cartilage health, three-dimensional patellar kinematics, contact areas and contact stresses. It is likely that the biomechanical environment contributes to the onset and progression of pathologies at the patellofemoral joint.

2.3 Knee Osteoarthritis

Osteoarthritis (OA) is a disease characterized by pain and joint dysfunction and is the most common musculoskeletal disorder, affecting 1 in 10 Canadians (IMHA OA consensus conference 2002). It is most prevalent in individuals over the age of 50 and can have grave affects on mobility, activities of daily living and quality of life in its sufferers. Knee OA is the most common form of the disease. The Framingham Osteoarthritis Study is a subSection of the Framingham cohort cardiovascular study which began in 1948 with 5209 participants. At the 22nd biennial examination (1992-3) the 1161 surviving members of the cohort were asked whether they experienced knee pain. If they gave an affirmative answer they underwent radiographic assessment of both knee compartments. 608 individuals (220 men and 388 women, mean age 80.7 ± 5 years) gave affirmative answers and of this group approximately 50% had some form of knee OA (radiographic joint space narrowing was used as an indicator)⁶⁹. This number included individuals with both tibiofemoral and patellofemoral OA. The tibiofemoral joint is perceived to be the more common knee compartment to find OA however this study discovered that the patellofemoral joint was involved in approximately half of all knee OA cases with 5.3% of the group having isolated PF OA and 19.7% of the group having combined TF and PF OA (Figure 2.4)¹²³.

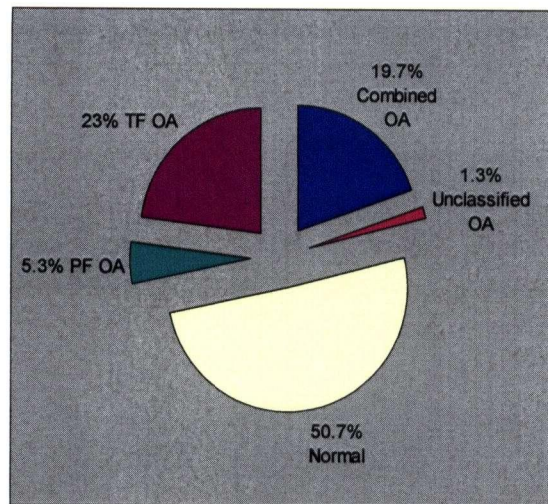


Figure 2.4: Distribution of knee osteoarthritis in the Framingham cohort knee pain group (n=608). Ref: McAlindon, 1996

2.3.1. Characteristics of Knee OA

Indicators of knee OA are the degeneration of articular cartilage within the joint, the presence of osteophytes (bony protrusions on the joint surface) and subchondral sclerosis (hardening of the bone)¹⁹. These three indicators (Figure 2.5) manifest themselves differently from person to person and a cause and affect relationship between them has yet to be established. Also, the order in which they present themselves is uncertain, i.e. does cartilage thinning, development of osteophytes or subchondral sclerosis occur first.

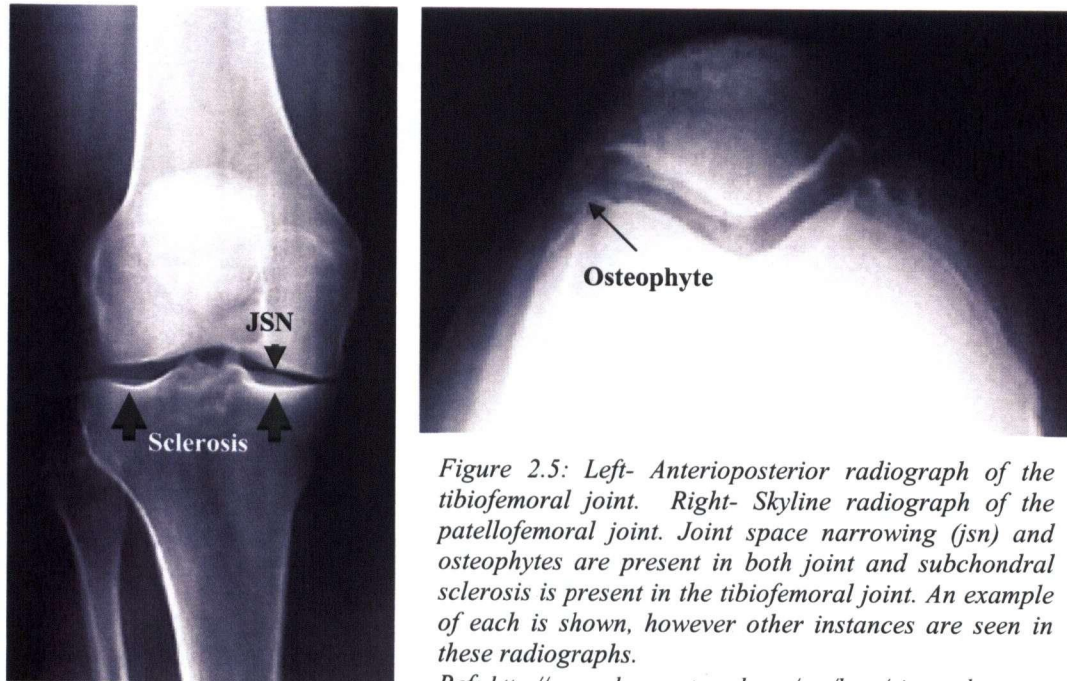


Figure 2.5: Left- Anteroposterior radiograph of the tibiofemoral joint. Right- Skyline radiograph of the patellofemoral joint. Joint space narrowing (jsn) and osteophytes are present in both joint and subchondral sclerosis is present in the tibiofemoral joint. An example of each is shown, however other instances are seen in these radiographs.

Ref: <http://www.physsportsmed.com/asr/knee/vitanzo.htm>

Cartilage has a limited ability to regenerate once damage has occurred. Two different mechanisms of cartilage wear have been proposed: 1) interfacial wear due to the articulation of the two joint surfaces and 2) fatigue wear due to the repetitive stressing of the cartilage¹³³. Interfacial wear occurs at the cartilage surface whereas fatigue wear occurs within the cartilage. Cartilage does not share the adaptive behaviour of bone although it does have a limited ability to repair and regenerate. Any mechanical insult to the cartilage, however, most likely results in permanent damage. Some degree of articular cartilage wear is a natural consequence of aging.

In knee OA, osteophytes initially occur in the peripheral regions of the bone-cartilage interface (Figure 2.4) and as the disease progresses develop in more central regions of the cartilage plate. Osteophytes in their early stages are covered by cartilage but in their later stages tend to ‘push through’ the cartilage surface and are exposed to the joint capsule. The exposed bone then articulates with the opposing cartilage causing further wear. It is

unknown whether the composition of the bone of the osteophyte and the cartilage covering the osteophytes differs from normal bone and cartilage.

Sclerosis is the hardening of the bone directly underneath the articular cartilage. It is attributed to increased bone density, trabecular microfractures and macroscopic collapse in subchondral bone. Sclerotic regions appear brighter on radiographs (Figure 2.4). There is disagreement about whether sclerotic changes are primary or secondary in osteoarthritis. A recent study suggests that sclerosis is a secondary change occurring as a result of increased loading due to changes in thickness and the biomechanical properties of articular cartilage¹⁸⁹. Other groups believe that changes in subchondral bone precede cartilage changes¹⁴³. Sclerosis most commonly occurs in subchondral regions of the weight bearing bone, such as the tibia¹⁹. It is hypothesized that the increased load in the bone causes more blood to flow to this area, stimulating the osteoblasts in the subchondral region to deposit bone on existing trabeculae to meet the loading needs¹⁹. Sclerosis is not often seen in patellofemoral OA. Cartilage degeneration and osteophytes are the two main indicators of OA at this joint.

2.3.2 Clinical and Radiographic Assessment of Knee OA

OA is a disease that affects different individuals in different ways. Some people experience severe pain and loss in mobility while others are hardly affected by the disease at all. Classification schemes have been created over the years in order to assess different stages of the disease. Two different definitions of OA are used when studying the disease: 1) radiographic OA which relates to the presences of cartilage degeneration, osteophytes and sclerosis and 2) clinical or symptomatic OA which refers to the pain and

loss of mobility an individual experiences as a result of the disease. A distinct difference between clinically relevant patellofemoral OA and radiographic patellofemoral OA has been established. The former describes how it affects individuals who are debilitated by their OA and the latter quantifies the destruction of cartilage and presence of osteophytes and is most often used in research studies. An interesting study showed that radiographic evidence of patellofemoral OA does not correlate with pain and loss of mobility¹⁰³. This has lead researchers to question the best methods of quantifying disease progression and to develop clinical and radiographic classification systems, both of which have their own merits.

2.3.2.1 Clinical OA

Clinical osteoarthritis is assessed by symptoms and signs identified usually by a family physician during physical examination. Common symptoms of OA include pain, stiffness, alteration in shape, functional impairment, anxiety and depression. There are signs associated with each of the symptoms which included crepitus, restricted movement, tenderness, bony swelling or deformity and muscle wasting and weakness¹⁹. Radiography is often used to support the clinical diagnosis of OA because the signs and symptoms of the disease are of quite a general nature, which can lead to misdiagnosis. Clinical diagnoses can be controversial, especially in early OA, because the signs and symptoms used are not specific to this disease.

Although research studies tend to use the radiographic definition of OA, the debilitation and pain component of the disease has also been studied and quantified. Questionnaires have been developed which assess the clinical status of OA, such as the

Western Ontario and McMaster Universities OA Index (WOMAC) (Appendix A)^{12,13}, the Comprehensive OA Test (COAT)²¹, the Rheumatoid and Arthritis Outcome Score (RAOS)²⁰, the German short musculoskeletal function assessment (SMFA-D)^{110,112}, the Knee Injury and OA Outcome Score (KOOS)^{150,151} and the short form -36 Arthritis-Specific Health Index (ASHI)¹⁸³. The most commonly used questionnaire is the WOMAC OA Index (Appendix A) which has been validated for use at the hip and knee^{12,13}. It measures clinically important symptoms of the disease by using activities of daily living to determine the pain, stiffness and physical function of the patient. It is most often used to assess treatment outcomes or disease progression in longitudinal studies but is also an important tool in assessing the clinically relevant stage of OA in cross-Sectional studies. Questionnaires are the clinical link in studies which use radiographic grade OA as a primary outcome measure.

2.3.2.2 Radiographic OA

Numerous grading scales have been developed for the radiographic assessment of patellofemoral OA. The first and still the most commonly used imaging modality to study OA is radiography. An atlas for the radiographic assessment of OA, the Kellgren-Lawrence scale, was developed to characterize stages of the disease^{108,109,125}. Grades 0 through 4 are based on varying degrees of osteophyte presence and joint space narrowing (Table 2.1). In the radiographic assessment of OA cartilage degeneration is often estimated by measuring joint space narrowing. The reasoning behind this is that the distance between bones in the joint ultimately decreases as a result of the cartilage wear.

Limitations of this method are that local cartilage deficits are not visible on radiographs and that cartilage is assumed to fill the entire space between the bones.

Grade	Indicators
0	No osteophytes
1	Doubtful osteophytes
2	Minimal osteophytes, possible joint space narrowing, cysts and sclerosis
3	Moderate or definite osteophytes with moderate joint space narrowing
4	Severe large osteophytes and definite joint space narrowing

Table 2.1: The Kellgran-Lawrence osteoarthritis grading scale.

Variations of this scale exist^{48,125,134,155,168,169}, some of which address the limitations of the Kellgran-Lawrence scale. The foremost limitation of the Kellgran-Lawrence protocol is that the radiographs are not taken in a weight bearing position, and therefore an accurate measurement of joint space is not obtained because cartilage compresses under load. New protocols have been established for obtaining weight bearing radiographs in conjunction with the Kellgran-Lawrence scale²⁴. A newer bone atlas^{89,155} is endorsed by the Osteoarthritis Research Society International (OARSI). The largest population-based OA studies to date (Framingham cohort, Chingford cohort) use radiographic assessment of the knee joint to quantify the stage of OA.

There are two inherent flaws in the radiographic assessment of knee OA. The first is that radiography provides a representation of a three-dimensional object in two dimensions; the image obtained will always be dependent on the angle at which it is taken. Protocols have been developed to standardize anatomical positioning for radiography of patellofemoral OA^{24,128,129}. These protocols have been validated for reliability however a technician trained in OA positioning protocol is required^{115,174}. The second flaw is that all radiographs must be taken in a weight bearing position in order to

obtain an accurate measure of joint space. For the tibiofemoral joint this is not much of a problem because the anterior-posterior radiograph with the leg in an extended position while standing will suffice. However, imaging the patellofemoral joint presents a greater challenge. The Buckland-Wright protocol dictates that the patient must stand with the knee flexed to 30° (with the aid of a support frame if necessary). The X-ray tube is then positioned directly above the patient's head and the cassette on a step above the patient's foot (Figure 2.6). Sometimes a trace of the patient's foot is taken in order to reposition correctly at another time point. The difficulty with this method is in positioning the knee at 30°. A goniometer is used to measure this angle, however in obese patients (as many osteoarthritic patients are) it may be more difficult to identify the location of the bones. A small study has also shown that the position of the x-ray tube is of substantial importance in calculating joint space¹²⁶. It found that a of 2° change in x-ray tube alignment caused an error of 1 mm in joint space measurement. In OA, a 1 mm difference in joint space measurement can change the Kellgran-Lawrence grade, which could lead to misclassification and mistreatment.

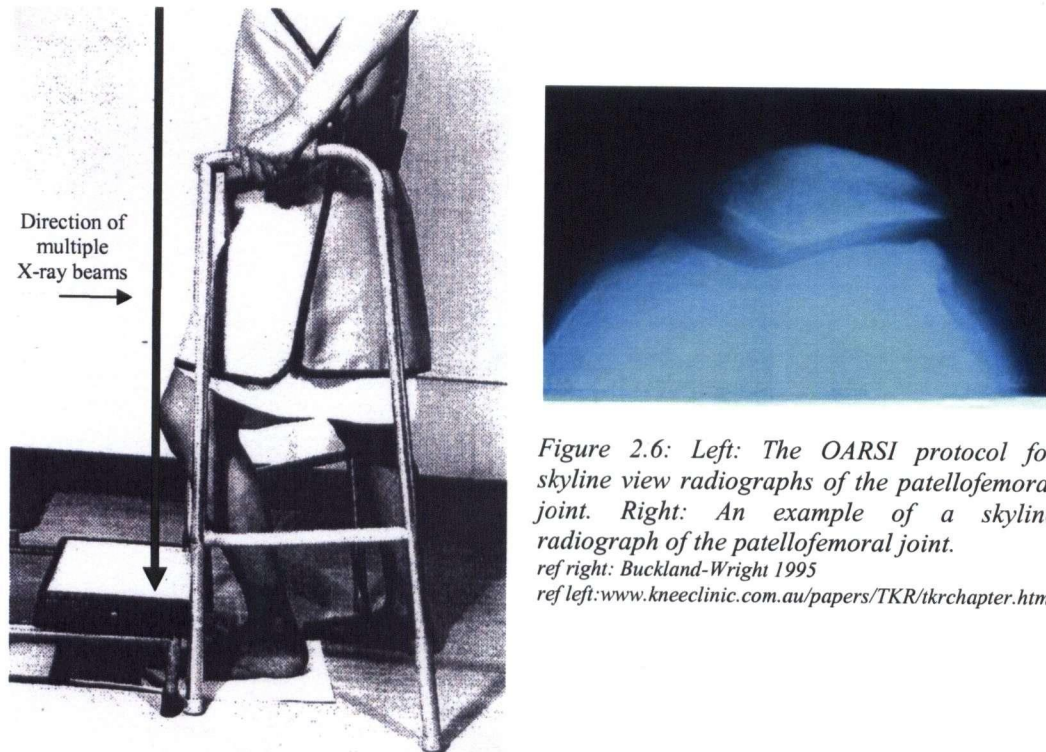


Figure 2.6: Left: The OARSI protocol for skyline view radiographs of the patellofemoral joint. Right: An example of a skyline radiograph of the patellofemoral joint.
 ref right: Buckland-Wright 1995
 ref left: www.kneeclinic.com.au/papers/TKR/TKRchapter.htm

2.3.3 Treatment

Currently there is no cure for OA. Treatment options focus on pain management and maintenance of mobility. Early treatment strategies have a systemic and biomechanical component and include the combination of drugs, exercise, bracing, education and acupuncture with the goal of slowing down onset and progression of the disease⁷⁰.

Systematic approaches have focused on reducing inflammation and pain. Oral drugs, such as acetaminophen in a first instance or nonsteroidal anti-inflammatory drug (NSAID) when acetaminophen has failed, are used for pain management⁷⁰. Glucosamine, which may aid in cartilage repair by increasing proteoglycan synthesis^{70,124,165}, and chondroitin, which may reduce degradation of cartilage^{9,10,124,177}, are in the clinical trial stages. Corticosteroid injections^{4,145,166} and capsaicin cream^{47,93} are also sometimes prescribed for

pain. Finally, some individuals have shown benefits when obtaining acupuncture treatment^{14,15,62}.

The biomechanical approaches have been primarily physiotherapy based. General exercise (strength and aerobic activities) is prescribed for knee OA^{63,130,156,178}. In particular, muscle strength in the quadriceps is stressed because it has been identified as a risk factor of OA^{75,165} in all knee compartments¹¹. Bracing, taping and corrective footwear have also been used to treat knee OA^{164,44,107,137,141,142,153,190} with the aim of reducing impact¹⁶⁴, reducing lateral thrust at the knee¹⁹⁰, increasing proprioception and reducing feelings of instability¹³⁷, controlling lateral instability¹⁴¹ and repositioning the patella⁴⁴.

Educational programs have also had success in the management of OA. Mail⁷⁶, telephone¹⁸⁴ and group education programs^{121,156,175,185} have also been shown to improve the health status of individuals with OA.

When all of the non-surgical treatments of knee OA have been exhausted surgical treatments are often sought. In younger patients high tibial osteotomy, which attempts to correct lower limb alignment, has been successful in reducing pain^{1,102} and delaying articular cartilage wear in the tibiofemoral joint⁷². Total knee arthroplasty (TKA) is the most popular and successful treatment for individuals with late stages of knee OA and less than a 20 year life expectancy^{70,116}. TKA has a success rate of 95% at the 15 year mark^{49,144,149}. Cartilage transplants and tissue engineering are also being explored as a treatment for knee OA^{25,70}.

2.3.4 Economics

The economic burden of OA is two fold, being a combination of direct costs and indirect costs. The direct costs include drugs, medical care, hospital, research funding and pensions and benefits⁷. The indirect costs can be summarized as lost wages and include premature mortality, chronic disability and short term disability⁷. The most recent report that discusses the costs associated with musculoskeletal illness in Canada, Economic Burden of Illness in Canada, was carried out in 1998 and found that 2.6 billion dollars were attributed to direct costs and 16 billion to indirect costs⁸⁹. Musculoskeletal disorders have the third highest indirect costs of all categories of disorders and have a similar economic burden as cancer⁷. Because arthritis accounts for approximately 60% of musculoskeletal disorders and OA for approximately 45% of all arthritis cases¹²² the cost of OA in particular runs over 5 billion dollars per year. Due to the aging population, it is estimated that the incidence of arthritis in Canada will increase by 124%, from 2.9 to 6.5 million sufferers, by 2031⁸.

2.3.5 Risk Factors

There is a wide body of literature on the topic the risk factors associated with knee OA, yet very little is understood about the etiology of the disease. The identification of risk factors allows treatment strategies to be developed that focus on modifying the detrimental factor in order to arrest the onset or progression of the disease. It is most likely that the etiology of the disease is related to both biomechanics and biochemistry, therefore interdisciplinary study is necessary to fully understand the origins of the disease. Many possible risk factors of knee OA have been studied independently or in

combination and tend to be classified in two distinct groups: systemic and biomechanical. Systemic factors include age, sex, ethnicity, bone density, hormonal status, nutritional factors and genetics⁶⁹, while biomechanical factors include obesity, mechanical environment (knee laxity, proprioception, knee alignment), loading, acute injury, occupation and sports participation⁶⁹. For example, it has been shown that obesity (most commonly quantified by a body mass index of 30 or above) is associated with knee OA⁶⁸ and that weight loss reduces the risk of symptomatic knee OA⁷³. It is likely a combination of some or all of the systemic and biomechanical risk factors that lead to the onset and progression of knee OA. Longitudinal research shows that treatment strategies must target a combination of these risk factors¹⁵⁶.

It has been suggested that the risk factors of tibiofemoral and patellofemoral knee OA are different⁷¹. However the risk factors associated with patellofemoral OA have had limited attention to date. One study found that obesity and meniscectomy were more strongly correlated with medial tibiofemoral OA than patellofemoral OA and that osteophytes are more strongly correlated with patellofemoral OA than tibiofemoral OA⁴³. The sample sizes of this study were, however, too small to say this conclusively. Another study found that obesity and meniscectomy were not greater risk factors of tibiofemoral OA than patellofemoral OA. However, they did not have any data on osteophytes¹²³. A different study looking at knee alignment found that the tibiofemoral joint is more vulnerable to the effects of alignment than the patellofemoral joint in disease progression³⁰. Previously, the patellofemoral joint was omitted from knee OA studies but now there is no question that the patellofemoral joint plays a large role in symptomatic

knee OA¹²⁵. It is apparent that the particular risk factors of patellofemoral OA should be studied more closely.

2.3.6 Lower Limb Alignment and Knee OA

Lower limb alignment has been associated with both tibiofemoral and patellofemoral knee OA^{31,34,61,159}. It is thought that the mechanical environment associated with a varus (bow-legs) or valgus (knock-knees) malalignment (Figure 2.7) may contribute to the onset and the progression of OA at the knee joint. Alignment may produce different mechanical changes at the tibiofemoral and patellofemoral joints and therefore it is important to study them separately.

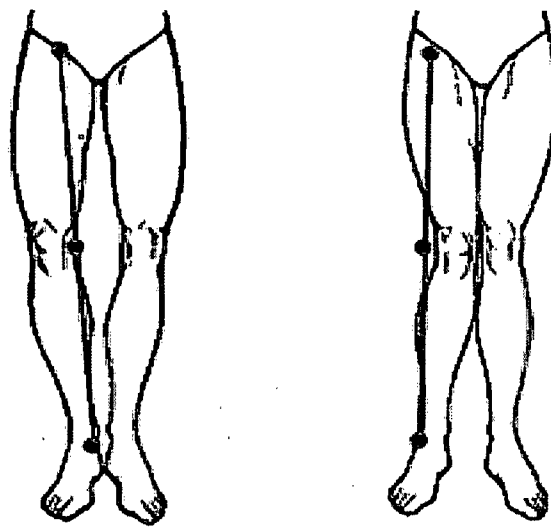


Figure 2.7: An example of varus alignment or bow-legs (left) and valgus alignment or knock knees (right). Ref Mast 2002

Knee alignment is a risk factor of knee OA and is most often measured from a leg lengths radiograph. Many protocols have been developed to ensure the proper positioning of patients for this radiograph^{42,132,152}. To assess OA, it is important that the radiograph is taken in the anteroposterior plane in a weight bearing position (i.e.

standing) and that normal shoes are worn in order to study the natural stance of the individual. Bony landmarks at hip, knee and ankle are used to identify the mechanical axes of the femur and tibia and measure the angle between the two lines. Women more commonly have a valgus deformity due to naturally wider hips. There are both manual and electronic methods of measuring the knee angles from radiographs.

Alignment is associated with compartment specific tibiofemoral OA progression. It has been shown that varus malalignment is associated with medial tibiofemoral OA progression and valgus malalignment is associated with lateral tibiofemoral OA progression¹⁵⁹. This study used Kellgran-Lawrence radiographic grading to study disease progression. Another study used quantitative MRI techniques to study changes in compartmental tibiofemoral cartilage volume in OA knees³⁴. This study found that rate of cartilage loss was associated with knee alignment in a compartment specific manner. For example, a large valgus angle was associated with a greater rate of cartilage loss in the lateral compartment of the tibiofemoral joint. One limitation of this study was that a full leg length radiograph was not obtained. Tibiofemoral angles were measured on images from the midshaft of the femur to the midshaft of the tibia. It has also been shown that varus, but not valgus, alignment makes the knees more vulnerable to the effects of obesity on disease progression¹⁵⁷. It was found that during gait the medial compartment transmits 60 to 80% of the axial load and the lateral compartment transmits the remainder of the axial load¹⁵⁴. Gait analysis of individuals with varus malalignment found more load is transmitted through the medial tibiofemoral compartment than the lateral, but analysis of individuals with valgus malalignment found that in order for the lateral tibiofemoral compartment to transmit more load than the medial a much greater

degree of malalignment was required¹⁰⁴. It is thought that the redistribution of loading creates a local environment in which OA progresses more quickly.

Varus or valgus alignment is also associated with the direction of the lateral reaction force vector at the patellofemoral joint. Q-angle (Figure 2.2) is affected by varus and valgus alignment (varus alignment decreases q-angle and valgus alignment increases q-angle). A decrease in q-angle reduces the lateral reaction force and an increase in q-angle increases the lateral reaction force¹⁰⁰. Increase in q-angle causes changes in the contact pressures at the patellofemoral joint. In a cadaver study in which they varied q-angle, half of the knees saw a lateral shift which unloaded the medial compartment and the other half saw a separation of specific contact areas in both the medial and lateral compartments with greater q-angles⁹⁷. A decrease in Q-angle resulted in the reverse effect with either a medial shift of the contact area, unloading the lateral compartment, or a separation of specific contact areas in the medial and lateral compartments⁹⁷.

The association between alignment and patellofemoral OA has also been studied. One study found that lateral patellofemoral OA is more common than medial patellofemoral OA, valgus malalignment was associated with lateral patellofemoral OA and varus malalignment was associated with medial patellofemoral OA⁶¹. This study also found that OA in individuals with valgus knees more often involved both the patellofemoral and tibiofemoral joint whereas individuals with normal alignment more often had isolated tibiofemoral OA. They took weight-bearing radiographs and used the Kellgran-Lawrence scale to define OA. Limitations of this study include that it wasn't population based and it was cross-Sectional, therefore the affects of alignment on development and progression of the disease were not studied. This study had a large

sample size (n=292) and there were many individuals who did not follow into the general trend seen. For example, the study found that of the individuals with knee OA and lateral patellofemoral joint narrowing, 43 had valgus alignment and 32 had varus alignment. Although there was an association with valgus alignment and lateral patellofemoral joint space narrowing, a large number of individuals with varus alignment displayed the same pattern. This suggests that there are additional factors involved in the compartmental cartilage thinning phenomenon.

Recently, a follow up study, from the same group, which looked at the progression of OA at the patellofemoral joint, was published³¹. It found that the progression of lateral patellofemoral OA is more common than medial patellofemoral OA and patellofemoral OA is affected by varus or valgus alignment in a compartment-specific manner. The study also found that individuals with varus alignment at baseline were twice as likely to have isolated medial patellofemoral OA progression and that individuals with valgus alignment at baseline were 1.6 times more likely to have isolated lateral patellofemoral OA progression. These results were expected, however there were some other interesting findings in this study.

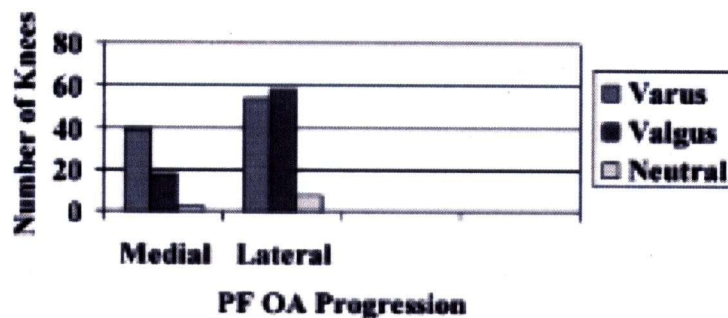


Figure 2.8: Results from Cahue et al. 2004. Number of varus and valgus knees undergoing medial and lateral patellofemoral OA progression. Ref Cahue, 2004

First, the group with lateral progression has almost the same number of varus knees as valgus knees (Figure 2.8). The medial group shows a greater distinction between alignment and medial progression.

Table 3. Knee osteoarthritis progression in specific compartments between baseline and 18 months*

Knee alignment at baseline	Compartment(s) in which progression occurred								
	Medial PF only	Medial PF and medial TF	Medial TF only	Medial PF and lateral TF	Lateral PF only	Lateral PF and lateral TF	Lateral TF only	Lateral PF and medial TF	Medial PF and lateral PF
Varus knees (n = 211)	28 (13)	8 (4)	24 (11)	3 (1)	33 (16)	1 (0.5)	1 (0.5)	18 (9)	26 (12)
Valgus knees (n = 158)	12 (8)	2 (1)	2 (1)	4 (3)	47 (30)	5 (3)	15 (9)	6 (4)	12 (8)

* Values are the number (%). PF = patellofemoral; TF = tibiofemoral.

Table 2.2: Results of distribution of tibiofemoral (TF) and patellofemoral (PF) OA progression from Cahue et. al.2004 Note only a small number of individuals had both lateral PF and TF progression.

Second, very few individuals have both lateral patellofemoral and tibiofemoral progression and both medial patellofemoral and tibiofemoral progression (table 2.2). There are likely other risk factors influencing the distribution of disease progression. Current understanding of OA mechanics predicts that varus alignment would be associated with the progression of both medial patellofemoral and medial tibiofemoral OA and that valgus alignment would be associated with the progression of both lateral patellofemoral and lateral tibiofemoral OA. However, this was not found. There were only 3 individuals with varus knees who had both forms of medial knee OA and only 5 individuals with valgus knees who had both forms of lateral knee OA, in a study of 237 individuals. One limitation of this particular study is that Q-angle, which might have provided some additional useful information, was not measured. These studies suggest further study is required in this area to understand other possible risk factors and indicators of the changes in local mechanical environment.

2.4 Methods for Assessing Articular Cartilage Morphology

Innovations in imaging technology have allowed researchers to visualize soft tissues *in vivo*. Articular cartilage is most commonly measured indirectly using radiography in OA research. However, radiographs only have the ability to assess total degeneration of both cartilage plates, no information with regards to the degeneration of one plate or any specific areas of cartilage degeneration can be obtained. This is a qualitative assessment of cartilage degeneration and is most often used in a clinical setting. Magnetic resonance imaging (MRI) and ultrasound are techniques which have been used to study articular cartilage *in vivo*. MRI has emerged as the most popular method of cartilage imaging, with some groups focusing on the quantitative assessment of articular cartilage morphology^{27,35} and others the biological content of the cartilage itself²⁹. Areas of cartilage degeneration found with MRI have been associated with joint space narrowing measurement from radiographs at the patellofemoral joint¹⁷. The quantitative assessment of cartilage is more useful in research settings. Both MRI and ultrasound have the potential to contribute to the further understanding of OA progression through longitudinal studies which can track changes in cartilage morphology and biochemistry.

2.4.1 MRI Methods

MRI is an imaging modality very popular in medical research because soft tissues can be visualized and there are no known side effects, such as ionizing radiation. In brief, MRI is based on the premise that by applying a radiofrequency (RF) pulse in a magnetic field the displaced waves can be detected and transformed into an image. Different tissues displace waves in different manners and these differences allow us to

differentiate between different tissues in the image. Different imaging sequences (type, length and order in which the RF pulse is applied) can be optimized for specific tissues. One current limitation of MRI is the long imaging time involved. Longer scans produce better images. The sequences chosen usually involve a trade off of image resolution to time. The usual time for an adequate cartilage scan is 10 to 15 minutes, depending on the purpose. The main reason for keeping imaging times to a minimum is that the patient must remain still for the duration of the scan because motion artefacts on the acquired image can distort images and measurements. It is not an easy task to remain in one position for extended periods of time, especially for individuals experiencing pain. Another drawback of MRI is that it is a very expensive imaging modality due to the cost of the machines themselves, the long imaging times and the technical staff required.

Several groups have developed methods of analyzing articular cartilage morphology with MRI^{38,88,138,140,147,167}. The knee joint is the most commonly studied with quantitative MRI (qMRI) due to its relatively flat cartilage plates, which reduces problems associated with the partial volume effect (not having sufficient resolution to detect abrupt changes in the object geometry) which occurs at curved cartilage surfaces. There is a substantial body of literature looking at many different groups of individuals of all ages in healthy and diseased knees. qMRI allows for the study of cartilage changes at a macroscopic level and provides insight into patterns in cartilage degeneration which have not been previously studied *in vivo*. There were three separate issues that had to be overcome in the development of qMRI analysis: 1) an MRI sequence protocol optimized for cartilage viewing, 2) a method of segmenting (delineating) the cartilage from the MR

images, and 3) a method to extract the morphological parameters from the segmented cartilage models.

The challenge in developing an MR sequence for articular cartilage is based on the tissue's complex composition and the composition of surrounding tissues. It is also important that the quality of the image is not compromised by cartilage that has degenerated. For quantitative analysis an extremely high in-plane resolution is desirable because cartilage is very thin, especially in osteoarthritic cases. Also, the slice thickness should be sufficiently small to reduce the chance of missing any features of cartilage morphology. Originally, high resolution 3D T1-weighted fat-suppressed gradient echo sequences were used on a 1.5 Tesla MR scanner for cartilage imaging. While the images it produces are of high quality the imaging times are over 16 minutes if a sufficiently high in-plane resolution is desired^{138,140}. Staying still for over 16 minutes is not an easy task, especially for participants with joint pain, therefore reducing the time of the MR without sacrificing resolution or image quality was a logical next objective for researchers. The high-resolution T1-weighted 3D fast low angle shot (FLASH) sequence with water excitation has been validated on a 1.5 Tesla MR scanner using CT arthrography, A-mode ultrasound and excised cartilage of individuals undergoing total knee arthroplasty. It is a faster sequence, taking 7 to 10 minutes depending on the size of the joint, and it does not sacrifice image resolution or quality^{79,27,82}. This sequence is now the most commonly used in qMRI of cartilage morphology. Research and clinical practice is slowly making a move to 3 Tesla scanners and unfortunately sequences which are optimized for a 1.5 Tesla scanner are not necessarily ideal at 3 Tesla. Groups are now attempting to

determine which sequences will optimize cartilage viewing on the 3 Tesla MR scanner and validation has been carried out⁵⁰.

The method of cartilage segmentation (manual or semi-automated) is a subject of contention in the field of qMRI. Originally manual cartilage segmentation was used in all qMRI studies. In this method researchers manually outline the cartilage area in a slice by slice fashion, often using custom software. Since manual segmentation is very labour intensive, taking up to 1 hour per cartilage plate, groups have begun to develop semi-automated techniques which have been shown to speed up the process by approximately 15%¹⁷². These semi-automated techniques include region growing^{138,140}, active shape modelling¹⁶⁷, edge detection¹¹³, B-spline snakes^{39,172} and active contours¹⁰⁶. Some degree of user interaction is required in all of these methods, for example to use B-spline snakes the user must identify the corners of the cartilage and correct any inconsistencies due to artefacts in the image and regions where two cartilage plates are in contact. It has also been shown that time savings have increased with user experience¹⁷². Progress in semi-automated tools for cartilage segmentation includes the addition of modules to decrease user interaction by employing cartilage templates or information from the previous MR slice. At this time it appears all of the large scale OA studies using qMRI are being carried out using manual segmentation.

Once a cartilage model is extracted from the MR images morphological parameters are calculated. The most commonly used morphological parameters are thickness, volume and surface area. In OA research other parameters are important such as denuded cartilage area (where the bone is exposed), percentage of cartilage coverage and number of cartilage fragments. For the thickness measurement a Euclidean distance

transformation is most often used¹⁷⁰ although others calculate the cartilage thickness by using normal vectors^{6,113}. The Euclidean distance transformation is a more sophisticated algorithm for calculating the distance between two surfaces (the bone-cartilage interface and the cartilage surface in this case) but is less time consuming than a simple normal distance calculation. The Euclidean distance transformation assigns distance maps to each voxel in the segmented volume⁴⁶. Volume calculations are based on the numerical integration of voxels by multiplying pixel size by slice thickness^{113,140}, by bilinear and cubic interpolation^{106,138}, or by a shape-based interpolation method¹⁷⁰. Surface area is calculated using a triangulation algorithm⁶⁴. All other parameters are derivatives of these three main algorithms.

qMRI methods have been validated and used to study cartilage morphology in numerous studies of healthy and diseased joints. Validation has been carried out using water displacement of surgically retrieved tissues^{138,140,172}, CT arthrography^{51,53}, stereophotogrammetry³⁸ or phantom MR images¹⁰⁶. qMRI has been used in many clinical trials. One study found that men tended to have more cartilage volume than women even when results were normalized to joint and body size³³. They also found that changes in tibial and femoral cartilage volume in osteoarthritic knees are related³⁶, and that women using estrogen replacement therapy (ERT) have more cartilage than controls¹⁸⁸. Other groups have found that muscle cross-sectional area was related to cartilage morphology⁹⁹; found that cartilage volume decreased at 3-7 minutes and at 8-12 minutes (to a lesser extent) after carrying out deep-knee bends⁵⁸; and that qMRI can accurately measure cartilage morphological parameters of severely deteriorated osteoarthritic cartilage^{83,84}.

Databases of normal and osteoarthritic cartilage morphology as assessed from qMRI are being created. Databases of osteoarthritic knees have the potential to relate morphological parameters to stages of OA and provide information on possible patterns in disease progression. One group in particular is attempting to compile databases of both normal and osteoarthritic knees in order to create thickness templates of the cartilage surface. Currently there are 2 knee templates, one based on 14 healthy patellofemoral joints and the other based on 33 osteoarthritic patellofemoral joints⁴⁰. qMRI also has great potential in longitudinal studies of disease/structure modifying OA drugs (D/SMOADs). These studies will have a large number of subjects therefore there is a great need to decrease processing time in qMRI without compromising precision. As previously mentioned, a 15% time savings can be realized with semi-automated algorithms. Interactive touch-sensitive screens also have the potential to decrease manual segmentation time by 15%¹²⁶. A combination of these two methods is likely the direction of future work.

2.4.2 Biochemical Methods

Delayed gadolinium enhanced MRI (dGEMRIC) is another method of assessing cartilage *in vivo*. In this method gadolinium, a contrast agent, is injected into the patient and over time it diffuses into the articular cartilage. The contrast agent distributes itself inversely to the concentration of glycosaminoglycans (GAG), a component of cartilage associated with cartilage stiffness. GAG concentration of the cartilage can be determined from this inverse relationship (Figure 2.9). The dGEMRIC method has been used in many cartilage and OA studies and is an important tool in understanding the degeneration of cartilage on a molecular level.

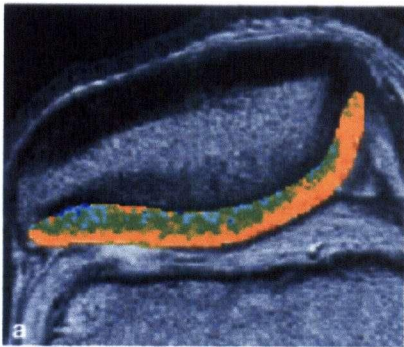


Figure 2.9: The distribution of gadolinium in the patellofemoral joint measured using the dGEMRIC protocol. Gadolinium distributes inversely to glycosaminoglycans. Ref Burstein 2001

2.5 Three-Dimensional *in vivo* Patellar Tracking

Researchers and physicians suspect that abnormal patellar tracking plays a role in patellofemoral OA. An early hypothesis was that tilting of the patella produced a hyper-pressure on the lateral compartment causing pain (Figure 2.10)⁷⁴.

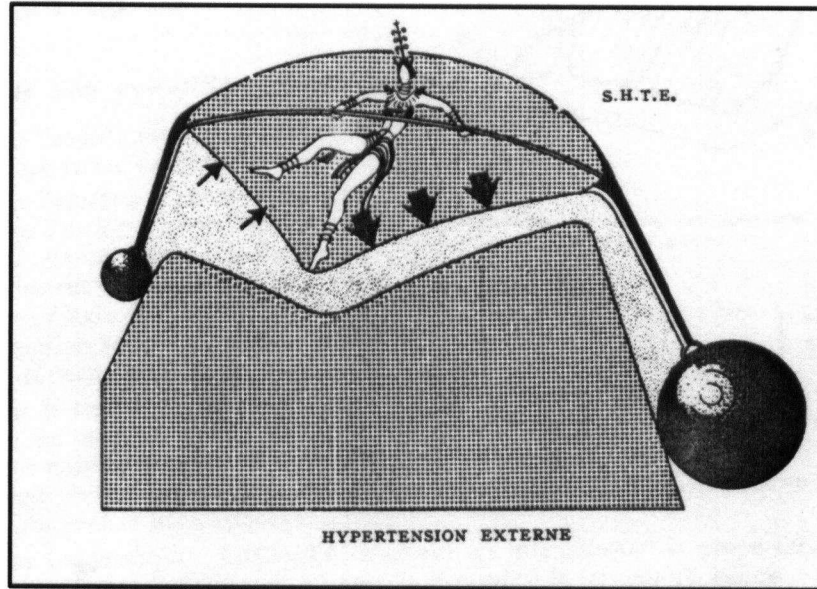


Figure 2.10: Hyper-pressure syndrome of the patella as described by Ficat *et al.* An excess pressure in the lateral compartment may be associated with anterior knee pain. Ref Ficat 1975

This work motivated other groups to study patellar kinematics. However, due to imaging limitations the patella was only studied in two dimensions and one position of knee flexion by means of skyline or sunrise radiographs. As new imaging technology became available, such as MRI, CT and ultrasound, patellofemoral kinematics were studied in more detail, first *ex vivo* and then *in vivo* with both invasive and non-invasive techniques. These methods are all very computationally intensive. The strength of these new methods is that we can now study patellofemoral kinematics in three dimensions and can describe patellar motion completely as medial-lateral translation, anterior-posterior translation, proximal-distal translation, flexion, tilt (internal/external rotation) and spin (varus/valgus rotation) (Figure 2.11). In order to replicate patellar motion in activities of

daily living such as walking, climbing up and down stairs and sitting in a chair some type of load must be applied to the joint when measuring patellar kinematics.

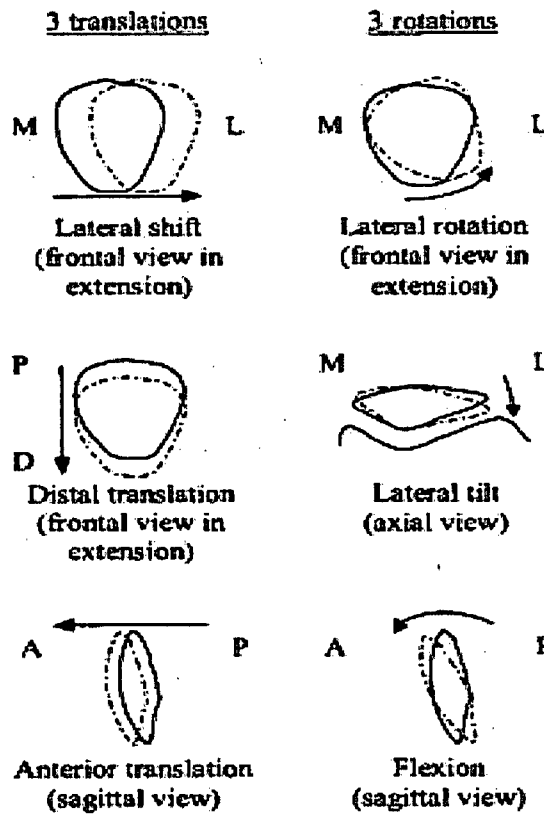


Figure 2.11: Patellar kinematics, 3 translations and 3 rotations. Katchburian, 2003

2.5.1 Invasive Methods

Patellar kinematics have been measured *in vivo* using invasive techniques such as photogrammetry¹⁸¹ or intracortical pins^{111,114}. The photogrammetry, often referred to as RSA, technique requires radio-opaque markers to be inserted in the bone. The joint is then x-rayed in a bi-planar reference frame at the position of the bones at various points in time be determined. Veress et al used this technique to study a group of 4 volunteers who had undergone high tibial osteotomy. 3 steel balls were surgically implanted, one in

the patella and one in each femoral condyle, and x-rays in the axial and sagittal view were taken of the volunteer's knee joint at intervals of 30° from 0 to 90° while they were lying prone and pushing isometrically on a loading rig. The patella tended to shift inferiorly but patterns of tilt were not as constant within the volunteers. No other kinematic parameters were reported. This study was limited by the limited number of balls and problems imaging the balls in some of the images. Three-dimensional quantities were not assessed.

The intracortical pin technique entails bone pins being drilled into the femur, tibia and patella. One study assessed one male volunteer with no history of knee pathology¹¹¹. Intracortical pins were inserted into the anteriolateral aspect of the patella, the medial condyle of the femur and the medial aspect of the tibia, slightly proximal to the tibial tuberosity. Optoelectric markers were attached to each pin and the volunteer performed various tasks while seated, while standing and while squatting. Kinematic data were acquired using a four camera system and joint kinematics were derived. It is obvious from this and from photogrammetry studies that non-invasive patellar tracking techniques are much more practical as there is no risk of pain or infection.

2.5.2 Non-invasive Imaging Methods

Groups have experimented with CT, ultrasound and optoelectronic systems for assessing patellar kinematics. The advantages of these other approaches are that they do not have the size constraint of traditional MR scanners, nor the complication of metal artefacts when imaging or when building rigs to be used in the studies. For example, Asano et al conducted a study using CT which assessed the knee from 0 to 120°. A

limitation of this technique however is the ionizing radiation exposure⁵. Another technique utilized ultrasound sonography which has the advantage of being less expensive than CT or MRI¹⁶³. This study found that the method had a mean error of 1.4 ± 3.2 mm. Lastly, Lin et al conducted a study in 12 healthy subjects using a clamp which mounted on the patella and an optoelectric system^{119,120}. This method has a range of motion of 20° and displayed kinematic results consistent with the literature. This study is limited by possible movement of the clamp, the altered mechanics that clamping might cause and that skin markers were used to define the femoral and tibial coordinate systems. These three novel examples of assessing patellar tracking have potential however they are not as advanced as the MRI methods as of yet.

2.5.3 Non-invasive Methods using MRI

MRI is the most commonly used imaging modality for assessing patellar kinematics. The risk to the volunteer is minimal because there is no ionizing radiation exposure. Also, different MR sequences allow for optimal imaging of different tissues depending on the application. For example, if joint kinematics are being assessed, a sequence optimized for bone will be applied.

One group developed an MRI-based technique of measuring three-dimensional patellar kinematics *in vivo*⁶⁷. In this method a geometric model of the joint is created from a high-resolution MR image using a T1-weighted spin echo sequence on a 1.5T scanner. Contours of the bone at 5 angles of loaded knee flexion are created from fast (under 1 minute), low-resolution MR images. The load applied during the low-resolution scans was approximately 100 N. The contours are matched to the geometric model using

an iterative closest points algorithm. Three-dimensional patellar kinematic parameters of flexion, internal/external spin, tilt, proximal translation, lateral translation and anterior translation are derived using the coordinate system described in Section 4.4. Tibiofemoral kinematics are also assessed with this method. One strength of this method is that it has been rigorously validated for both accuracy and precision (repeatability)^{66,67}. The accuracy study was carried out by comparing results using the MRI based technique to results obtained using bi-planar x-rays and CT in three cadaver knees. The results of the accuracy study found an error of 1° for rotations and 0.88 mm for translations. The repeatability study was carried out in three volunteers and both intra-observer and repositioning error were assessed and found to be less than 3° for rotations and less than 2.5 mm for translations and less than 2.15° for rotations and less than 0.7 mm for translations, respectively. A study of individuals undergoing high tibial osteotomy found that after the surgical treatment tibiofemoral and patellofemoral joint kinematics were altered⁹¹. Specifically, the subjects showed a 6.5° decrease in mean tibial adduction, a 0.8 mm decrease in lateral tibial translation, a 5.1° decrease in patellar flexion and a 1.2° decrease in patellar spin and a 1.6° increase in mean medial patellar tilt and a 4.2 mm increase in proximal patellar translation. These changes alter the loading pattern at the joints. A strength of this method is that allows individuals with knee pathologies to be assessed because the imaging time in loaded flexion is short, in contrast to other methods that require individuals to hold the loaded position for 6 minutes¹³⁵.

Another *in vivo* method of measuring patellar kinematics in weight-bearing also measured contact areas in the patellofemoral joint¹³⁵. Normal patellar tracking was studied 10 healthy volunteers (mean age 30). A sagittal image was taken to measure

tibiofemoral flexion. An axial spoiled gradient echo MR sequence was taken on a 1.5 T scanner in order to visualize both the bone and soft tissue at the patellofemoral joint. In particular, 5 images at angles of knee flexion ranging from -10° to 60° . A 13.61kg load was applied to the knee using a foot plate attached to a pulley system. Five kinematic parameters were assessed (3 rotations, medial-lateral and proximal-distal translations). Details on the coordinate system used to define the kinematic parameters were not given. The patellar translations and rotations were calculated with respect to the femur in the extended position. The transformation matrices used to measure the movement from the extended position were measured by registration using *Analyze* software (Mayo Clinic, Rochester, MN). An accuracy of 1.5 mm for translations and 3° for rotations was reported however the validation was carried out by measuring the orientation of a phantom (an invisible goniometer and four vials of gadolinium saline solution). Contact area was measured using B-splines and then calculated the centroid of the line on each slice in order to track the contact area through the range of flexion. This study showed that through the range of tibiofemoral flexion the patella translated inferiorly and medially, flexed at similar angles as the tibiofemoral joint, tilted medially with a peak at 30° and returning to the original position at 60° , and rotated externally by an average of 2° at 30° of tibiofemoral flexion. The contact area increased from a mean of approximately 200 mm^2 at 0° to approximately 560 mm^2 at 60° and it tended to move medially mirroring and surpassing the movement of the patella, inferiorly until 60° and posteriorly with the femoral condyle curve¹³⁵. Limitations of this study include the small field of view making measurement of tibiofemoral flexion difficult, the static loading condition and lack of reporting the anterior-posterior translation which is important when

defining ‘normal’ kinematics. Also, the volunteers had to hold the weight-bearing position for over 6 minutes which may be difficult if the method is extended to pathological knees.

Open MR is a valuable tool for studying the patellofemoral joint in deep flexion. The range of knee flexion that can be studied at is not limited by the size of the traditional MR scanner’s bore^{176,182}. One study examined the patellofemoral joint of 10 healthy volunteers at 30° and 90° of flexion in an open MR. The knee was loaded by applying a 10 Nm torque to the lower third of the shank. 2D and 3D sulcus angles (β), patellofemoral angle (between S and F), patellar shift (displacement between P_{max} and C) and tilt angle (α) were assessed with respect to a patellar based coordinate system (Figure 2.12).

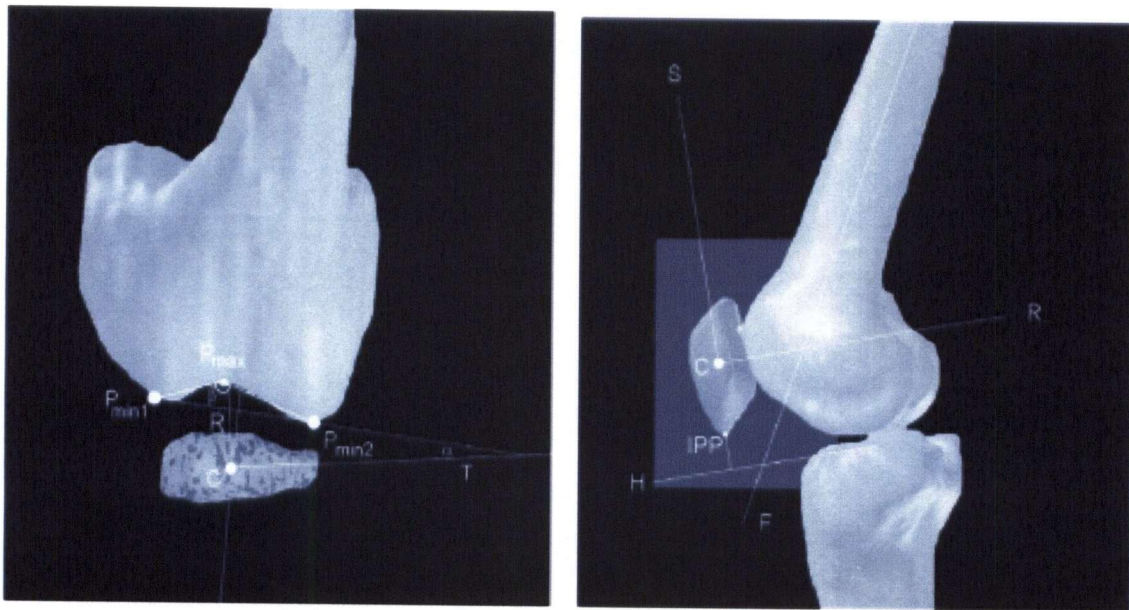


Figure 2.12: Coordinate system used by von Eisenhart-Rothe et al, 2004.

The repeatability of the method was found to be between 1.2% and 8.3% (CV%). No data have been published regarding the accuracy of the method. They found differences in patellar height (anterior-posterior translation), flexion, tilt and lateral shift between 30°

and 90°. Limitations of this study include the lower resolution images due from the low field open MR (0.2T as opposed to 1.5 T of a normal MR), the omission of kinematic analysis in the coronal plane and the static loading condition. In a second open MR study, volunteers stood in the open MR scanner while images were taken from full extension to 60° or 70°. The only kinematic parameters studied were medial-lateral translation and tilt. A lateral translation through the range of flexion in 6 subjects bilaterally and 7 subjects unilaterally and a tilt in 3 knees in hyperextension and 5 knees at 0° was found. The kinematic parameters were assessed qualitatively and no information regarding accuracy or precision was reported.

Cine phase and fast phase contrast MRI is a dynamic means of assessing joint kinematics *in vivo*^{23,160}. Cine phase contrast MRI (cine-PC MRI) is the combination of cine MRI and phase-contrast MRI. Cine MRI collects data at specified time points. Phase-contrast MRI provides the velocity components of the phase signal (x, y, z) associated with the anatomical images. The combination of the two techniques allows specific anatomical points to be tracked over time. One group used cine-PC MRI as well as a newer version of this method called fast PC-MRI (which uses segmented phase encoding) to study patellofemoral and tibiofemoral kinematics¹⁴⁸. In this method the volunteer lies prone in the MR scanner and bends and extends his or her lower leg in time with a metronome throughout the scan. Three different sets of scans are taken. The first is an axial slice at the femoral condyle level in order to select the second which is in the sagittal or oblique sagittal plane (this is the cine- or fast-PC scan which takes approximately 5.5 and 3 minutes, respectively) from which the kinematics are derived and last is 3 axial scans at the femoral epicondyle, midpatellar and tibia 2 cm below the

patellar tendon insertion. Kinematics can then be derived with minimal manual input, i.e. the task of bone segmentation from each image slice is eliminated, the only task of the user is to identify specific anatomical points to create the coordinate system (Figure 2.13).

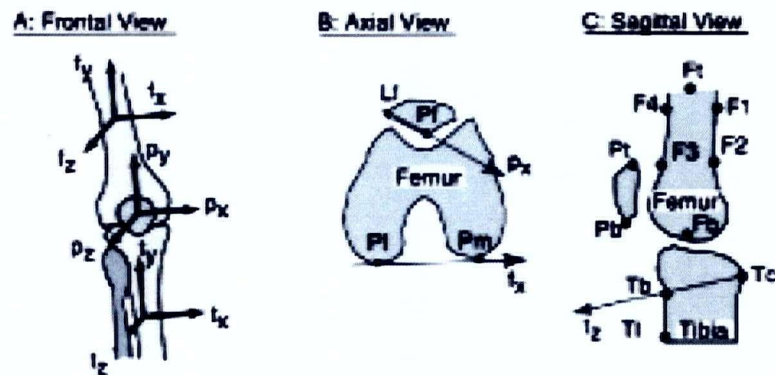


Figure 2.13: Anatomical coordinate system assignment, Sheehan et al 1998.

Accuracy for the method was assessed using a motion phantom (a gelatine doped plate) that moved at a known velocity. The accuracy using the phantom was less than 0.7 mm for in plane motion and 4.0 mm for out of plane motion (Sheehan 1998). The precision of cine-PC MRI was reported to be 0.46 mm and 0.21° and the subject inter exam variability is 1.6° to 2.4° for fast-PC MRI and 2.4° to 6.1° for cine-PC MRI¹⁴⁸. Limitations of this method are that there is little or no resistance during the motion. Even though the muscles are active, the method does not simulate activities of daily living. Motion artefact can result in the images if changes in speed occur within a cycle. Motion outside of the plane of motion cannot be accurately quantified. People with knee pathology may not be able to carry out the knee motion over extended periods of time.

2.5.4 Summary of MRI-based Methods

Many groups use MRI to assess patellar kinematics *in vivo*. Differences in coordinate axes assignment, loading direction and angles of tibiofemoral flexion studied create difficulties in comparing results of studies (table 2.3). Further, differences in methods of validation raise questions as to the accuracy of the reported results.

Method	MR Technique	Loading	Range of Flexion	Kinematic Parameters Measured	Validation
Fellows et al	Closed Bore MRI	axial ≈100 N	0° to 45°	1. flexion 2. spin 3. tilt 4. anterior translation 5. proximal translation 6. lateral translation	Accuracy: Cadaver study - < 1° and < 0.88 mm Repeatability: < 3° and < 2.5 mm (intra-observer) < 2.15 and < 0.7 mm (repositioning)
Patel et al	Closed Bore MRI	Axial ≈ 130 N	-10° to 60°	1. flexion 2. spin 3. tilt 4. proximal translation 5. lateral translation 6. inferior tilt	Accuracy: Orientation Phantom – < 3° and < 1.5 mm Repeatability: none reported for patellar kinematics, for tibiofemoral kinematics 3.8 to 15.6 CV % (intra-observer) and 6.3 to 26.0 CV % (inter-observer)
Von Eisenhart-Rothe et al	Open MRI	Torque 10 Nm	0°, 30°, 90°	1. tilt 2. lateral translation	Accuracy: None Repeatability: error between 1.2 and 8.3 CV%
Sheehan et al	Cine-phase MRI	none (fast-PC) 34 N (cine-PC)	10° to 30°	1. flexion 2. spin 3. tilt	Accuracy: Motion Phantom- in-plane < 0.7mm, out of plane < 4.0mm Repeatability: < 0.46 mm and < 0.21° (precision), 1.6° to 2.4° (fast-PC inter-exam variability), 2.4° to 6.1° (cine-PC inter-exam variability)

Table 2.3: Summary of in vivo MRI based techniques for assessing patellar kinematics.

2.6 Summary

1. The local biomechanical environment at the patellofemoral joint is a very complex interaction between geometry, cartilage health, three-dimensional patellar kinematics, contact areas and contact stresses. It is likely that the local biomechanical environment contributes to the onset and progression of pathologies at the patellofemoral joint.
2. Knee OA is a disease characterized by pain and limited mobility to its sufferers and there is no known cure. The patellofemoral joint is involved in approximately half of knee OA cases. Identifying risk factors of OA is important in the development of treatment strategies to arrest the onset and progression of OA.
3. OA can be defined radiographically or clinically. Radiographic OA is characterized by the presence of osteophytes, joint space narrowing and sclerosis. Clinical OA is determined by physical examination and questionnaires.
4. Cartilage cannot be imaged using conventional radiography. Therefore specific feature of cartilage degeneration cannot be identified.
5. Varus and valgus alignment are associated with the progression of patellofemoral OA in a compartment specific manner. Varus alignment is associated with medial OA progression and valgus alignment is associated with lateral OA progression. Alignment explains only some isolated compartmental progression. The affect of malalignment on the local biomechanical environment of the patellofemoral joint is not clear.
6. qMRI is a method of measuring cartilage morphology *in vivo*. Features such as cartilage thickness, volume, surface area and denuded area can be quantified. qMRI

allows each cartilage plate to be assessed individually and specific regions of cartilage degeneration to be identified.

7. Three-dimensional patellar kinematics can now be assessed accurately and non-invasively *in vivo* using MR imaging techniques. Assessing patellar kinematics provides important information regarding the local biomechanical environment at the patellofemoral joint.

Chapter 3: Methods A – Patellofemoral Cartilage Morphology

3.1 Introduction

We will use quantitative MRI (qMRI) to assess cartilage morphology at the patellofemoral joint in order to answer research questions number 2 and 3. qMRI is a validated method of assessing cartilage morphology in individuals with osteoarthritis (OA). In qMRI cartilage thickness, volume and surface area, among other parameters, can be assessed from MR images. qMRI is becoming a key tool used in the most recent and comprehensive osteoarthritis studies. Parameters calculated with qMRI are area of bone/cartilage interface, cartilage surface area, cartilage volume and mean cartilage thickness. Other parameters relevant to OA can be derived from these. In this study, we used qMRI to assess total, medial compartment and lateral compartment cartilage morphology of the patella and femur at the patellofemoral joint.

We used a manual segmentation technique and a touch-sensitive screen to delineate cartilage areas from the MR images. One limitation of qMRI is the labourious manual segmentation process (identifying cartilage on images) and although semi-automated techniques are being developed, time savings of only 15% (or about 10 minutes per dataset) are being realized^{27,172}. New input devices, such as digitizing tablets and touch-sensitive screens, have the potential to speed up the manual segmentation process. These new input devices have not been assessed in the context of qMRI. We compared the new input devices to a traditional mouse, which is most commonly used in manual segmentation, in terms of time, precision and percentage difference between devices.

“Section 3.2 of this chapter has been accepted for publication. McWalter EJ, Wirth W, Siebert M, von Eisenhart-Rothe R, Hudelmaier M, Wilson DR, Eckstein F. Use of novel interactive input devices for segmentation of articular cartilage from magnetic resonance images. *Osteoarthritis Cartilage* In Press”

3.2 Input Device Study

In this study, we compared cartilage segmentation time, precision (reproducibility) and measurement consistency for three input devices (mouse, digitizing tablet, touch-sensitive screen). The comparison was made by following the progress of an individual, myself, being trained to segment cartilage in order to avoid user bias towards one input device. Two new interactive computer input devices were compared to a traditional mouse (Optical Mouse, Logitech, Fremont, California). The first device was an interactive digitizing tablet (Graphire3, Wacom, Krefeld, Germany), which consists of a 4 x 5 inch active region within which the user writes with an electronic pen. Each point in the active region corresponds to a point on the screen in a scaled down manner. The tablet enables the user to navigate the cursor throughout the workspace by drawing and clicking within the active region. The second device was an interactive touch-sensitive screen with a 1280 x 1024 pixel matrix (Cintiq 18SX, Wacom, Krefeld, Germany). The user segments directly on this screen using an electronic pen similar to the one used with the digitizing tablet. The screen can be angled from an upright to a horizontal position to suit the user's preference.

3.2.1 Subjects and Imaging

We used each of the three devices to process MR images of the knee from 12 subjects using a qMRI technique⁸⁵. Six of the images were from six individuals with no history of knee symptoms and signs (3 females, 3 males, mean age 23.3 ± 2.1 years) and six of the images were from six individuals with severe knee osteoarthritis (6 females, mean age 66.8 ± 7.2 years). Two sets of images were acquired in each subject, one in the axial plane

and one in the coronal plane^{28,28,55,55,78,78,85,179,179}. Images were acquired using a T1 weighted fast low angle shot (FLASH) 3D gradient echo sequence with water excitation, which has been previously validated in terms of technical accuracy^{28,28,85} and reproducibility upon repositioning^{28,54,54,55,55,85,85,101,101}. For the individuals with no history of knee problems a 1.5 T Siemens Magnetom Vision scanner was used and the MRI parameters were as follows: repetition time (TR) = 17.2 ms, echo time (TE) = 6.6 ms, and flip angle (FA) = 25°. For the individuals with knee OA a 1.5T Siemens Symphony Quantum scanner was used and the MRI parameters were as follows: TR = 19ms, TE = 8.6 ms, and FA = 20°. For all images the in plane resolution was 0.31 mm x 0.31 mm, the slice thickness was 1.5 mm, the pixel matrix was 512 x 512, and the field of view was 16 cm. The acquired image is anisotropic, therefore to obtain an isotropic representation of cartilage an interpolation algorithm is applied to the volume (described in Section 3.3.3.1).

3.2.2 Image Analysis

With no previous experience in cartilage segmentation, I received preliminary training with the proprietary software created specifically for cartilage segmentation¹⁸⁷ and an introduction to established, validated protocols prior to performing the cartilage segmentation with all three devices. I was allowed one week to become familiar with the input devices. In contrast to previous studies which apply semi-automated techniques¹⁷³, segmentation was performed using a fully manual technique in this study. For each acquired dataset from the normal subjects, the cartilage from the patella was segmented three times (once with each input device) within one sitting. To avoid bias associated

with user training or fatigue, the order in which the input devices were used within the sitting differed for each dataset (Table 3.1). All six possible orders were used. The order in which the datasets were segmented was not varied to ensure that the user did not recall features of the particular dataset; if the same dataset is segmented last in one session and first in the next a bias would be introduced.

dataset	Session 1	5 days	Session 2
1	abc	→	abc
2	bca	→	bca
3	cab	→	cab
4	acb	→	acb
5	cba	→	cba
6	bac	→	bac

Table 3.1: Investigator schedule for cartilage segmentation. a = interactive digitizing tablet, b = interactive touch-sensitive screen, c = traditional mouse. Session 1 was completed in its entirety before session 2 commenced.

To limit bias associated with familiarization with the dataset, the user thoroughly studied each dataset before beginning the session. Once all six datasets had been segmented (session 1), segmentation was repeated (session 2) according to the schedule found in Table 3.1, which dictated a five day interval between datasets. The entire process was then repeated for the six normal medial tibiae (coronal images), the six OA patellae (axial images), and the six OA medial tibiae (coronal images). The patellar and medial tibial cartilage plates were selected to represent the segmentation of cartilage in the axial and coronal views, respectively. Due to the labour intensive nature of manual cartilage segmentation it did not seem practical to segment more than one cartilage plate in each plane.

Once the segmentation was complete, quantitative descriptions of cartilage were obtained using established techniques. Cartilage volume was calculated by numerically

integrating of all segmented voxels (Section 3.3.3.1)^{52,52,139}. Mean cartilage thickness calculations were made using a three-dimensional Euclidean distance transformation (Section 3.3.3.2)^{171,187,187} and surface area calculations made using a triangulation technique (Section 3.3.3.3)^{95,95,187}.

3.2.3 Statistical Analysis

We compared the input devices using the following three parameters: 1) Time required for segmentation, 2) consistency between devices for volume, mean thickness and surface area results, and 3) precision (reproducibility) of the analysis of cartilage morphology.

The time spent to segment each cartilage plate (i.e. patella or medial tibia) for each subject (n=12) was recorded for each device in each session. The mean and standard deviation of the segmentation time were calculated for each input device. Only the times recorded for session 2 were used in the analysis of time because session 1 was considered an orientation session. We tested the null hypothesis that there was no significant difference in segmentation time between devices with a Wilcoxon Signed Rank Test. The Wilcoxon Signed Rank Test is a non-parametric version of a t-test and is therefore suitable in this situation as a normal distribution of results could not be assumed for the small samples in this study.

We compared volume, surface area and mean thickness calculations (mean of sessions 1 and 2) made after segmenting for all three input devices. We tested the null hypothesis that there were no significant differences between input devices for measured volume, surface area and mean thickness again using a Wilcoxon Signed Rank Test.

The precision of each input device was determined by calculating the root mean square (RMS) of the coefficient of variation expressed as a percentage (CV%) and RMS standard deviation⁸⁰ (n=6) of cartilage volume, surface area, and mean thickness between the two sessions. We tested the null hypothesis that there were no significant differences in precision errors between the input devices with a Wilcoxon Signed Rank Test.

3.3 Cartilage Morphology of Individuals with Varus/Valgus Alignment

3.3.1 Image Acquisition

Axial MR images of each subject's symptomatic knee were acquired using a 1.5 T General Electric Signa MR scanner (Figure 3.1). The symptomatic knee was the one the subject identified as being more severely affected by OA. The participant lay supine with the leg in a relaxed position and the knee flexed to approximately 30°, measured with an MR safe goniometer (which has an error of 10° to 15°). The knee was flexed in order to include both the patellar and femoral patellar groove cartilage of the patellofemoral joint within a 16 cm x 16 cm field of view. A receive-only cardiac phased array coil was used because its flexibility allowed for knee flexion (the knee coil could not accommodate flexion). This coil also allowed for the positioning of saline filled plastic bags around the knee, which were used to obtain uniform fat suppression and to enhance signal to noise ratio. The MR sequence used was a three-dimensional T1-weighted spoiled fast low angle shot (FLASH) with fat suppression, a sequence that is optimized for quantitative analysis of cartilage and that is the most commonly accepted and used for qMRI⁷⁹. The data were collected with a matrix of 256 x 256 pixels, the data were interpolated to 512 x 512 within the GE software. The cardiac coil did not allow for the image to be collected at 512 x 512 initially. A 512 x 512 matrix is desirable for carrying out cartilage segmentation. The slice thickness was 1.5 mm and had an in-plane resolution of 0.31 mm (after interpolation), the repetition time was 21.4 ms, the echo time was 4.2 ms, the flip angle was 20° and the scan time was 7 minutes and 40 seconds for 1 repetition (Table 3.2).

Parameter	Image Parameters
Slice thickness	1.5 mm
In-plane Resolution	0.31 mm
Repetition Time (TR)	21.4 ms
Echo Time (TE)	4.2 ms
Flip Angle (FA)	20°
Number of Excitations (NEX)	1
Field of View (FOV)	160 mm
Matrix Size	512 x 512
Time	7 min 40 s
Coil	Cardiac

Table 3.2: qMRI imaging parameters.



Figure 3.1: MRI image of patellofemoral joint cartilage using a T-1 weighted FLASH 3D sequence with fat suppression.

3.3.2 Cartilage Segmentation

The cartilage was segmented from the MR images using a custom, proprietary software package (Chondrometrics GmbH, Munich, Germany) and an interactive touch-sensitive screen (Cintiq 18SX, Wacom, Krefeld, Germany). Segmentation refers to the

process of classifying pixels according to the type of tissue they represent. In this case the segmented pixels represent cartilage. First the images were converted from the DICOM or .dcm format to a proprietary .chm format using a program called CHM Read. The .chm file contains all information in the original DICOM file and documentation of every modification made to the dataset, i.e. all of the information regarding the segmented Sections of the image is saved in this file.



Figure 3.2: The Cintiq 18SX by Wacom, a touch-sensitive screen on which the user can write with a digitizing pen to move the cursor through the workspace. Ref: <http://www.wacom.com/lcdtablets/index.cfm>

CHM Works was used for the manual segmentation of the patellar and femoral cartilage. The touch-sensitive screen, Cintiq 18SX (Wacom, Krefeld, Germany), allows the user to navigate about the desktop using a digitizing pen, as seen in Figure 3.2. It provides a more comfortable method of manual segmentation than the mouse and reduces segmentation time by approximately 15% (see Section 3.3 for details)¹²⁷. This finding was obtained as a result of a study we carried out and a description of it can be found in Section 3.3. In this method of manual segmentation each slice was studied in a sequential manner to identify the bone/cartilage interface. Specifically, the user manually draws a line along the bone/cartilage interface on each slice. The segmented line is one

pixel thick and is colour coded green (Figure 3.3). A second sequential pass of the slices was then carried out to identify the cartilage surface. The user draws a single pixel line along the cartilage surface (articulating surface) which is colour coded pink (Figure 3.3). The area between the bone/cartilage interface line (green) and the cartilage surface line (pink) was identified as cartilage. This process was carried out for the patellar cartilage and then for the femoral cartilage. A description of how the segmented cartilage was divided into medial and lateral compartments can be found in Section 5.5.2.

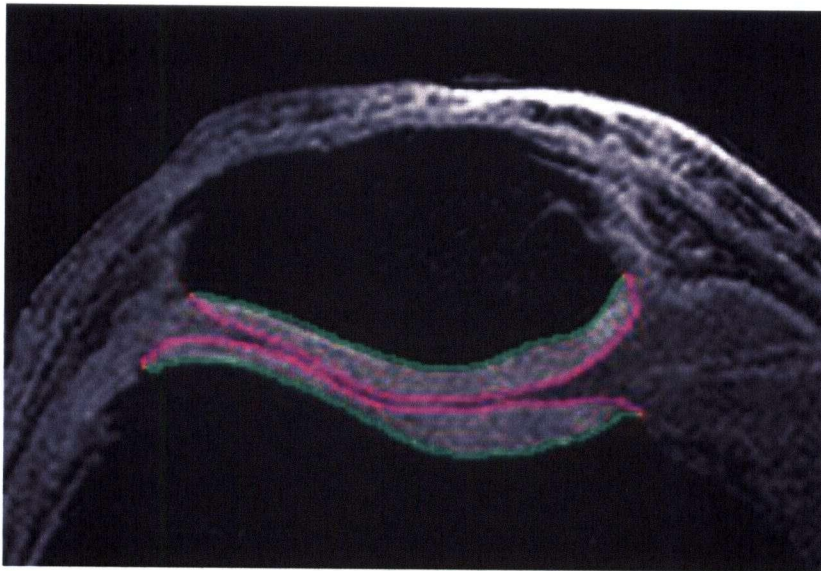


Figure 3.3: Manual Cartilage Segmentation. The green line indicates the bone cartilage interface and the pink line indicates the cartilage surface. Both patellar and femoral cartilage was assessed.

Cartilage segmentation involves judgement by the user, especially in the case of osteoarthritis where there are often defects in the cartilage and osteophytes present. For this reason, whenever doubt existed an anatomist (a medical doctor who specializes human in anatomy) was consulted. Once the segmentation was complete, the

segmentation of each dataset was verified by an anatomist very experienced in cartilage segmentation from MRI.

3.3.3 Assessment of Morphological Parameters

The .chm file containing the segmented cartilage information was then loaded into the calculation program. The program uses the area identified as cartilage on each slice and calculates morphological parameters. The primary calculated morphological parameters are volume, thickness and surface area. In osteoarthritic knees parameters such as percentage of cartilage coverage provides valuable information about the stage of the osteoarthritis present. The areas identified during segmentation are processed using various algorithms to extract the desired morphological parameters.

3.3.3.1 Volume

Volume of the patellar and femoral cartilage was assessed using a shape-based interpolation method¹⁴⁶. This algorithm was developed to allow calculation from objects for which the in-plane resolution is not equal to the slice separation. The interpolation step creates isotropic volume information and can be carried out before or after segmentation. By carrying out the interpolation step after segmentation, segmentation time is drastically reduced, as fewer slices require segmentation. The steps involved in the interpolation algorithm are as follows:

1. The bone/cartilage interface line and cartilage surface line defined during cartilage segmentation was described as a series of points.

2. A line was drawn between a point on one slice and the nearest point on the adjacent slice.
3. A three-dimensional surface was created for the bone/cartilage interface and the cartilage surface according to the lines drawn between adjacent slices (Figure 3.4).
4. An isotropic binary volume was created. The edge voxels were determined from the three-dimensional surfaces.
5. The volume was determined by the numerical integration of voxels in the isotropic binary volume.

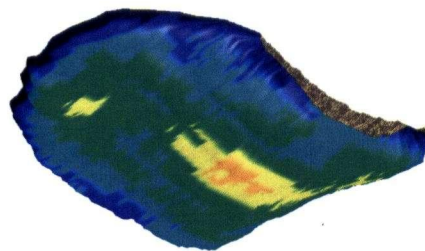


Figure 3.4: Three-dimensional representation of a patellar cartilage plate. The bone/cartilage interface (top) and cartilage surface (bottom) have been created using the shape-based interpolation algorithm. The differences in colour indicate regions of differing cartilage thickness (yellow thickest, dark blue thinnest).

3.3.3.2 Thickness

Thickness of the patellar and femoral cartilage was assessed using a three-dimensional Euclidean distance transformation (EDT) algorithm^{18,170}. The strength of the EDT lies in the efficiency and accuracy it achieves when compared to other algorithms used for this application, which often entail computing all the normal vectors of a discrete surface. It does however act on two three-dimensional surfaces (the bone/cartilage

interface surface and cartilage surface), therefore the edge interpolation step described in Section 3.2.2.1 must be first carried out. The algorithm progresses as follows:

1. A shape-based interpolation was used to define the three-dimensional bone/cartilage interface and cartilage surface.
2. A binary assignment system was used to identify voxels belonging to the cartilage.
3. Each voxel is encoded with the minimal distance normal to the nearest bone/cartilage interface voxel. These distances were defined by passing a series of local 3D coordinate masks containing local distance vectors over the data volume and then recalculating the global distance for each one.
4. Cartilage thickness was determined by reading the distance values of the cartilage surface voxels.
5. Mean cartilage thickness was determined by finding the mean of all thickness values.

3.3.3.3 Surface Area

Surface area for the bone cartilage/interface and the cartilage surface were assessed for the patella and the femur. The measurement of surface area of the cartilage was based on a triangulation technique which uses information from the Euclidean distance transformation⁹⁴. The algorithm is as follows:

1. A triangle was created for each point on the surface with its nearest neighbour (on the same slice) and closest point on the next adjacent slice.
2. The surface area was calculated by integrating the size of all triangles.

3.3.4 Measured Parameters

Other morphological parameters were extracted using the volume, thickness and surface area algorithms. The morphological parameters assessed in this study are listed below and the unit of measurement of each is shown in table 3.3.

1. **Area of Bone/Cartilage Interface**– The bone/cartilage interface is the surface at which the bone and cartilage meet. It is an important parameter in determining the size of the particular joint and is used to normalize size dependent variables. The surface area algorithm was used to calculate bone/cartilage interface (Section 3.2.3.3).
2. **Cartilage Surface Area**– Cartilage surface area refers to the area of the cartilage adjacent to the synovial fluid. In osteoarthritic knees, areas of bone without cartilage coverage are taken into consideration. This measure is dependent on joint size. The surface area algorithm was used to calculate cartilage surface area (Section 3.2.3.3).
3. **Cartilage Volume** – A three-dimensional measure of the amount of cartilage in the particular cartilage plate. This parameter is dependent on the size of the bone itself. Cartilage volume was calculated using an interpolation algorithm (Section 3.2.3.1).
4. **Normalized Volume**– This parameter is calculated by dividing cartilage volume by bone/cartilage interface area. This parameter is sometimes considered a surrogate measure of mean cartilage thickness, however the thickness assessed is not necessarily normal to the bone/cartilage interface.
5. **Mean Cartilage Thickness**– The mean of the thickness measurements taken over the entire volume of cartilage. This measurement is taken normal to the bone/cartilage interface using a Euclidean distance transformation algorithm (Section 3.2.3.2).

6. Percentage Cartilage Coverage – This parameter is important in osteoarthritic knees because it describes the amount of bone that still has cartilage coverage. When segmenting the cartilage surface any regions that are not covered in cartilage are identified along the bone/cartilage interface. Percentage cartilage coverage can then be calculated by dividing the area of the covered bone/cartilage interface by the total bone/cartilage interface.

Parameter	Unit of measurement
Bone/Cartilage Interface:	cm ²
Surface Area:	cm ²
Volume:	mm ³
Normalized Volume:	mm
Mean Cartilage Thickness:	mm
Percentage Cartilage Coverage:	-

Table 3.3: Units of measurement for cartilage morphologic parameters assessed in this study.

3.3.5 Accuracy and Precision

The qMRI method has been validated for accuracy and precision in normal and osteoarthritic cartilage. Initially the volume, thickness and surface area calculation algorithms were validated using test objects or phantoms and knee joint cartilage data^{56,94}. The accuracy, precision and diagnostic value of the method as a whole has also been assessed in normal^{57,51,56,59,170} and osteoarthritic knees²⁷. Root-mean square (RMS) coefficient of variation (CV%) is used to define accuracy. In osteoarthritic cartilage the accuracy is $\pm 4.6\%$ for surface area, $\pm 8.9\%$ for cartilage thickness and $\pm 9.1\%$ for cartilage volume⁸⁴. Precision was defined as the root mean square (RMS) of the coefficient of variation expressed as a percentage (CV%) and RMS standard deviation. The precision (with a five day interval between segmentation) in normal knees has been found to be

$\pm 4.3\%$ for volume, $\pm 2.7\%$ for surface area and $\pm 4.4\%$ for cartilage thickness and in osteoarthritic knees has been found be $\pm 5.6\%$ for volume, $\pm 2.6\%$ for surface area and $\pm 6.1\%$ for cartilage thickness¹²⁷. qMRI of osteoarthritic knees appears to be less repeatable than normal cartilage. But the increased CV% is related to the relatively smaller amounts of cartilage as compared to normal knees. Therefore, the magnitude of the repeatability error is similar between normal and OA knees.

Chapter 4: Methods B – Three-dimensional Patellar Kinematics

4.1 Introduction

To answer research questions 1 and 3, we assessed three-dimensional patellar kinematics in individuals with knee osteoarthritis (OA) and varus or valgus malalignment using a novel, non-invasive MRI-based method developed by our group^{66,67}. We used the method to assess differences in patellar kinematics between the varus and valgus groups. The method consists of a series of imaging and post processing steps (Figure 4.1).

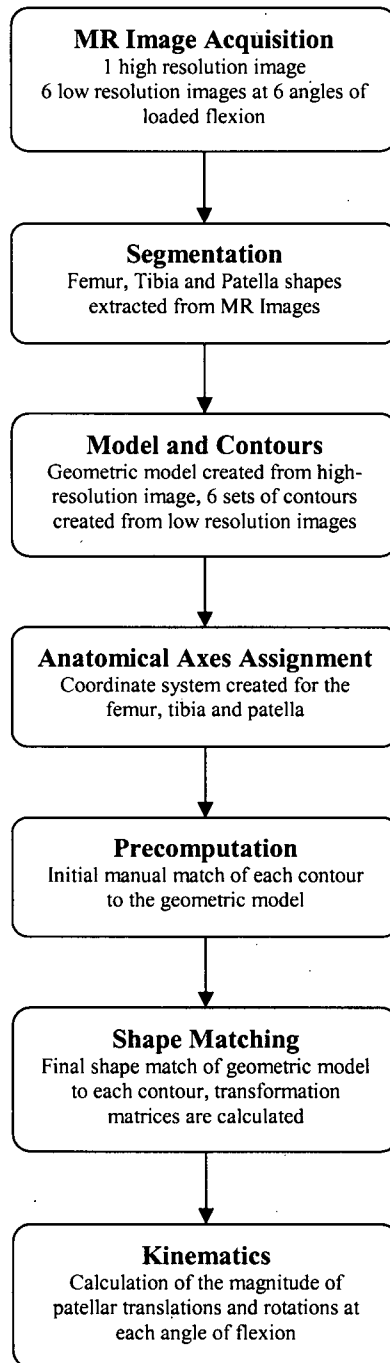


Figure 4.1: Flow chart of three-dimensional patellar kinematics method.

4.2 High-resolution Scan

One high-resolution MR scan of the knee joint in a relaxed, extended position was acquired in the sagittal plane with a T1-weighted spin echo sequence using a 1.5 Tesla scanner (GE Genesis-Signa, General Electric, LX, USA). The slice thickness of this scan was 2 mm and the in-plane resolution was 0.625 mm. Other imaging parameters can be found in table 4.1. The parameters have been optimized for time and image quality⁶⁵.

Parameter	High-Resolution Image
Slice Spacing	2 mm
In-plane Resolution	0.625 mm
Repetition Time (TR)	750 ms
Echo Time (TE)	21 ms
Flip Angle (FA)	90°
Number of Excitations (NEX)	1
Field of View (FOV)	320 mm
Matrix Size	512 x 512
Scan Time	10:20 min
Coil	Body

Table 4.1: High-resolution imaging parameters

The femur, patella and tibia were segmented from the high-resolution scan in a slice-by-slice fashion using Analyze software (Mayo Clinic, Rochester, MN). As mentioned in Chapter 3, segmentation refers to the process of classifying pixels according to the type of tissue they represent. In this instance we are identified the femur, tibia and patella. A semi-automated, region growing technique based on pixel intensity was used to identify the contours of each bone in each MR slice in which they appeared. Manual corrections were made to these contours to account for motion and intensity artefacts in the original image. The contour was then filled in to identify all the bony regions as a single intensity (Figure 4.2). Each bone was identified as a different object map. Visually, the distinction between object maps was colour coded: the femur in red, the tibia in green and the patella in yellow.

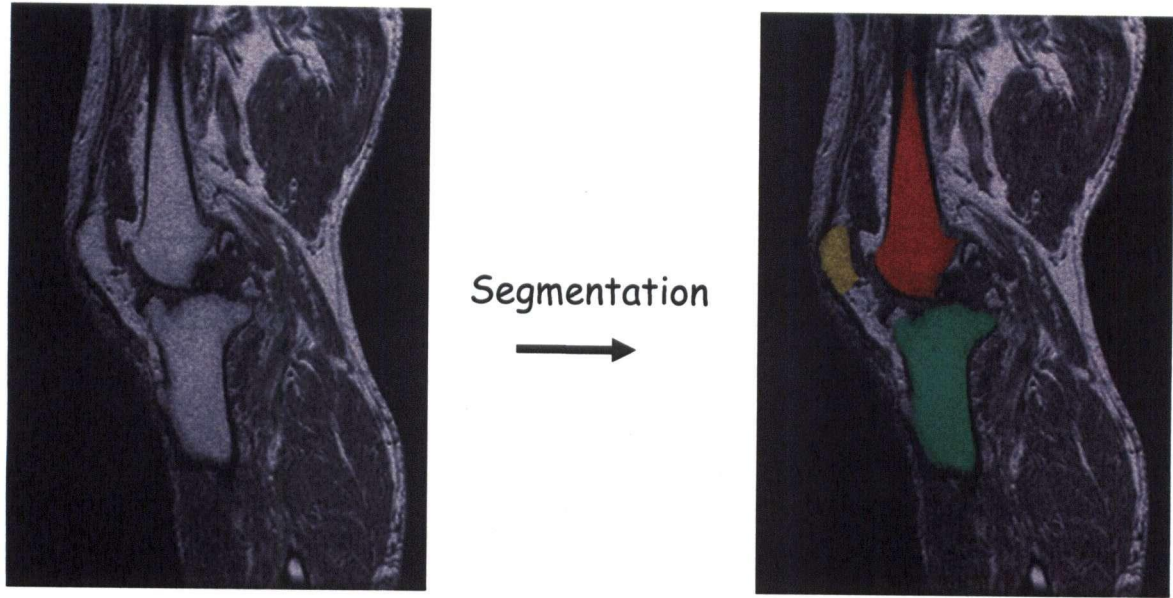


Figure 4.2: Segmentation of the femur (red), the tibia (green) and the patella (yellow) from one MR slice. The image on the left is the original image and on the right is the segmented image. Each slice in the MR dataset was segmented in this fashion.

Three-dimensional geometric models of the femur, tibia and patella were created using an adaptive deformation algorithm. The object map was imported into the surface extractor module of Analyze. This module creates a three-dimensional point cloud model from the object map of each bone using a built in algorithm. This algorithm initially fits polygons to the object map surface, essentially covering the spaces between the original segmented slices. The algorithm considers all of the edges of the polygons as individual springs attached together at the polygon nodes. The polygon edges are deformed in an iterative fashion, according to a mass-spring model, until the nodes reach an equilibrium position. The final position of the nodes approximates the surface of the object. The Cartesian coordinates of the nodes were imported into Matlab (The Mathworks, Natick, MA, USA) to create a three-dimensional point cloud model which describes the surfaces of the femur, tibia and patella (Figure 4.3).

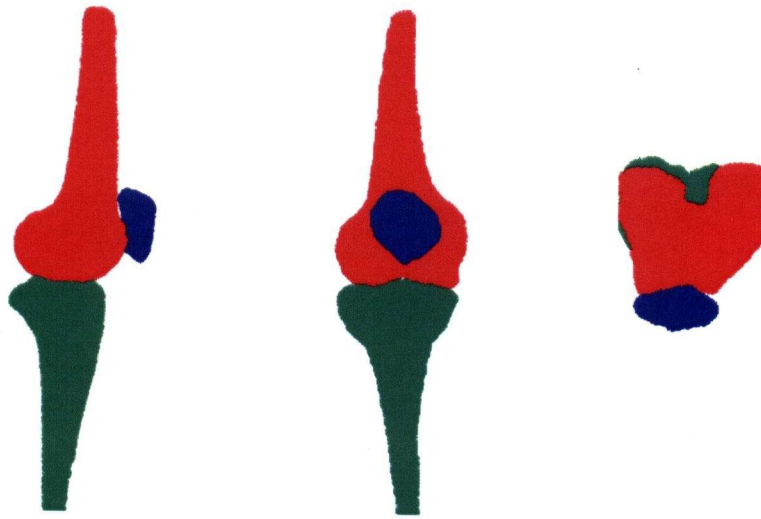


Figure 4.3: Three-dimensional point cloud model of the femur, tibia and patella. Left: sagittal view, Centre: frontal view, Right: axial view.

4.3 Loading Rig Design

An axial force in the leg was applied using a loading apparatus in order to simulate the type of loading experienced when standing. In order to load the knee in a flexed position a custom, MRI compatible rig was designed. The participant lies supine within the MR scanner therefore the load had to be applied approximately normal to the axial plane. The rig had to meet the size constraints of the MR scanner's bore (width 57 cm, height from table to ceiling 40 cm), had to be designed and constructed using non-metallic, MR compatible parts only, had to permit the application of different load magnitudes and had to be adjustable for use with the right or left foot. It was also important that our rig be portable because it may be used in different MR scanners.

The final apparatus (Figure 4.4) consists of a pedal attached to a loading bed mounted on a U-shaped frame. The pedal and loading bed can freely rotate about the cross-bar of

the frame and can be positioned on the left or right side of the cross-bar depending on which knee is being loaded. The pedal was oriented at 30° from the horizontal when in the loaded state and the amount of load applied by the pedal is dependent on both position of the foot on the pedal and the amount of weight placed on the loading bed (Figure 4.5).



Figure 4.4: MR compatible loading rig. Left: Side view of the loading rig showing pedal, loading bed and frame. Right, Oblique view of the loading rig showing the pedal and loading bed rotating about the U-shaped frame.

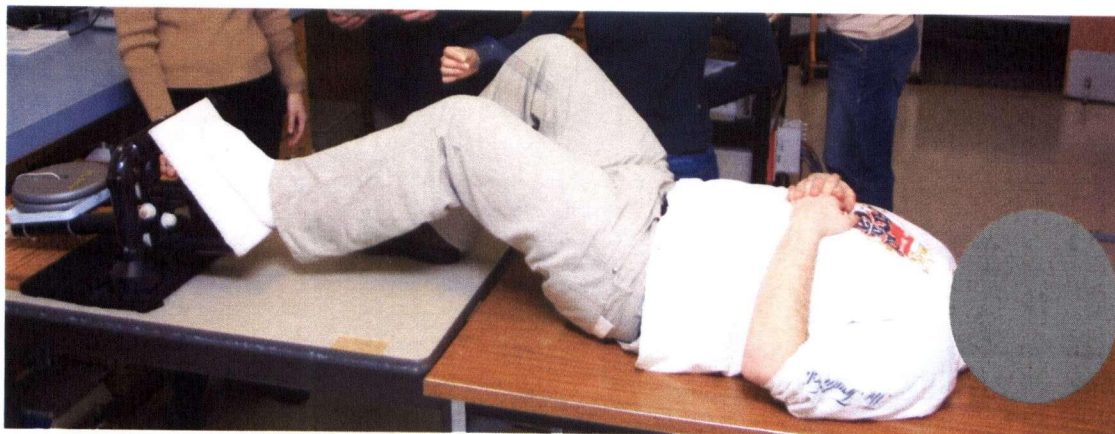


Figure 4.5: An example of loading a participant's knee. During actual imaging the leg is supported by padding.

In this study the applied load was set to 80 N. This load is small relative to normal activities (ground reaction force in the vertical/axial direction during gait is in the order of 700 N, depending on body weight). However a load had to be chosen which would allow people with symptomatic knee osteoarthritis, which entails some degree of pain or reduced mobility, to carry out the loading task. The participant was positioned with the knee at the desired angle of flexion and with his or her foot in the required position on the pedal. This position was defined so the approximate centre of each individual's foot was in the same position and the foot was oriented in the correct direction. The pedal was set at a loading angle of 30°. Various foam pads were placed under the flexed leg to ensure the initial angle of flexion remained constant. Immediately prior to the commencement of the scan the load was applied and the participant was instructed to 'maintain' the original position, but not move the pedal. The experimenter ensured that the participant had in fact maintained this position by observing a visual mark on the rear side of the loading rig. Each participant had a practice session holding the pedal in position prior to the scan.

4.4 Low-resolution Scan

Six low-resolution MR scans were acquired in the sagittal plane with a T1-weighted spin echo sequence. These six datasets were acquired at six different angles of loaded knee flexion between 0° and 40°. The slice thickness was 7 mm and the in-plane resolution was 1.25 mm. Further imaging parameters can be found in table 4.2. In the first low-resolution scan the participant's knee was placed in approximately 40° of tibiofemoral flexion with his or her foot placed on the pedal of the loading rig (described

in Section 4.3 Loading Rig Design). The angle of tibiofemoral flexion was decreased by approximately 6° per scan by instructing the individual to move slightly further away from the rig itself. The loading position rig remained fixed. Immediately prior to the commencement of the scan an 80 N load was applied to the rig and the participant was instructed to ‘maintain’ the flexed knee position for the duration of the scan (approximately 40 seconds).

Parameter	Low-Resolution Image
Slice Spacing	7 mm
In-plane Resolution	1.25 mm
Repetition Time (TR)	283 ms
Echo Time (TE)	13 ms
Flip Angle (FA)	90°
Number of Excitations (NEX)	1
Field of View (FOV)	320 mm
Matrix Size	256 x 256
Scan Time	38 seconds
Coil	Body

Table 4.2: Low-resolution imaging parameters

The femur, tibia and patella were segmented from each of the 6 low resolution images in a slice-by-slice fashion, in the same manner as was carried out for the high resolution images. However, they were not assembled into models. Instead, the Cartesian coordinates of the outlines of the femur, tibia and patella were extracted from the segmented images and imported into and displayed in Matlab (Figure 4.6).



Figure 4.6: Low resolution contours.

4.5 Anatomical Axes Assignment

An orthogonal, anatomical axis system was individually assigned to the femur, tibia and patella using anatomical landmarks identified from the high resolution image. The sign conventions were based on the Joint Coordinate System⁸⁷. In the right knee the positive directions are proximal, lateral and anterior. To maintain a right handed coordinate system in this study the positive directions of the coordinate axes in the left knee are proximal, lateral and posterior. As with the Joint Coordinate System model rotations and translations were referred to using the clinical terms: flexion/extension, adduction/abduction, internal/external rotation, medial/lateral translation, anterior/posterior translation and superior/inferior translation. This naming system is adequate for tibiofemoral kinematics. However more descriptive names were used for the patella to help visualize the actual movements. The six kinematic parameters for the

patella are therefore named flexion, spin, tilt, proximal translation, lateral translation and anterior translation. A more complete description of each is provided in Section 4.6.

To define the coordinate axes in each bone, anatomical landmarks were identified on the original high resolution MR scan. Since not all of these landmarks were visible in the imaging plane (sagittal), Analyze was used to resample the data and create an isotropic raw volume from the high resolution scan using an input driven linear interpolation algorithm. The three orthogonal views were then displayed. The in-plane resolution of the isotropic volume was 0.625 mm (this was also the in-plane resolution of the high resolution scan). The anatomical landmarks definitions for the femur and tibia were based on those described by Lerner et al.¹¹⁸ and for the patella were based on those described by¹⁶¹. The femoral, tibial and patellar coordinate systems used have also been described previously (Appendix B)^{65,90}. The positive directions for the right knee are lateral, anterior and superior and for the left knee are lateral, posterior and superior.

4.6 Shape-matching

The aim of the shape-match was to accurately match the outlines of the femur, tibia and patella created from the low resolution images to the geometric models of the femur, tibial and patella created from the high resolution image. Custom software written in Matlab by former lab members, Robert Fellows and Nicholas Hill, was used to carry out this task. The shape-matching process was based on an Iterative Closest Points (ICP) algorithm¹⁶ and the final output of this step is 6 transformation matrices relating the position of the geometric model to the position of each set of outlines. This process is carried out in 2 steps, a pre-computational shape-match and the actual shape-match itself.

4.6.1 Iterative Closest Points Algorithm

The ICP algorithm is a method of registering a data shape to a model shape using a mean-square distance metric¹⁶. Registration is the process of identifying the geometric transformation required to align two different representations of the same shape. In the present situation the geometric model (high resolution) is the model shape and the outline (low resolution) is the data shape. This algorithm can be summarized by three steps:

1. The shortest Euclidean distance between each point in the outline and the geometric model was determined in an iterative fashion. The shortest distance is determined by finding the distance between all combinations of outline points to geometric model points and identifying the shortest distance. When the shortest distance was found the point pair was considered to be ‘closest points’.
2. The rigid body transform, seen below, which described the motion of the geometric model from its original to a new position based on the ‘closest point’ pair was determined¹⁸⁰. X, Y and Z is the translation vector and the 3 x 3 R matrix describes the rotation (Equation 4.1).

$$[FlexedPosition] = T[InitialPosition] \quad \text{Equation 4.1}$$

where

$$T = \begin{bmatrix} 1 & 0 & 0 & 0 \\ X & R_{11} & R_{12} & R_{13} \\ Y & R_{21} & R_{22} & R_{23} \\ Z & R_{31} & R_{32} & R_{33} \end{bmatrix}$$

3. The transformation, according matrix calculated in 2, was applied and the mean-square error of the mean distance between the outline points and the geometric model points.

These three steps were iterated until the change in the mean square error was less than a predetermined value. The smaller this value is the more accurate the transformation will be, however a smaller desired change in error results in more iterations and a longer processing time.

4.6.2 Pre-computation

The pre-computation to define the starting position for the ICP is carried out for the purpose of speeding up the actual shape-match process. It also ensures that the desired convergence on the global minimum distance between the geometric model and the bone outlines occurs. ICP can be very sensitive to the initial position of the geometric model and outlines, especially to rotations. The pre-computation step requires the user to translate and rotate the geometric model until a relatively good match with the outline is obtained (Figure 4.7). First, an initial match of the centres of mass of the geometric model and the outline was carried out. Next, translations and rotations were input into the program by the user and were adjusted until the user was satisfied with the initial match. The femur, tibia and patella were each matched individually. A fast version of the ICP algorithm (the number of points in the geometric model and the outline is reduced) was run in which the system was deemed to have converged when the error had not changed by more than 0.001 mm. The output of the pre-computation is initial

transformation matrices for each individual bone match between the geometric model and each outline position.

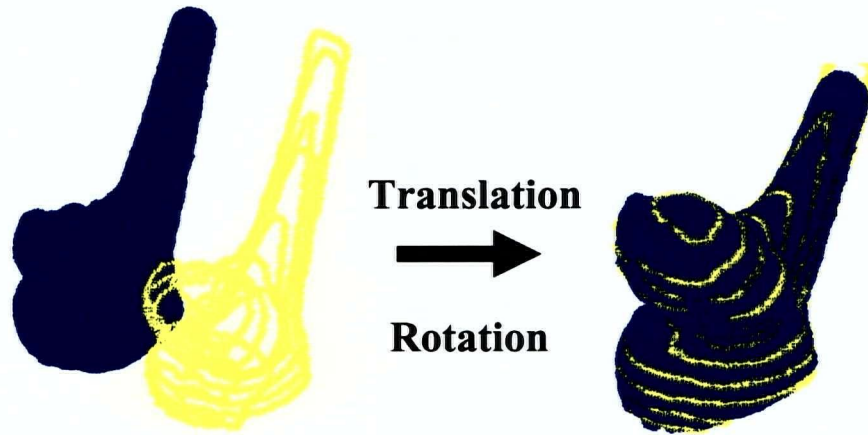


Figure 4. 7: A manual trial and error translation and rotation of the geometric model is carried out to create an initial match to the outline.

4.6.3 Shape-Match

The shape-match program takes as input the geometric models, all the low resolution outlines and all the initial transformation matrices calculated in the pre-computation step and outputs the final transformation matrices between each bone and outline. In this program the ICP algorithm was run and the stable condition was met when the error had not changed by more than 0.00001 mm. Images of the final shape-match of each outline with the geometric model were displayed in order to confirm the shape-match (Figure 4.8). An image of the relative motion of the patella and the tibia with respect to the femur at each angle of flexion (Figure 4.8) was also plotted.

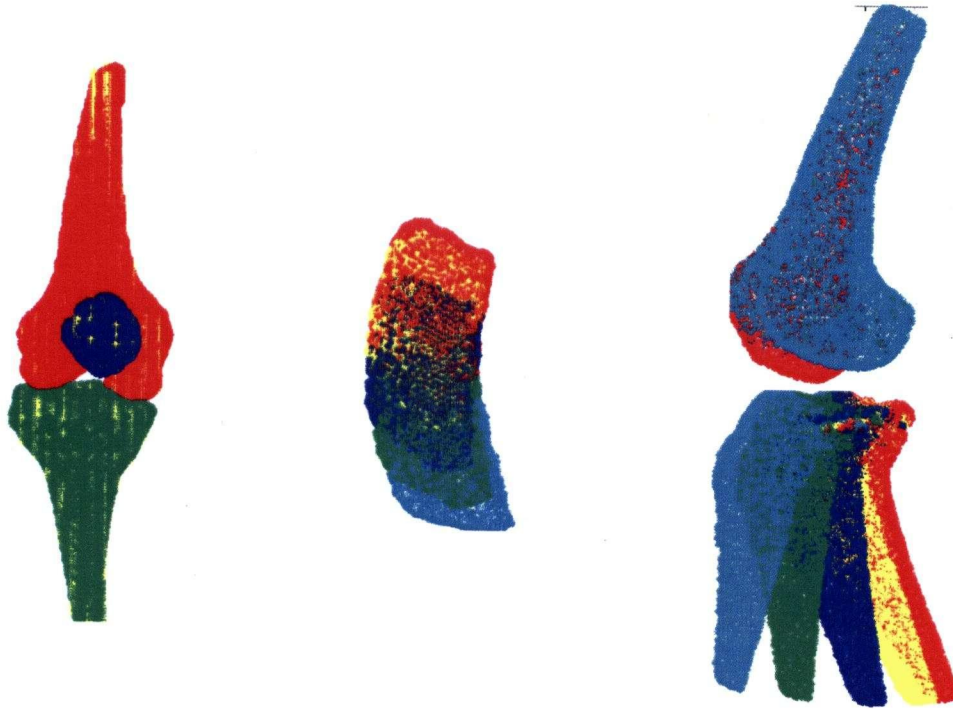


Figure 4. 8: Left: final shape match, yellow lines are the outlines from the low-resolution model. Middle: Motion of the patella. Upper right: Motion of the femur, note virtually no movement. Lower left: motion of the tibia.

4.7 Kinematics

Patellofemoral kinematic parameters were calculated using the coordinate axes assigned to each bone and the transformation matrices determined by the shape-match. The angle of tibiofemoral flexion associated with each transformation was calculated as the degree of rotation about the medial/lateral axis of the femur using the Joint Coordinate System⁸⁷. The following 6 patellofemoral kinematic parameters (Figure 4.9) were calculated for each angle of tibiofemoral flexion^{41,87}:

1. Flexion – the rotation of the patella about the medial/lateral femoral axis
2. Tilt – the rotation of the patella about the superior/inferior patellar axis
3. Spin – the rotation of the patella about the axis perpendicular to the medial/lateral femoral axis and the superior/inferior patellar axis

4. Proximal translation – translation of the patella along the superior/inferior femoral axis
5. Lateral translation – translation of the patella along the medial/lateral femoral axis
6. Anterior patellar translation – translation of the patella along the anterior/posterior femoral axis.

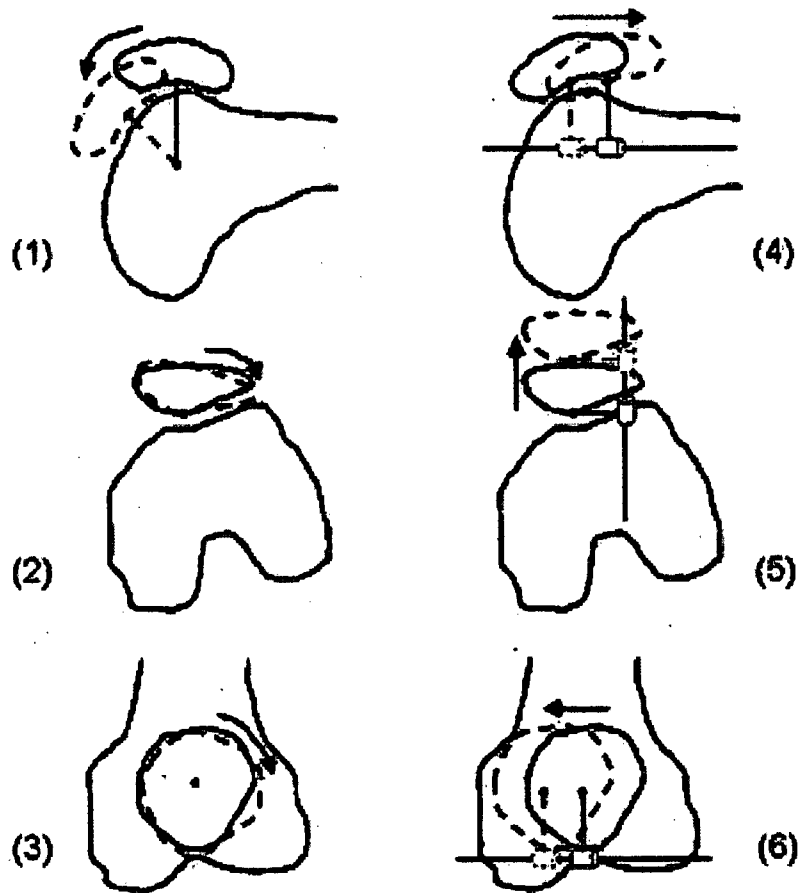


Figure 4.9: Patellofemoral kinematics positive directions. Ref: Robert Fellows, Thesis, 2003

4.8 Accuracy and Precision

The accuracy of this novel, MRI-based technique for measuring three-dimensional patellar kinematics *in vivo* was assessed using roentgen stereophotogrammetric analysis (RSA)⁶⁷. Former lab member Robert Fellows carried out a study using three cadaver knee specimens. Three-dimensional patellar kinematics were assessed using two different methods:

1. The MRI based technique described above, with modification to the MRI compatible loading apparatus
2. Taking simultaneous bi-planar x-rays in various static positions and creating a geometric model from a computed tomography (CT) scan

The accuracy of the method was determined to be 1.75° for rotations and 0.88 mm for translations, calculated as the mean absolute difference between the RSA and MRI measurements.

The precision (repeatability) of the method was measured in terms of intra-subject variability and inter-experimenter variability⁶⁶. Three healthy subjects underwent numerous assessment of three-dimensional kinematics (two high resolution scans and 4 low resolution loading cycles). The error in intra-subject variability was less than 1.5° for rotations and less than 1 mm for translations which was based on two high resolution scans and four separate loading cycles for each subject. The inter-experimenter error was measured between 3 experimenters and was found to be less than 2.15° for rotations and less than 0.7 mm for translations. Patellar spin showed the greatest variation, however the patterns of all parameters were consistent between experimenters.

Chapter 5: Methods C – Study Design

5.1 Study Population

Individuals with early knee osteoarthritis were recruited to participate in this study. Participants were identified through a database maintained by the Mary Pack Arthritis Centre, Vancouver, BC. Individuals listed in this database had previously participated in osteoarthritis studies and had expressed an interest in being contacted to participate in future studies. Dr. Jolanda Cibere, a Rheumatologist at the Centre, accessed the database and identified possible candidates for this study based on the following criteria:

1. Knee osteoarthritis in at least one compartment of the knee (tibiofemoral or patellofemoral) assessed from an anterior/posterior and/or skyline radiograph
2. Detectable varus (bow-legs) or valgus (knock-knees) knee malalignment by visual inspection
3. No contraindication for MRI (which was then again confirmed prior to imaging)

Twenty individuals were identified through the database and were contacted via regular mail. The letter outlined the study's objectives and procedures which had been approved by the University of British Columbia and the Vancouver Coastal Health Research Institute Ethical Review Committees.

5.2 Measurements

Twelve individuals agreed to participate in the study and gave informed consent (Appendix C). They each underwent measurements in the knee they identified as being more severely affected. Measurements included:

1. Assessment of varus or valgus leg alignment from a leg lengths radiograph
2. Assessment of patellofemoral cartilage morphology with qMRI
3. Assessment of three-dimensional patellar tracking with novel MRI procedure
4. Assessment of clinical OA severity with the Western Ontario and McMaster University (WOMAC) osteoarthritis questionnaire
5. Measurement of height and weight

5.2.1 Assessment of Varus-Valgus Knee Alignment

One standing, full leg, anteroposterior radiograph was taken to assess the femorotibial angle of the lower leg¹³¹. Dr. Savvas Nicolaou, a radiologist at Vancouver General Hospital, read the radiographs for this study and assessed the angle. First the mechanical axis of the femur was identified as the line from the centre of the femoral head to the centre of the intercondylar notch. Next the mechanical axis of the tibia was identified as the line from the centre of the anterior crest of the tibial plateau to the centre of the talus bone. The angle of intersection of these two lines was measured and the participant was classified into the varus (less than 180°) or valgus group (greater than 180°) (Figure 5.1). Individuals were required to display a minimum of 3° of malalignment in order to be included in this study.

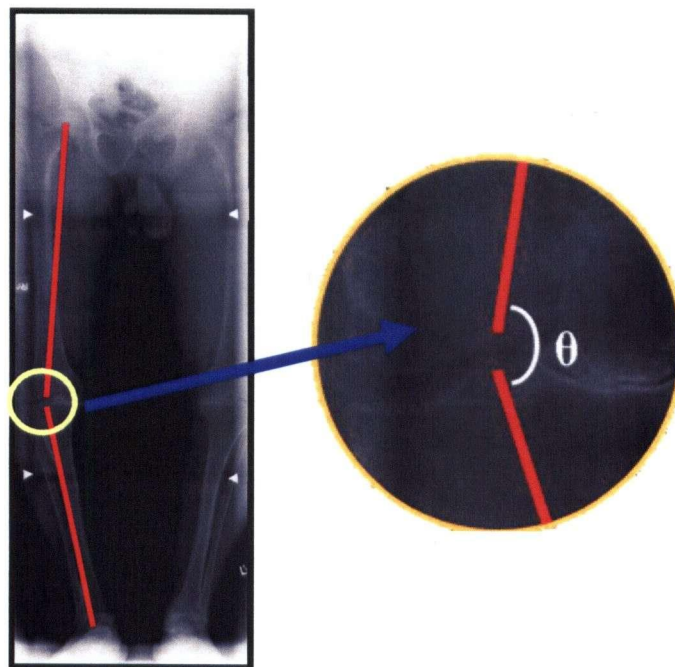


Figure 5.1: The measurement of femorotibial angle from radiographs using the Moreland protocol. The mechanical axis of the femur and tibia are defined and the angle between them is measured. An angle of $< 180^\circ$ is varus and $> 180^\circ$ is valgus.

5.2.2 Assessment of Patellofemoral Cartilage Morphology

Patellar and femoral cartilage morphology at the patellofemoral joint was assessed using the qMRI method outlined in Chapter 3. First, patellar and femoral cartilage was segmented and measured (Figure 5.3). Femoral cartilage in this study refers to the cartilage that covers the trochlear groove of the femur (Figure 5.2). The entire patellar cartilage plate was used in this assessment. However, due to the limitation of the field of view in the axial plane it was not possible to assess the entire femoral plate. Instead, the number of slices of femoral cartilage assessed was dependent on the number of patellar cartilage slices that the individual participant displayed. The amount of femoral cartilage assessed was $\frac{3}{4}$ the size of the patellar cartilage plate. For example, if the patella had 20 cartilage slices, 15 femoral slices were assessed. The first femoral slice to be assessed was the most proximal of the trochlear groove of the femur.

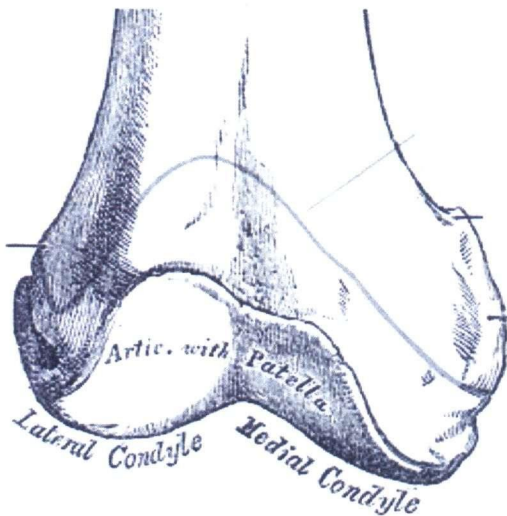


Figure 5.2: Articular surface of the femur with the patella, the trochlear groove. Ref: Gray's Anatomy

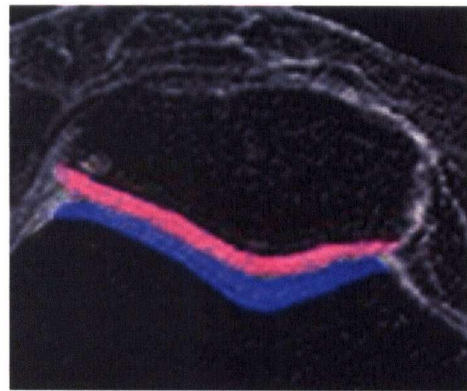


Figure 5.3: Segmented patellar (pink) and femoral (blue) cartilage.

Next both the patellar and femoral cartilage plates were divided into medial and lateral compartments (Figure 5.4). The patellar cartilage was divided along the median ridge and the femoral cartilage was divided along the deepest point of the trochlear groove. The cartilage morphology of the compartments was assessed separately.

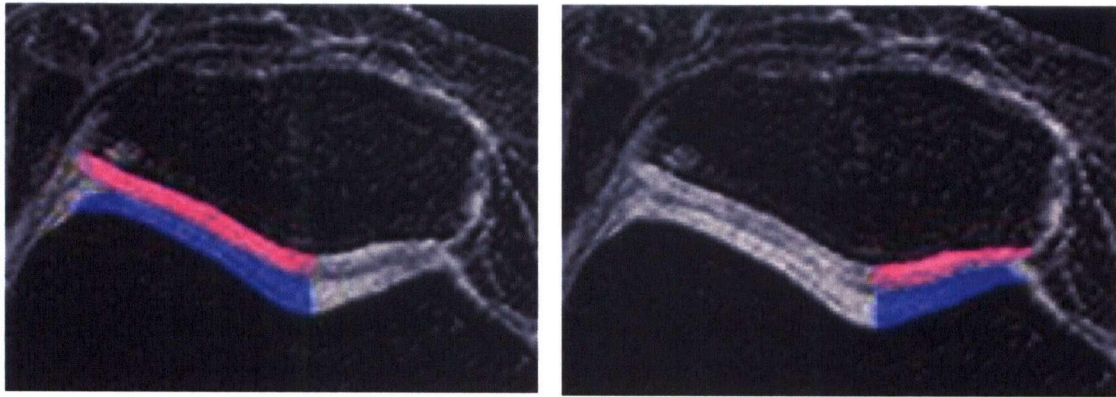


Figure 5.4: The medial and lateral division of patellar and femoral cartilage. The patellar cartilage is divided into medial (right) and lateral (left) compartments along the median ridge and the femoral cartilage is divided along the depth of the patellar groove.

The following cartilage morphologic parameters were assessed for the patella and femur (details of each measurement can be found in Section 3.2.4):

1. Area of Bone/Cartilagel Interface
2. Surface Area
3. Volume
4. Normalized Volume
5. Mean Thickness
6. Percentage Cartilage Coverage

5.2.3 Assessment of Three-Dimensional Patellar Kinematics

The assessment of three-dimensional patellar kinematics was carried out using the method described in Chapter 4. Six angles of loaded flexion were assessed for each

participant. In some cases the individual moved during the scan or two of the angles of tibiofemoral flexion were similar, therefore only 5 scans were analyzed for all participants. If all 6 scans were good, the scan that caused the least difference in angle between the two adjacent scans was removed.

5.2.4 WOMAC Questionnaire

The WOMAC questionnaire (Appendix A) is a self-administered questionnaire which addresses pain, stiffness and physical function in individuals with OA at the knee and hip. It was developed and validated for use as a research tool in knee and hip OA studies¹³. The researcher specifies which knee or hip (right or left) the patient should assess when completing the questionnaire. The questionnaire takes only five minutes to complete. It focuses on a combination of pain and mobility questions that have been identified as specific to OA by the questionnaire developers. The WOMAC can be administered in a Likert scale format where the patient answers each question as none, mild, moderate, severe or extreme or in a visual analog format where the patient places an x on a line that ranges from none to extreme. We administered the WOMAC LK3.1 questionnaire in the more severely affected knee.

5.2.5 Height and Weight Measurement

Height and weight were measured on a manual scale like those found in a doctor's office. Body mass index (BMI) was then calculated (equation 5.1).

$$BMI = \frac{(\text{weight})}{(\text{height}^2)} \quad \text{Equation 5.1}$$

5.3 Statistical Analysis

All statistical analysis was carried out using a 0.05 level of significance. Statistical analysis was carried out using Statview (SAS, Cary, NC, USA) and Minitab Student Package (Minitab, State College, PA, USA). When t-tests were performed, a two-sample t-test was used when comparing between the varus and valgus groups and a paired t-test was used when comparing side or compartment differences between individuals. We used the t-tests under the assumption that the data was normally distributed.

5.3.1 Varus/Valgus Alignment Groups

We tested the null hypothesis that there was no significant difference in alignment between the right and left knee using a paired t-test. We also tested the null hypothesis that there was no difference in BMI between the varus and valgus groups using a two-sample t-test. We tested the null hypothesis that there was no difference in WOMAC score between the varus and valgus groups using a two-sample t-test.

5.3.2 Varus/Valgus Alignment vs. Cartilage Morphology

We tested the null hypothesis that there was no difference in total cartilage morphology between the varus and valgus groups using a two-sample t-test. Each of the 6 morphologic parameters was tested for both patellar and femoral cartilage.

We tested the null hypothesis that there was no difference in compartmental patellar and femoral cartilage morphology between the varus and valgus groups using a two-way analysis of variance (ANOVA). The two factors were compartment (medial or lateral) and alignment (varus or valgus).

5.3.3 Varus/Valgus Alignment vs. Three-dimensional Patellar Kinematics

We tested the null hypothesis that there was no difference in patellar tracking value or slope between the varus and valgus groups using a linear random effects model. The linear random effects model is a hierarchical or multilevel model and in this case we used a 2-level model. This test is often chosen when the experimenter would like to make inferences on the data outside the particular independent variables measured. It was suitable in this case because the angles of loaded tibiofemoral flexion varied from participant to participant and inferences were desired for other angles between measured values. The random effects model has been used previously in a patellar kinematics study¹³⁵. Dr. Michael Schulzer, a statistician with the Centre for Clinical Evaluation and Epidemiology, was the statistical advisor for this Section and carried out the statistical analysis using specialized multilevel modelling software (MLwiN, London, UK).

As mentioned, we used a 2-level model. Level 1 is the subject's individual patellar tracking data and level 2 is the alignment group's (varus or valgus) combined data. First, a linear regression line was fit to each individual's patellar kinematic data, therefore each individual had 6 regression lines associated with him or her, one for each patellar kinematic parameter (flexion, spin, tilt, anterior translation, lateral translation and proximal translation). A slope and an intercept were defined for each individual. The mean slopes and intercepts were used to create a group specific (varus or valgus) model of the data. In this instance we have defined the intercept as a random variable (allowed to vary normally about the mean) and the slope as a fixed variable (was considered to be the mean). The final model is displayed in equation form (Equation 5.2).

$$y = \text{intercept} + \text{slope} * x + \text{level} * \text{grp} + \text{interaction} * \text{grp} * x \quad \text{Equation 5.2}$$

The independent variable, x , was angle of tibiofemoral flexion. For the varus group $\text{grp}=0$ and for the valgus group $\text{grp}=1$. The intercept and slope terms were mean values of the individual data. The interaction term shows how one independent variable varies as a function of the other. The standard error (SE) for each term in the equation is also calculated within this model. By dividing the mean value by the SE a z-score can be calculated showing the significance of the term.

If the interaction term was not significant a random effects model without the interaction term was created (Equation 5.3).

$$y = y\text{-int} + \text{slope} * x + \text{level} * \text{grp} \quad \text{Equation 5.3}$$

The 95% confidence interval for each line was also calculated.

The random effects model allowed differences in values of kinematic parameters and differences in rates of change of parameters between the varus and valgus group to be identified.

5.3.4 Three-dimensional Patellar Kinematics vs. Patellar Cartilage Morphology

We tested the null hypothesis that there was no relationship between patellar kinematic parameters and compartmental cartilage morphology using a regression model. This model was suitable because we wished to examine correlations rather than differences between groups. In order to carry out this regression both of these parameters had to be summarized as single number for each participant. Each patellar kinematic parameter (PKP) was summarized two different ways:

1) The mean value of the initial 5 kinematic measurements

2) The slope of the regression line fit to the initial 5 kinematic measurements.

Each compartmental cartilage morphologic parameter (CCMP) for each participant was summarized as the ratio of the medial compartment value to the lateral compartment value using a logarithmic representation (Equation 5.4):

$$[\text{Ln}(\text{CCMP}_{\text{med}}) - \text{Ln}(\text{CCMP}_{\text{lat}})] \quad \text{Equation 5.4}$$

Cartilage volume was not assessed in this model as the normalized volume parameter provided a more accurate means of comparison.

Each of the 6 mean PKP were individually related to 5 compartmental cartilage morphologic parameter ratios according to the following regression model (Equation 5.5):

$$[\text{Ln} (\text{CCMP}_{\text{med}}) - \text{Ln} (\text{CCMP}_{\text{lat}})] = \text{mean (PKP)} \quad (\text{equation 5.5})$$

This was also carried out for the slope of the patellar kinematic parameter (Equation 5.6):

$$[\text{Ln} (\text{CCMP}_{\text{med}}) - \text{Ln} (\text{CCMP}_{\text{lat}})] = \text{slope (PKP)} \quad \text{Equation 5.6}$$

Therefore 30 regressions using the mean patellar kinematic parameter value and 30 different regressions using the slope of the patellar kinematic parameter value were carried out (i.e. 6 patellar kinematic parameters x 5 cartilage morphologic parameter ratios). A p-value for the order of fit for the regressions is also reported and refers to the most appropriate curve fit to the data, for example a significant p-value for a first order polynomial indicates that a higher degree polynomial should be considered for fitting the points.

The femoral cartilage was not assessed in this manner because a complete description of the entire cartilage plate could not be obtained due to the limited field of view of the MRI images and the curvature of the cartilage plate. Because the movement of the patella across the femur is dependent on the angle of tibiofemoral flexion and because the inferior portions of the femoral cartilage plate are not included in the model as they follow the curvature of the femur, an accurate representation of the relationship between patellar kinematics and femoral cartilage morphology would not be obtained.

Chapter 6: Results

6.1 Introduction

The participants in this study were divided into groups according to the knee alignment that they displayed. Group specific relationships between cartilage morphology and patellar kinematics were then assessed. Finally, the relationship between patellar kinematics and cartilage morphology, independent of knee alignment was assessed.

Section 6.4 of this chapter has been accepted for publication. McWalter EJ, Wirth W, Siebert M, von Eisenhart-Rothe R, Hudelmaier M, Wilson DR, Eckstein F. Use of novel interactive input devices for segmentation of articular cartilage from magnetic resonance images. *Osteoarthritis Cartilage* In Press.

6.2 Varus/Valgus Alignment

The angle of alignment of the more severely affected knee was considered in assessments of varus and valgus alignment (highlighted in red in table 6.1).

Participant	Alignment	Right Knee Angle	Left Knee Angle
1	Varus	178.1	179.0
2	Valgus	183.5	184.5
3	Valgus	183.5	183.4
4	Varus	165.5	164.5
5	Valgus	184.5	182.5
6	Valgus	182.9	181.3
7	Valgus	182.2	184.3
8	Varus	174.2	173.1
9	Varus	178.3	179.9
10	Varus	170.7	175.0
11	Varus	172.5	170.9
12	Varus	174.9	169.5

Table 6.1: Angles of lower limb alignment for 12 study participants. Both knee angles were assessed, only the imaged knee (highlighted in red) was considered in the study.

Two individuals, participant 1 and 9, were excluded from the study due to the minimal malalignment. The study was then conducted with 10 individuals, 5 with varus alignment (4 men, 1 woman) and 5 with valgus malalignment (5 women). The mean and standard deviation femorotibial angle of the varus group was $169.7^{\circ} \pm 3.2^{\circ}$ and of the valgus group was $183.3^{\circ} \pm 0.8^{\circ}$. A normal femorotibial angle is close to 180° . No significant difference was seen in angle of alignment between the right and left knee. The mean BMI of the varus group was 25.9 ± 4.4 and the valgus group was 27.4 ± 3.3 . For the number of subjects assessed, there was no statistically significant difference in BMI between the groups ($p=0.5694$).

6.3 WOMAC

The mean WOMAC scores for pain, stiffness and difficulty carrying out activities of daily living (ADLs) were not significantly different between groups ($p=0.05$). The mean and standard deviation of the WOMAC scores for the varus and valgus groups are shown in table 6.2.

	Varus	Valgus	P-value
Pain (20)	5.6 (3.2)	5.2 (2.8)	0.84
Stiffness (8)	1.4 (0.5)	2.4 (1.5)	0.22
Difficulty performing ADLs (68)	16.4 (8.0)	21 (10.5)	0.46

Table 6.2: Mean and standard deviation () of the pain, stiffness and difficulty performing activities of daily living for the WOMAC questionnaire. The p-value for the difference between groups were not significant in any case.

6.4 Input Device Study

Segmentation using the interactive touch-sensitive screen was on the order of 15% faster than segmentation using the optical mouse for three of the four cartilage plates (Table 6.3). Use of the tablet involved tended to increase segmentation time when compared to the mouse, although the increase was not statistically significant (Table 6.3).

	tablet	screen	mouse
normal patella	75 ± 6 min	60 ± 9 min*	71 ± 9 min
normal tibia	69 ± 10 min	60 ± 6 min	64 ± 8 min
OA patella	75 ± 14 min	57 ± 7 min*	71 ± 8 min
OA tibia	78 ± 12 min	60 ± 8 min*	74 ± 8 min
total time	1784 min	1421 min	1680 min

Table 6.3: Mean and standard deviation of time for each segmentation input device (interactive digitizing tablet, interactive touch-sensitive screen and traditional mouse) for the normal patella, normal tibia, OA patella and OA tibia for session 2 only. The total time spent using each input device in session 2 is also shown. * identifies a statistically significant differences as compared to the mouse ($p=0.032$ for all significant values).

We found no systematic differences in cartilage volume, surface area, or mean cartilage thickness between the different segmentation input devices (Table 6.4).

We found no significant difference in the precision (reproducibility) of the results for the different input devices (Table 6.5). Resegmentation precision errors for volume ranged from 1.9% to 3.7% in normal cartilage for the mouse, from 3.8% to 5.2% for the tablet, and from 3.6% to 4.3% for the screen. In the OA cartilage surfaces, resegmentation precision errors for volume ranged from 4.7% to 5.2% for the mouse, from 4.7% to 5.0% for the tablet, and 3.9% to 5.6% for the screen. Similar precision errors were obtained for surface area and mean cartilage thickness (Table 6.5).

	tablet vs mouse	screen vs mouse	tablet vs screen
volume:			
normal patella	-0.5% ± 2.2	-0.8% ± 2.2	0.3% ± 0.6
normal tibia	0.6% ± 3.0	0.4% ± 3.1	0.2% ± 2.7
OA patella	-2.4% ± 1.9	-1.8% ± 3.9	-0.4% ± 4.8
OA tibia	1.0% ± 2.0	0.7% ± 3.2	0.3% ± 3.1
surface area:			
normal patella	0.1% ± 1.3	-0.7% ± 1.9	0.8% ± 1.3
normal tibia	0.5% ± 1.4	-0.1% ± 1.0	0.5% ± 0.6
OA patella	0.3% ± 0.8	-0.2% ± 1.3	0.6% ± 1.8
OA tibia	-0.8% ± 1.5	0.4% ± 1.1	-1.1% ± 2.4
mean thickness:			
normal patella	-0.2% ± 1.9	0.5% ± 1.8	-0.6% ± 0.7
normal tibia	1.2% ± 3.6	1.6% ± 3.6	-0.3% ± 4.1
OA patella	-1.8% ± 2.5	-1.6% ± 4.1	0.0% ± 5.3
OA tibia	2.6% ± 1.4	1.0% ± 4.7	1.7% ± 4.3

Table 6.4: Systematic differences and standard deviation in cartilage volume, surface area, and mean thickness for the digitizing tablet versus the mouse, the touch-sensitive screen versus the mouse and the digitizing tablet versus the touch-sensitive screen.

	tablet	screen	mouse
Volume (mm³):			
Normal patella	3.8% (3688.5±138.8)	3.6% (3677.5±132.2)	3.7% (3704.4±131.5)
Normal tibia	5.2% (2005.9±109.8)	4.3% (1998.6±102.9)	1.9% (1990.1±31.1)
OA patella	4.7% (1847.2±95.1)	3.9% (1864.5±75.6)	5.2% (1894.8±99.9)
OA tibia	5.0% (1824.7±83.6)	5.6% (1821.8±82.1)	4.7% (1805.7±66.4)
surface area(mm²):			
Normal patella	2.7% (14.36±0.39)	1.8% (14.24±0.27)	2.0% (14.34±0.28)
Normal tibia	2.0% (11.84±0.23)	1.8% (11.77±0.24)	1.4% (11.77±0.15)
OA patella	2.7% (11.23±0.32)	2.0% (11.16±0.24)	2.2% (11.19±0.24)
OA tibia	2.1% (10.63±0.24)	2.6% (10.75±0.26)	2.0% (10.71±0.19)
mean thickness (mm):			
Normal patella	2.2% (2.66±0.06)	3.2% (2.68±0.09)	2.8% (2.66±0.08)
Normal tibia	5.0% (1.47±0.07)	4.4% (1.47±0.07)	1.9% (1.45±0.03)
OA patella	4.6% (1.35±0.07)	5.3% (1.36±0.07)	6.1% (1.38±0.09)
OA tibia	5.9% (1.16±0.06)	5.6% (1.14±0.05)	5.3% (1.13±0.05)

Table 6.5: Precision (reproducibility) expressed as CV% and mean and standard deviation (mean ± standard deviation) in cartilage volume, surface area, and mean thickness for each segmentation input device (digitizing tablet, touch-sensitive screen and traditional mouse).

6.5 Varus/Valgus Alignment vs. Cartilage Morphology

6.5.1 Patellar Cartilage

Volume, normalized volume and mean thickness of the varus group were approximately twice those of the valgus group (Table 6.6). For the number of subjects assessed, no difference was seen for bone cartilage interface or % cartilage coverage. Surface area was approximately 40% greater in the varus group.

Parameter	Varus	Valgus	P-value
Bone Cartilage Interface (cm²)	14.43 (1.87)	12.25 (1.33)	0.0580
Surface Area (cm²)	15.13 (2.13)	10.94 (3.12)	0.0220*
Volume (mm³)	3796 (1083)	1668 (581)	0.0079*
Normalized Volume (mm)	2.60 (0.49)	1.37 (0.48)	0.0047*
Mean thickness (mm)	2.32 (0.50)	1.07 (0.44)	0.0028*
% Cartilage Coverage	96.6 (3.8)	82.2 (21.0)	0.2000

Table 6.6: Difference in total patellar cartilage morphology for the varus and valgus groups. Mean, (standard deviation) and P-value. * identifies a significant difference

In both groups the lateral patellar compartment was larger than the medial. In the valgus group the lateral compartment bone/cartilage interface was approximately 85% larger ($p=0.0230$). In the varus group, the lateral compartment was approximately 60% larger for bone/cartilage interface ($p=0.0050$), 50% for surface area ($p=0.0040$) and 70% for volume ($p=0.0110$). For the number of subjects assessed, no significant difference was seen for any of the other parameters (Table 6.7).

Parameter	Varus		Valgus	
	Medial	Lateral	Medial	Lateral
Bone Cartilage Interface (cm²)	5.5 (0.8)	8.8 (1.3)	4.2 (0.5)	7.8 (1.8)
Surface Area (cm²)	6.6 (1.2)	10.0 (1.6)	4.5 (0.8)	6.9 (3.5)
Volume (mm³)	1411 (446)	2379 (704)	568 (141)	1093 (562)
Normalized Volume (mm)	2.6 (0.6)	2.7 (0.5)	1.4 (0.2)	1.4 (0.7)
Mean thickness (mm)	2.1 (0.5)	2.3 (0.5)	0.9 (0.3)	1.1 (0.4)
% Cartilage Coverage	92 (11)	99 (1)	89 (8)	77 (33)

Table 6.7: Mean and standard deviation() values for patellar cartilage morphologic parameters the medial and lateral compartments of the varus and valgus groups.

6.5.2 Patellar Cartilage vs Varus/Valgus Alignment

For the number of subjects assessed, no statistically significant difference was found in compartmental cartilage morphology (medial and lateral) between the varus and valgus groups using a two-way ANOVA (Table 6.8). We did not find that the cartilage had degenerated more in the lateral compartment for the valgus group or in the medial compartment for the varus group.

Parameter	P-Value for Interaction
Bone Cartilage Interface (cm²)	0.7400
Surface Area (cm²)	0.6080
Volume (mm³)	0.3440
Normalized Volume (mm)	0.8970
Mean thickness (mm)	0.8880
% Cartilage Coverage	0.2330

Table 6.8: P-values for 2-way ANOVA of patellar cartilage morphology and varus/valgus alignment.

6.5.3 Femoral Cartilage

Volume and mean thickness of the varus group were approximately twice those of the valgus group (Table 6.9). The varus group also displayed an approximately 30% larger bone/cartilage interface, 40% larger surface area and 60% greater normalized volume. For the number of subjects assessed, no difference was seen in percentage cartilage coverage.

Parameter	Varus	Valgus	P-value
Bone Cartilage Interface (cm²)	11.85 (1.50)	9.25 (0.47)	0.0210*
Surface Area (cm²)	11.37 (0.79)	8.02 (2.50)	0.0460*
Volume (mm³)	2724 (141)	1342 (568)	0.0031*
Normalized Volume (mm)	2.34 (0.45)	1.45 (0.61)	0.0340*
Mean thickness (mm)	2.00 (0.43)	1.00 (0.03)	0.0320*
% Cartilage Coverage	89.4 (9.9)	82.5 (24.6)	0.5800

Table 6.9: Difference in total femoral cartilage morphology for the varus and valgus groups. Mean, (standard deviation) and P-value. * identifies a significant difference

The bone/cartilage interface in the lateral compartment of the varus group was approximately twice that of the medial compartment ($p=0.0020$) (Table 6.10). The valgus group displayed an approximately 80% larger bone/cartilage interface ($p=0.0020$) and twice the surface area ($p=0.0020$) and mean thickness ($p=0.0090$) in the lateral compartment.

Parameter	Varus		Valgus	
	Medial	Lateral	Medial	Lateral
Bone Cartilage Interface (mm²)	3.2 (0.6)	6.4 (0.7)	4.2 (0.9)	7.6 (1.0)
Surface Area (mm²)	3.1 (0.7)	5.6 (2.4)	4.0 (0.5)	8.3 (0.8)
Volume (mm³)	556 (256)	827 (448)	937 (180)	1782 (308)
Normalized Volume (mm)	1.7 (0.6)	1.3 (0.7)	2.4 (0.8)	2.4 (0.4)
Mean thickness (mm)	1.2 (0.6)	1.0 (0.6)	1.9 (0.6)	1.9 (0.3)
% Cartilage Coverage	91 (18)	79 (32)	77 (23)	96 (5)

Table 6.10: Mean and standard deviation() values for femoral cartilage morphology of the medial and lateral compartments of the varus and valgus groups.

6.5.4 Femoral Cartilage vs Varus/Valgus Alignment

For the number of subjects we assessed, medial and lateral cartilage morphology was not related to varus or valgus alignment (Table 6.11).

Parameter	P-Value for Interaction
Bone Cartilage Interface (cm²)	0.7950
Surface Area (cm²)	0.2150
Volume (mm³)	0.0570
Normalized Volume (mm)	0.4900
Mean thickness (mm)	0.5880
% Cartilage Coverage	0.1290

Table 6.11: P-values for 2-way ANOVA of femoral cartilage morphology and varus/valgus alignment.

6.6 Varus/Valgus Alignment vs. Patellar Kinematics

A linear random effects statistical model was used to study the difference between the varus and valgus groups for all six patellar kinematic parameters. By combining the data of all subjects, the model created a linear equation for each kinematic parameter in the following form:

$$y = y\text{-int (SE)} + \text{slope (SE)} * \text{flexion} + \text{level (SE)} * \text{grp} + \text{interaction (SE)} * \text{grp} * \text{flexion}$$

The linear equation includes:

- the **y-intercept** of the line
- the **slope** of the line
- the **level** or height of the line which is different for the varus and valgus groups
- the **interaction** term which indicates an interaction between groups (in this case it indicates the slope of the line is different between the varus and valgus groups)
- **grp**: 0 for the varus group, 1 for the valgus group
- **flexion**: the angle of tibiofemoral flexion (independent variable)

The y-intercept, slope, level and interaction terms are mean values from each individual in the varus and valgus groups (Section 5.3.3). The standard error (SE) in the mean values is reported in brackets next to the term itself. Z-scores were found by dividing the mean by the SE (the population mean, μ , is assumed to be 0). The p-value was calculated from the Z-score. If a significant difference ($z > 1.96$) is found in the interaction term it was included in the model when plotting the lines for varus and valgus groups. If there was no significant difference in the interaction terms a simplified model, without the interaction term, was used to plot the lines. In the latter case the p- and z-values reported for slope and level are those of the simplified model. A significant difference in the slope term refers to a non-zero slope. A significant difference in level is only meaningful if there is no interaction between the groups, i.e. if the groups have the same slope.

6.6.1 Patellar Flexion

Patellar flexion increased for both groups as tibiofemoral flexion increased and the patella was initially in a greater angle of extension for the valgus group (Equation 6.1, Figure 6.1). The difference in initial positions between groups was about 7° ($p=0.0047$, $z=-2.60$, $n=10$). For the number of subjects we assessed, the interaction term was not significant between the varus and valgus groups ($p=0.2297$, $z=-0.74$, $n=10$) therefore the model without the interaction term was used. There was a significant, increasing slope for both groups ($p=0.0000$, $z=-13.73$, $n=10$).

$$y = -9.667(2.152) + 0.564(0.041) flex - 7.459(2.874)grp \quad \text{Equation 6.1}$$

$$y = -9.667 + 0.564 flex - 7.459 grp$$

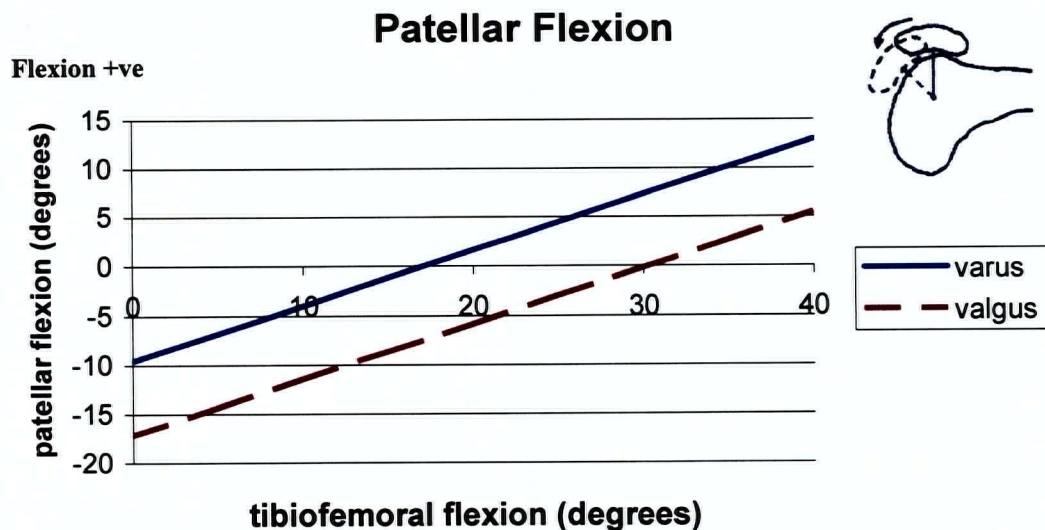


Figure 6.1: Linear random effects model of mean patellar flexion. Patellar flexion increased with increasing tibiofemoral flexion. The patellae of the valgus group begin in a greater angle of extension than the varus group.

6.6.2 Patellar Spin

The varus group displayed a constant angle internal spin and the valgus group displayed a constant angle of external spin (Figure 6.2). The overall difference between the angle of spin was about 6° ($p=0.0048$, $z=-2.59$, $n=10$). For the number of subjects we assessed, slope was not significant between groups ($p=0.4052$, $z=-0.24$, $n=10$) therefore the line is horizontal. The interaction term was not significant between the varus and valgus groups ($p=0.2810$, $z=-0.58$, $n=10$) therefore the model with out an interaction term was used (Equation 6.2).

$$y = 2.010(1.829) - 0.008(0.032) flex - 6.382(2.461)grp \quad \text{Equation 6.2}$$

$$y = 2.010 - 0.008 flex - 6.382 grp$$

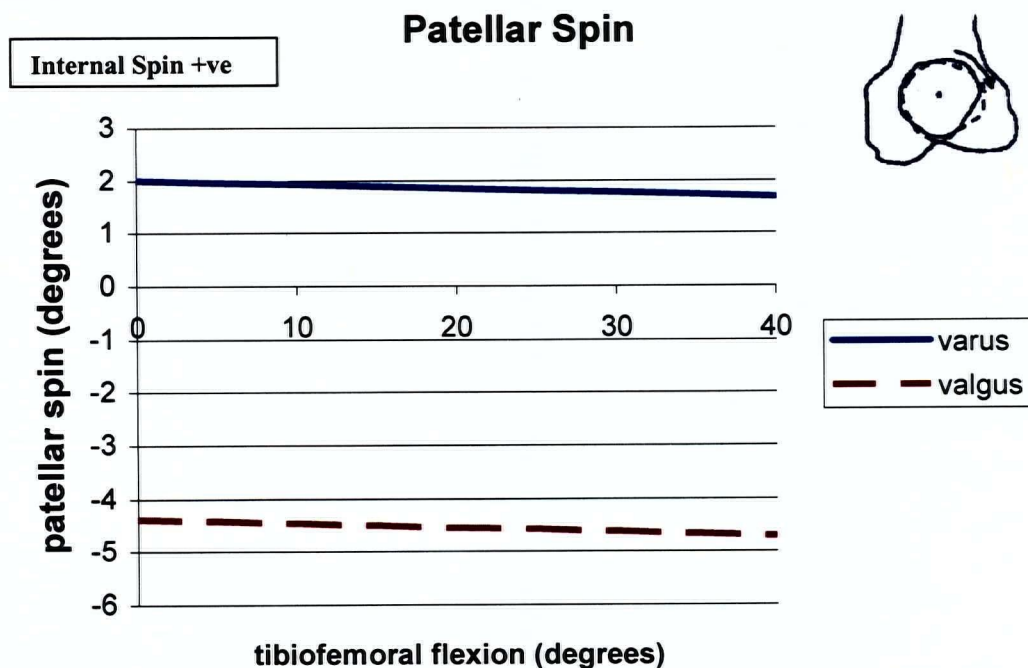


Figure 6.2: Linear random effects model of mean patellar spin. The varus group maintains an external spin and the valgus group maintains an internal spin through the angles of tibiofemoral flexion.

6.6.3 Patellar Tilt

The varus group displayed a constant angle of medial tilt of approximately 10° throughout the range of knee flexion and the valgus group was less tilted at full extension and tilted medially as the knee flexed at a rate of approximately 2° per 10° of knee flexion (Equation 6.3, Figure 6.3). The patterns of tilt were significantly different between the varus and valgus groups ($p=0.0028$, $z=2.77$, $n=10$).

$$y = 9.602(3.256) - 0.005(0.049)flex - 3.891(4.642)grp + 0.153(0.070)grp \cdot flex$$

Equation 6.3

$$y = 9.602 - 0.005flex - 3.891grp + 0.153grp \cdot flex$$

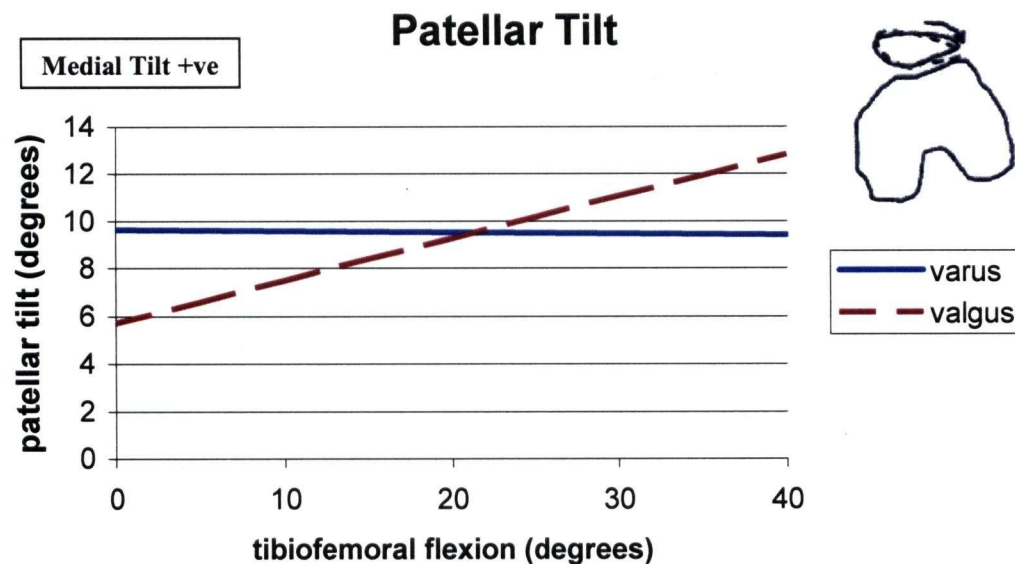


Figure 6.3: Linear random effects model of mean patellar tilt. The varus group displayed a constant angle of medial tilt and the valgus group was less tilted initially and tilted medially with increasing tibiofemoral flexion.

6.6.4 Proximal Patellar Translation

The patellae of the valgus group were positioned about 10 mm more proximally than the varus group ($p=0.0078$, $z=2.42$, $n=10$) and in both groups the patellae moved distally as the knee flexed at a rate of approximately 10 mm per 10° ($p=0.0000$, $z=-21.11$, $n=10$) (Figure 6.4). For the number of subjects assessed, the interaction term was not significant signifying the pattern of proximal translation was not different between groups ($p=0.0527$, $z=1.63$, $n=10$). The model without the interaction term was therefore used (Equation 6.4).

$$y = 29.106(2.606) - 0.566(0.026) flex + 8.794(3.627) grp \quad \text{Equation 6.4}$$

$$y = 29.106 - 0.566 flex + 8.794 grp$$

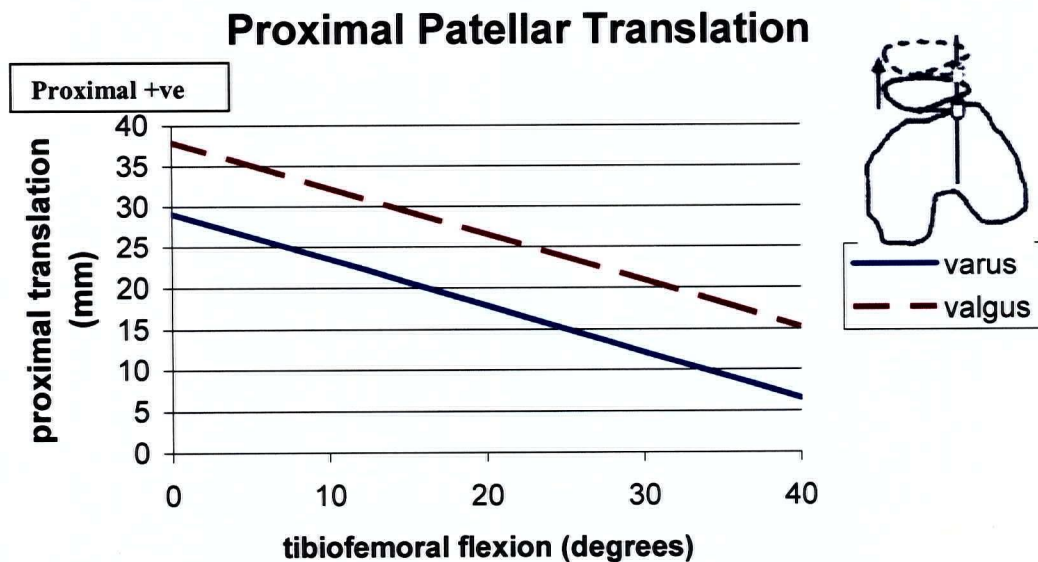


Figure 6.4: Linear random effects model of mean proximal patellar translation. The patellae of both groups translated distally as the knee flexed, in extension the valgus patellae are positioned more proximally.

6.6.5 Lateral Patellar Translation

For the number of subjects assessed, there was no significant difference in pattern of lateral translation between the varus and valgus groups ($p=0.4403$, $z=0.15$, $n=10$) (Equation 6.5). The position in the mediolateral plane did not change for either group ($p=0.4522$, $z=0.12$, $n=10$) nor was there a difference in position ($p=0.3336$, $z=0.43$, $n=10$). The patellae of both groups remained centred in the trochlear groove throughout the range of tibiofemoral flexion for both the varus and valgus groups according to the linear random effects model (Figure 6.5).

$$y = -0.344(1.730) + 0.003(0.028) flex + 1.0141(2.351) grp \quad (\text{Equation 6.5})$$

$$y = -0.344 + 0.003 flex + 1.014 grp$$

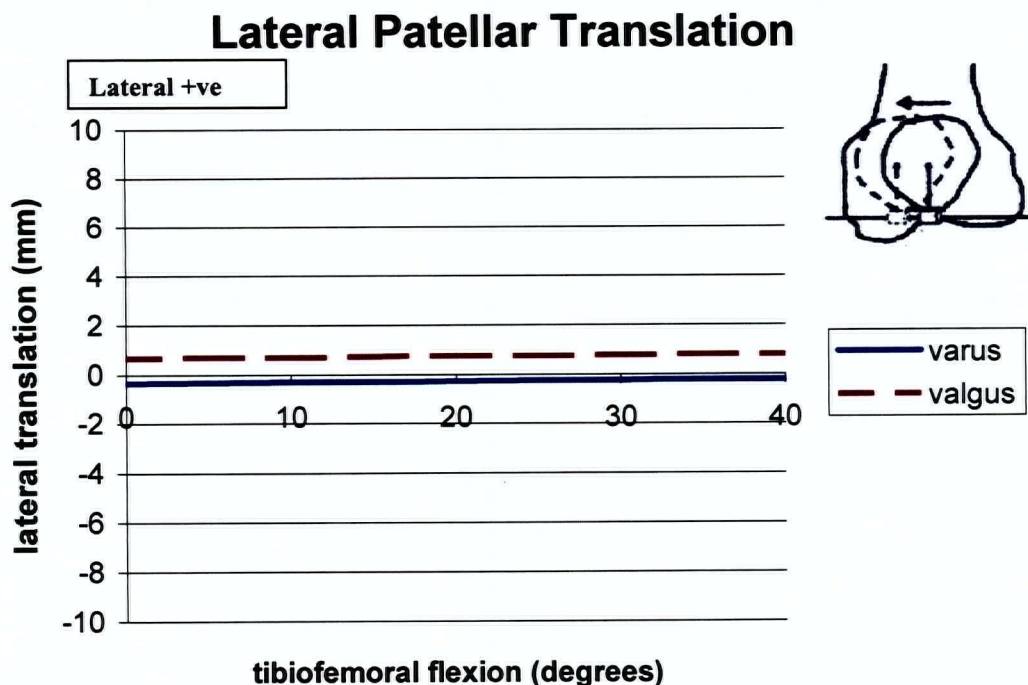


Figure 6.5: Linear random effects model of mean lateral patellar translation. The mean patellar translation of both groups was approximately 0 throughout the range of tibiofemoral flexion.

6.6.6 Anterior Patellar Translation

The anterior translation of the valgus group remained relatively constant at 25 mm while the varus group's patellae tend to move posteriorly by about 1mm per 10° of tibiofemoral flexion ($p=0.0005$, $z=3.27$, $n=10$) (Equation 6.6, Figure 6.6).

$$y = 31.627(0.754) - 0.123(0.020) flex - 6.584(1.0930) grp + 0.088(0.027) grp \cdot flex$$

Equation 6.6

$$y = 31.627 - 0.123 flex - 6.584 grp + 0.088 grp \cdot flex$$

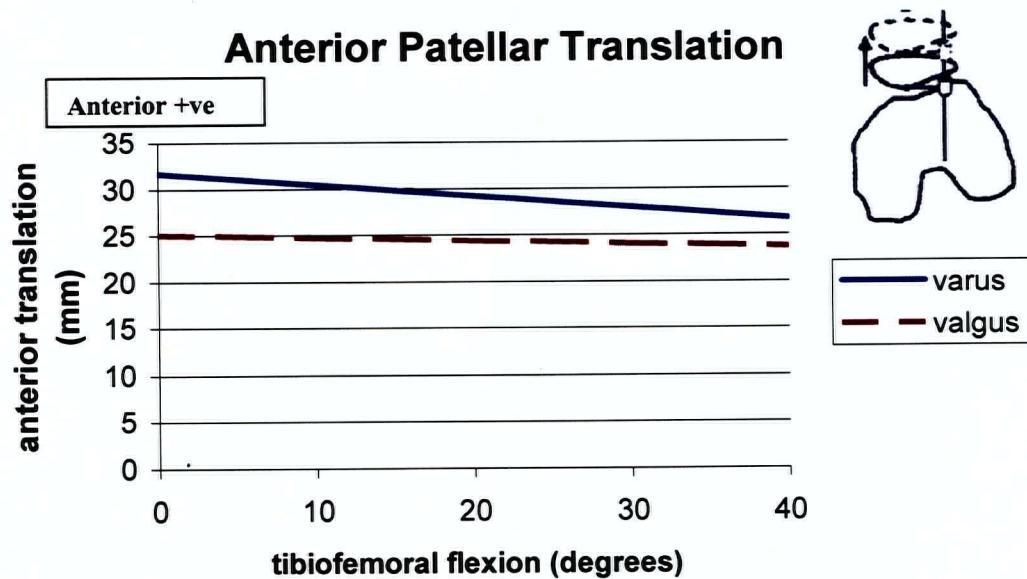


Figure 6.6: Linear random effects model of mean anterior patellar translation. The valgus group maintained a constant position and the varus group slowly moved posteriorly through the range of tibiofemoral flexion.

6.6.7 Summary of Significant Differences

A summary of the differences in kinematic parameters between the varus groups can be seen below (Table 6.12).

	Slope		Level		Interaction	
	p	z	p	z	p	z
Flexion/Extension	0.0000*	13.73*	0.0047*	-2.60*	-	-
Internal/External Spin	0.4052	-0.24	0.0048*	-2.59*	-	-
Abduction/Adduction Tilt	0.4602	-0.10	0.2005	-0.84	0.0028*	2.77*
Proximal Translation	0.0000*	-21.11*	0.0078*	2.42*	-	-
Lateral Translation	0.4522	-0.12	0.3336	0.43	-	-
Anterior Translation	0.0000*	-6.12*	0.0000*	-6.02*	0.0005*	3.27*

Table 6.12: Summary of significant p- and z-values for the linear random effects model parameters (slope, level and interaction). The p- and z-values are those of the actual models used, not all of which contained an interaction term. * identifies significant differences.

6.7 Patellar Kinematics vs Patellar Cartilage Morphology

The results of the regression analysis using the mean patellar kinematic parameters have not been included because the range of tibiofemoral flexion angles assessed for three-dimensional patellar kinematics was not consistent for all participants. The mean kinematic parameter for each individual was associated with a particular mean tibiofemoral angle. The maximum difference in mean tibiofemoral angle between subjects was 15°.

The regression analysis for slope of the patellar kinematic parameters is presented in the following Sections.

6.7.1 Bone/Cartilage Interface

Patellae with proportionally larger lateral compartments (area of bone/cartilage interface) tilted medially through the range of tibiofemoral flexion at a greater rate. A 1st and 2nd order regression was carried out (Figure 6.7 and 6.8) and resulted in R² values of 77% and 82%, respectively (Table 6.14). For the number of subjects assessed, no relationship was found between the rate of change of other kinematic parameters and compartmental bone/cartilage interface ratio (Table 6.13).

Kinematic Parameter	R ²	P-value (quality of fit)	P-value (order of fit)
Flexion	22%	0.1695	0.3720
Internal/external Spin	3%	0.6537	0.8788
Medial/Lateral Tilt	77% *	0.0009*	0.0027*
Proximal Translation	0%	0.9151	0.4254
Lateral Translation	34%	0.0771	0.2237
Anterior Translation	11%	0.3414	0.4922

Table 6.13: Results of linear regression for bone/cartilage interface and kinematic parameters. P-value (quality of fit) identifies the p-value associated with the regression). P-value (order of fit), indicates a higher order polynomial should be considered for the regression fit. * identifies a significant difference

Polynomial	R ²	P-value (order of fit)
1 st order	77%	0.0027
2 nd order	82%	0.2121

Table 6.14: First and second order regression fit for bone/cartilage interface to tilt as described by the R² value and a P-value indicating the appropriateness of fit.

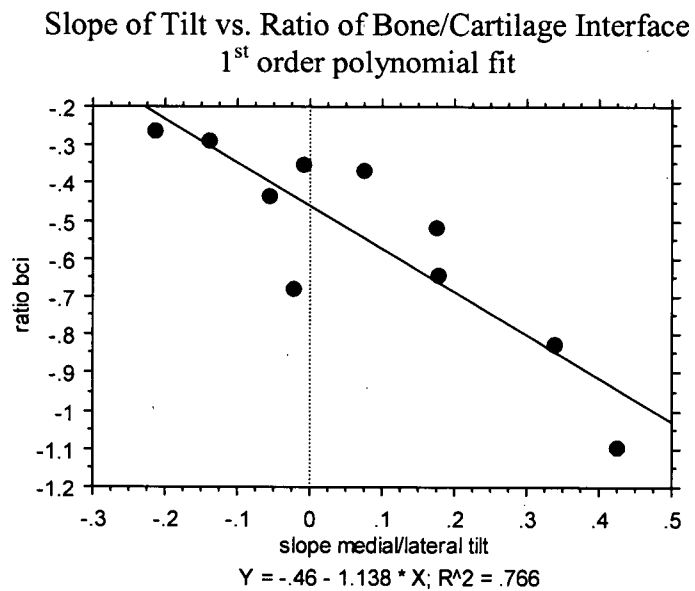


Figure 6.7: Linear regression fit of the ratio of medial to lateral bone/cartilage interface to the slope of patellar tilt. The regression equation and the R² values are shown.

Slope of Tilt vs. Ratio of Bone/Cartilage Interface
2nd order polynomial fit

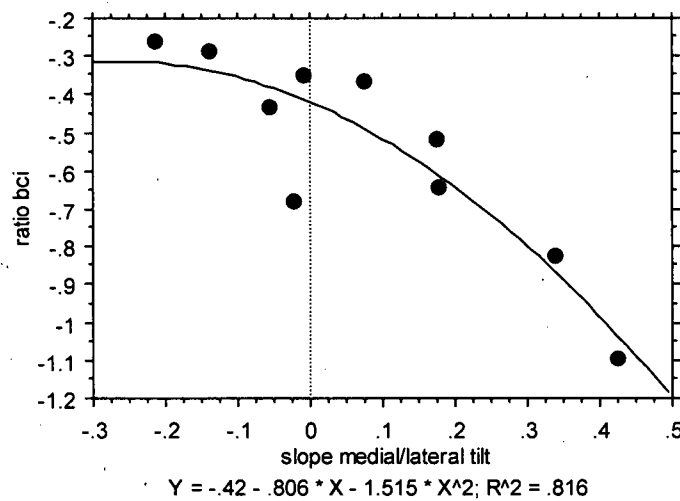


Figure 6.8: 2nd order polynomial regression fit of the ratio of medial to lateral bone/cartilage interface to the slope of patellar tilt. The regression equation and the R^2 values are shown.

6.7.2 Surface Area

For the number of subjects assessed, no correlation was seen between any kinematic parameter and proportion of medial to lateral cartilage surface area using a linear regression model (Table 6.15). The results suggest that a higher order polynomial may provide a better fit to the lateral translation data ($p=0.0158$). The majority of the data points showed a similar compartmental cartilage surface area ratio and approximately no change in rate of medial or lateral translation (i.e. maintained a constant mediolateral position). The R^2 value increased from 18% to 69% to 72% for the linear, 2nd order and 3rd order polynomial fits, respectively (Table 6.16). The increase in R^2 value with higher order fits is influenced greatly by a few outlying points (Figure 6.9 and Appendix D).

Kinematic Parameter	R ²	P-value (quality of fit)	P-value (order of fit)
Flexion	7%	0.4569	0.4881
Internal/external Spin	0%	0.8764	0.9899
Medial/Lateral Tilt	39%	0.0537	0.1775
Proximal Translation	13%	0.2979	0.5084
Lateral Translation	18%	0.2232	0.0158 *
Anterior Translation	6%	0.5145	0.7973

Table 6.15: Results of linear regression for surface area and kinematic parameters. P-value (quality of fit) identifies the p-value associated with the regression. P-value (order of fit), indicates a higher order polynomial should be considered for the regression fit. * identifies a significant difference

Polynomial	R ²	P-value (order of fit)
1 st order	18%	0.0158
2 nd order	69%	0.0109
3 rd order	72%	0.5272

Table 6.16: 1st, 2nd and 3rd order regression fit for surface area to lateral translation as described by the R² value and a P-value indicating the appropriateness of fit.

Slope of Lateral Translation vs. Ratio of Surface Area 1st order polynomial fit

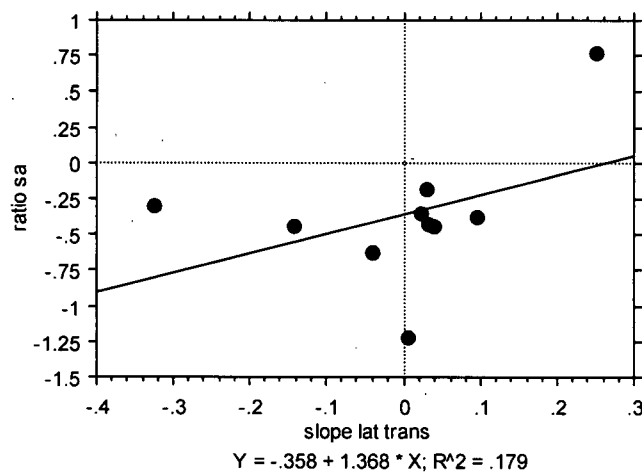


Figure 6.9: 1st order polynomial (linear) regression fit of the ratio of medial to lateral surface area to the slope of lateral patellar translation. The regression equation and the R² values are shown.

6.7.3 Normalized Volume

For the number of subjects assessed, no correlation was seen between any kinematic parameter and proportion of medial to lateral normalized volume using a linear regression model (Table 6.17). The results suggest that a higher order polynomial may provide a better fit to the lateral translation data (0.0030). The majority of the data points showed a very small or no difference between medial and lateral compartment normalized volume and approximately no change in rate of medial or lateral translation (i.e. maintained a constant mediolateral position). When assessing this relationship using higher order polynomials the R^2 value increased from 15% to 81% to 91% to 91% for the linear, 2nd order, 3rd order and 4th order polynomial fits, respectively (Table 6.18). The increase in R^2 value with higher order fits is influenced greatly by a few outlying points (Figure 6.10 and Appendix D).

Kinematic Parameter	R^2	P-value (quality of fit)	P-value (order of fit)
Flexion	1%	0.7456	0.6004
Internal/external Spin	0%	0.9800	0.9950
Medial/Lateral Tilt	14%	0.2808	0.4608
Proximal Translation	10%	0.3628	0.6755
Lateral Translation	15%	0.3749	0.0030*
Anterior Translation	4%	0.5458	0.5053

Table 6.17: Results of linear regression for normalized volume and kinematic parameters. P-value (quality of fit) identifies the p-value associated with the regression. P-value (order of fit), indicates a higher order polynomial should be considered for the regression fit. * identifies a significant difference

Polynomial	R^2	P-value (order of fit)
1 st order	15%	0.0030
2 nd order	81%	0.0014
3 rd order	91%	0.0488
4 th order	91%	0.8087

Table 6.18: 1st, 2nd, 3rd and 4th order regression fit for normalized volume to lateral translation as described by the R^2 value and a P-value indicating the appropriateness of fit.

Slope of Lateral Translation vs. Ratio of Normalized Volume
1st order polynomial fit

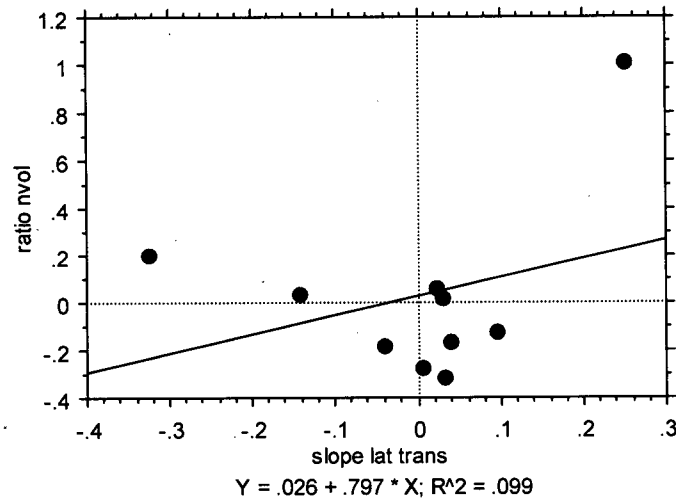


Figure 6.10: 1st order polynomial (linear) regression fit of the ratio of medial to lateral normalized volume to the slope of lateral patellar translation.. The regression equation and the R² values are shown.

6.7.4 Mean Thickness

For the number of subjects assessed, no correlation was seen between any kinematic parameter and proportion of medial to lateral mean thickness proportions using a linear regression model (Table 6.19). The results suggest that a higher order polynomial may provide a better fit to the lateral translation data ($p=0.0116$). The majority of the data points showed a very small or no difference between medial and lateral compartment mean thickness and approximately no change in rate of medial or lateral translation (i.e. maintained a constant mediolateral position). When assessing this relationship using higher order polynomials the R² value increased from 14% to 72% to 79% for the linear, 2nd order and 3rd order polynomial fits, respectively (Table 6.20). The increase in R² value with higher order fits is influenced greatly by a few outlying points (Figure 6.11 and Appendix D).

Kinematic Parameter	R ²	P-value (quality of fit)	P-value (order of fit)
Flexion	4%	0.5705	0.3067
Internal/external Spin	0%	0.8483	0.9842
Medial/Lateral Tilt	33%	0.0819	0.2447
Proximal Translation	10%	0.3695	0.6690
Lateral Translation	14%	0.2808	0.0116 *
Anterior Translation	4%	0.5675	0.6730

Table 6.19 : Results of linear regression for mean thickness and kinematic parameters. P-value (quality of fit) identifies the p-value associated with the regression. P-value (order of fit), indicates a higher order polynomial should be considered for the regression fit. * identifies a significant difference

Polynomial	R ²	P-value (order of fit)
1 st order	14%	0.0116
2 nd order	72%	0.0067
3 rd order	79%	0.2110

Table 6.20: 1st, 2nd and 3rd order regression fit for mean thickness to lateral translation as described by the R² value and a P-value indicating the appropriateness of fit.

Slope of Lateral Translation vs. Ratio of Mean Thickness
1st order polynomial fit

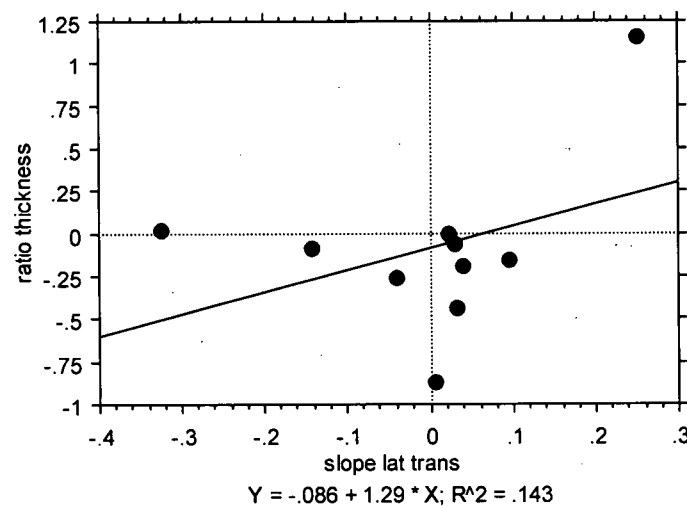


Figure 6.11: 1st order polynomial (linear) regression fit of the ratio of medial to lateral mean thickness to the slope of lateral patellar translation.. The regression equation and the R² values are shown.

6.7.5 Percentage Cartilage Coverage

For the number of subjects assessed, no correlation was seen between any kinematic parameter and proportion of medial to lateral mean thickness using a linear regression model (Table 6.21). The results suggest that a higher order polynomial may provide a better fit to the lateral translation data ($p=0.0002$). The majority of the data points showed a very small or no difference between medial and lateral compartment percentage cartilage coverage and approximately no change in rate of medial or lateral translation (i.e. maintained a constant mediolateral position). When assessing this relationship using higher order polynomials the R^2 value increased from 6% to 91% to 94% for the linear, 2nd order and 3rd order polynomial fits, respectively (Table 6.22). The increase in R^2 value with higher order fits is influenced greatly by a few outlying points (Figure 6.12 and Appendix D).

Kinematic Parameter	R^2	P-value (quality of fit)	P-value (order of fit)
Flexion	0%	0.8821	0.7957
Internal/external Spin	0 %	0.9171	0.9751
Medial/Lateral Tilt	18%	0.5232	0.7041
Proximal Translation	22 %	0.1691	0.4117
Lateral Translation	6%	0.5143	0.0002 *
Anterior Translation	0 %	0.8045	0.7592

Table 6.21 : Results of linear regression for percentage cartilage coverage and kinematic parameters. P-value (quality of fit) identifies the p-value associated with the regression. P-value (order of fit), indicates a higher order polynomial should be considered for the regression fit. * identifies a significant difference

Polynomial	R^2	P-value
1st order	6%	0:0020
2nd order	91%	0.0010
3rd order	94%	0.1110

Table 6.22: First and second order regression fit for percentage cartilage coverage to lateral translation as described by the R^2 value and a P-value indicating the appropriateness of fit.

Slope of Lateral Translation vs. Ratio of Percentage Cartilage Coverage
1st order polynomial fit

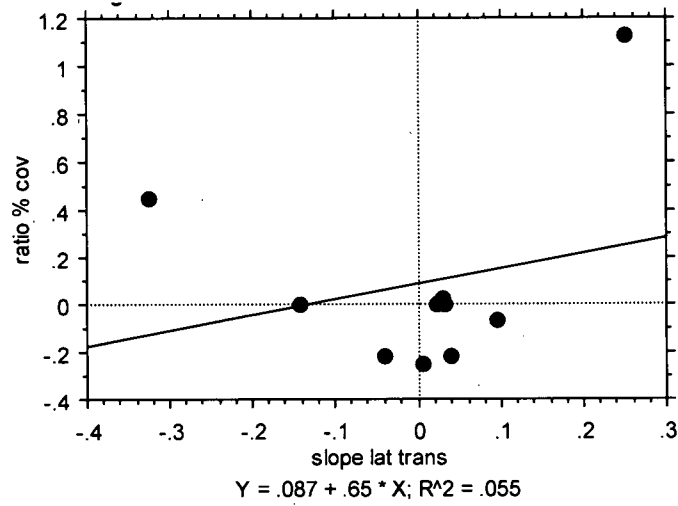


Figure 6.12: 1st order polynomial (linear) regression fit of the ratio of medial to lateral percentage cartilage coverage to the slope of lateral patellar translation.. The regression equation and the R^2 values are shown.

6.8 Summary

1. The varus group displayed a greater degree of malalignment ($169.7^\circ \pm 3.2^\circ$) than the valgus group ($183.3^\circ \pm 0.8^\circ$), which is consistent with other studies.
2. The WOMAC questionnaire showed that the varus and valgus groups were at similar stages of clinical OA.
3. A 15% time savings is obtained when using the touch-sensitive screen for cartilage segmentation.
4. The varus group had greater total patellar cartilage surface area, volume, normalized volume and mean thickness than the valgus group.
5. There was no relationship between compartment specific cartilage morphology and varus/valgus alignment.
6. The varus and valgus groups displayed similar patterns (slopes) for flexion, spin and anterior translation however the initial position of the patella were different.
7. The varus and valgus groups displayed different patterns (slopes) for tilt and proximal translation. The varus group displayed a constant angle of medial tilt and the valgus group an increasing medial tilt through the range of tibiofemoral flexion. The varus group displayed a slight posterior translation through the range of tibiofemoral flexion while the valgus group maintained a constant position.
8. For the number of subjects assessed, no difference was seen in lateral patellar translation between varus and valgus groups.
9. Patella with proportionally larger lateral patellar compartment bone/cartilage interface area tilted medially at a greater rate with increasing tibiofemoral flexion.

10. The relationship between patellar cartilage surface area, normalized volume, mean thickness and percentage cartilage coverage and lateral translation were influenced by a few inconsistent data points.

Chapter 7: Discussion

7.1 Introduction

We assessed the relationship between three-dimensional patellar kinematics, cartilage morphology and varus/valgus alignment in individuals with early knee osteoarthritis (OA). The techniques of assessing three-dimensional patellar kinematics and cartilage morphology were both MRI based and have been independently validated for both accuracy and precision^{27,67}. To date, the most comprehensive OA studies of varus/valgus alignment have relied on radiographic assessment of OA, in which cartilage is measured by joint space narrowing. We used qMRI in our study which allowed us to assess the cartilage morphology directly. The relationship between patellar kinematics and OA has received little attention in the literature. Only one other group has assessed three-dimensional kinematics in individuals with OA, however, their method has not been validated for accuracy. Because our method has been rigorously validated, we are confident that the relationships we have discovered between patellar kinematics and varus/valgus alignment in knee OA are accurate. To our knowledge, we are the first group to assess the relationship between cartilage morphology and patellar kinematics, independent of leg alignment.

Section 7.3.1 of this chapter has been accepted for publication. McWalter EJ, Wirth W, Siebert M, von Eisenhart-Rothe R, Hudelmaier M, Wilson DR, Eckstein F. Use of novel interactive input devices for segmentation of articular cartilage from magnetic resonance images. *Osteoarthritis Cartilage* In Press.

7.2 Synthesis – A Comparison to the Literature

7.2.1 Alignment

The amount of varus and valgus alignment in our groups was comparable to that found in other studies⁶¹. Individuals with varus alignment had a more severe malalignment than the individuals with valgus alignment³¹. The mean valgus alignment was 3.3° and since 3° was the minimum malalignment required for this study the valgus group displayed a relatively minor malalignment, however other studies report valgus malalignment of $3.9^\circ \pm 2.9^\circ$ ^{31,61}. The varus group's mean alignment of 10.3° is higher than the malalignment of $5.0^\circ \pm 3.7^\circ$ reported in previous studies^{31,61}.

7.2.2 BMI

The mean body mass index (BMI) was consistent with that seen in the general Canadian population⁷⁷. Both the varus and the valgus groups had mean body mass index's (BMI's) in the overweight range. In the varus group two individuals were obese, one was overweight and two were in the normal range. In the valgus group one individual was obese, one was overweight and three were in the normal range. Obesity (but not being overweight) is a risk factor of OA^{68,69} therefore obesity may be related to OA in the three individuals who were obese but not to the study sample as a whole. Because the majority of individuals in this study were in the normal weight range we believe that the risk factor of alignment could be adequately isolated to obtain meaningful results.

7.2.3 WOMAC

The results of the WOMAC were consistent with those of individuals suffering from early OA. The questionnaire studies the clinical symptoms of osteoarthritis in a specified joint¹². The results showed no significant difference in clinical symptoms of pain, stiffness or difficulty carrying out daily activities between the varus and valgus groups. The scores in all categories were all quite low, confirming that this study was in fact examining a group with clinical symptoms of early knee osteoarthritis. As previously mentioned, clinical symptoms of osteoarthritis do not correlate well with radiographic evidence of the disease (joint space narrowing and osteophytes). Therefore even though the groups have similar clinical severity this does not suggest that their state of cartilage health should be similar.

7.2.4 Cartilage Morphology and Alignment

7.2.4.1 Comparison to Normal Cartilage

When comparing the absolute values of total cartilage morphology to those reported in the literature for normal individuals the results suggest some cartilage degeneration has occurred. Our finding of patellar cartilage volume of 3.80 ± 1.08 ml for the varus group (predominantly men) was consistent with the normal range for men reported in the literature, which has been reported to be 4.22 ± 0.77 ml³³ and 3.56 ± 0.48 ml⁶⁴ for men. The valgus group's (all women) patellar volume measurement was 1.67 ± 0.58 ml which is lower than reported normal values of 2.87 ± 0.89 ³³ and 2.97 ± 0.72 ml⁶⁴ for women. The standard deviation for our varus group was much larger than those reported in the literature which is not surprising because some individuals may have had

more severe OA. Also it must be noted that the measure of volume in the valgus group appears to be normal however it is not uncommon for inflammation of the cartilage to occur in early stages of OA¹⁹. We found the mean thickness measurement in the normal range for the varus group to be 2.32 ± 0.50 mm which was slightly lower than the value reported in the literature for men of 2.93 ± 0.42 mm⁶⁴. For the valgus group we found the mean thickness to be 1.07 ± 0.44 mm which again was lower than the value of 2.20 ± 0.43 mm reported in the literature⁶⁴. Cartilage degeneration in the valgus group appears to have progressed further than in the varus group.

7.2.4.2 Compartment Specific Progression of OA

It is not surprising that we did not observe a compartment specific difference in cartilage degeneration between the varus and valgus groups. Previous studies that found a compartment specific difference^{31,61} defined progression as a change in Kellgran-Lawrence grade in one compartment only using radiography. Cartilage morphology was not assessed. Joint space narrowing, the radiographic measure of cartilage degeneration, does not occur until later Kellgran-Lawrence grades (Section 2.3.2.2). In the valgus group we saw a 15% less percentage cartilage coverage in the lateral compartment. After carrying out a power analysis we found that for this difference to be significant we would require 30 individuals in each group. The study was in not powered sufficiently to find a significant difference in percentage cartilage coverage between the medial and lateral compartments.

7.2.5 Kinematics and Alignment

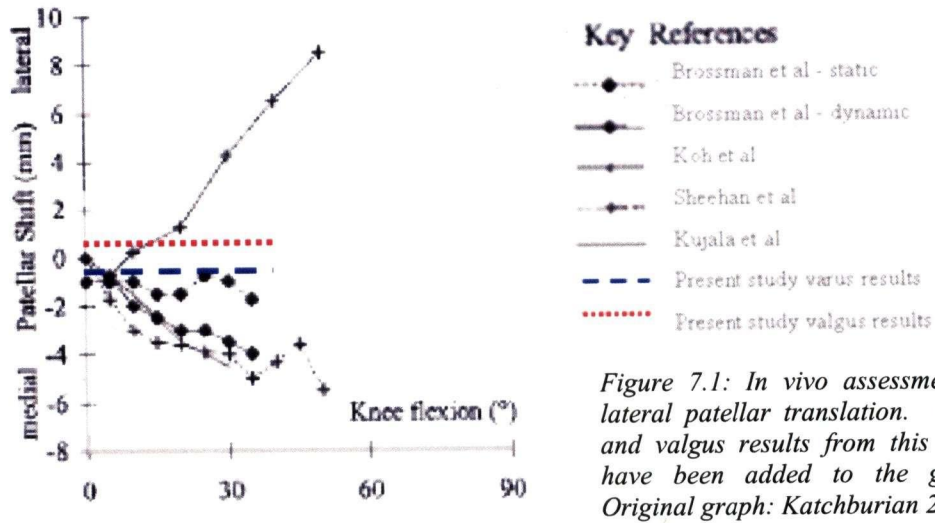
Comparing three-dimensional patellar kinematics to other literature is difficult because patterns of normal patellar tracking remain unclear. One reason for this is that there is not agreement on which parameters should be studied. The most commonly studied parameters are lateral patellar shift or translation, lateral patellar tilt and spin (internal/external rotation). Some groups consider only rotational parameters¹⁴⁸, some study two-dimensional parameters from three-dimensional models¹⁸² and others study every parameter possible about many different coordinate axes¹³⁵. It is also difficult to compare measured parameters in these instances because there is no consensus about how the coordinate systems should be defined. Parameters are highly dependent on the origin of the coordinate system as well as the bony landmarks chosen to determine axes directions. There have been attempts to standardize coordinate systems²⁶ however this has yet to be widely accepted. We used a coordinate system similar to that used by some groups^{161,162}, but very different from others¹⁸². Some groups did not report the details of axes assignment¹³⁶.

Groups have also suggested that the direction of movement will affect the measured values. For example, the position of the patella at 30° of tibiofemoral flexion may be dependant on whether the tibiofemoral joint is on a path of flexion or extension. This phenomenon has been shown in a gait study¹¹⁴. Differences in patellar position have also been observed when static and dynamic methods have been used²², therefore care must be taken when comparing static and dynamic studies. Finally, factors such as loading and muscle actions can affect the location of the patella. Some groups apply axial loads^{67,136}, torsional loads¹⁸² or no load¹⁴⁸. Some groups have observed that the type

of muscle contraction (concentric, eccentric or isometric) can also affect patellar position. The aim of most studies is to achieve a loading condition which mimics the movement from standing and bending in a weight-bearing position while others are attempting to mimic patterns of gait. The limitation of all imaging studies to date is the supine, prone or side position that loading is carried out in. All of these differences in methodology make numerical comparisons between studies and the establishment of normal values difficult therefore comparing patterns of tracking between studies is a more reasonable approach.

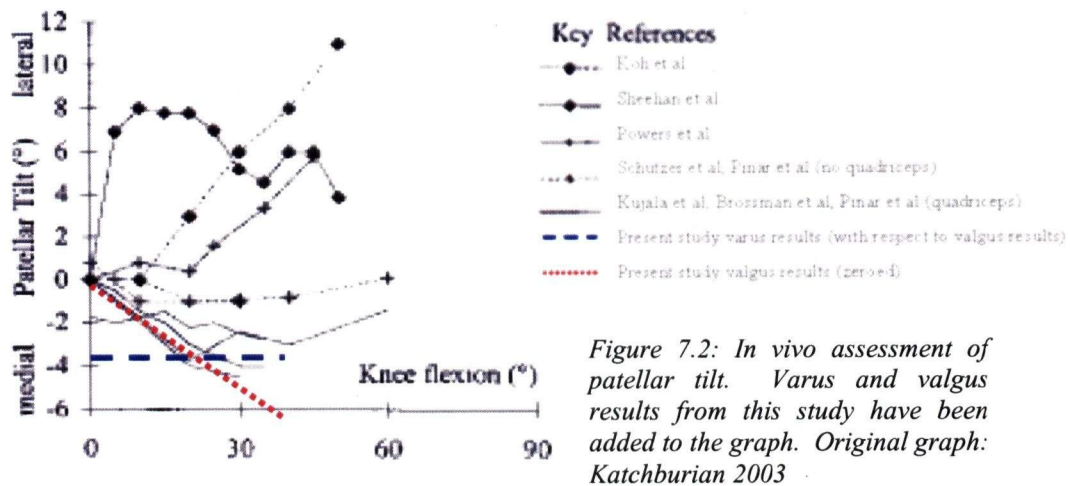
7.2.5.1 Lateral Translation

Our finding was different from that seen in previous *in vivo* studies which have shown a medial shift of between 4-5.5mm in early angles of knee flexion (0° to 30°) but no consensus in later angles of flexion¹⁰⁵. Some studies showed a lateral translation and other showed a constant or increase in the medial translation in greater angles of flexion (Figure 7.1)¹⁰⁵. In particular, one group found a parabolic shape of medial translation, beginning at 0mm at -10° of flexion, peaking at 3.2mm of medial translation at 30° flexion and returning to a central location (0mm) at 60° of flexion¹³⁵.



7.2.5.2 Tilt

Our finding of a constant angle of approximately 10° of medial tilt for the varus group and an increasing in medial tilt at a rate of approximately 2° per 10° in the valgus group was consistent with some studies and inconsistent with others. Other *in vivo* imaging based studies showed a parabolic pattern of tilt beginning and ending at 0° for 10° and 60° of knee flexion and peaking at 4.4° of medial tilt at 30° of knee flexion¹³⁵ and a constant angle of medial tilt at approximately 10° at knee angles between 10° and 30° of knee flexion⁹². A synthesis of *in vivo* studies, found patterns of patellar tilt were variable between studies, some increasing and others decreasing (Figure 7.2)¹⁰⁵.



7.2.5.3 Spin

Our findings were not consistent with those found in the literature. However there is not consensus between many studies. One *in vivo* MRI based studies revealed a similar finding consistent angle of external spin of 5° ¹⁴⁸ and the other an increasing angle of external spin beginning at 1° at -10° of knee flexion (internal spin position), then -2° at 30° of flexion and finally -5° at 60° of knee flexion¹³⁵. There is no clear pattern of spin between studied other *in vivo* studies (Figure 7.3)¹⁰⁵. Our results were very similar to those reported by Sheehan et al because similar coordinate systems were used, the coordinate system used by Patel et al is not described in detail and therefore it is uncertain whether or not this is the source of differences.

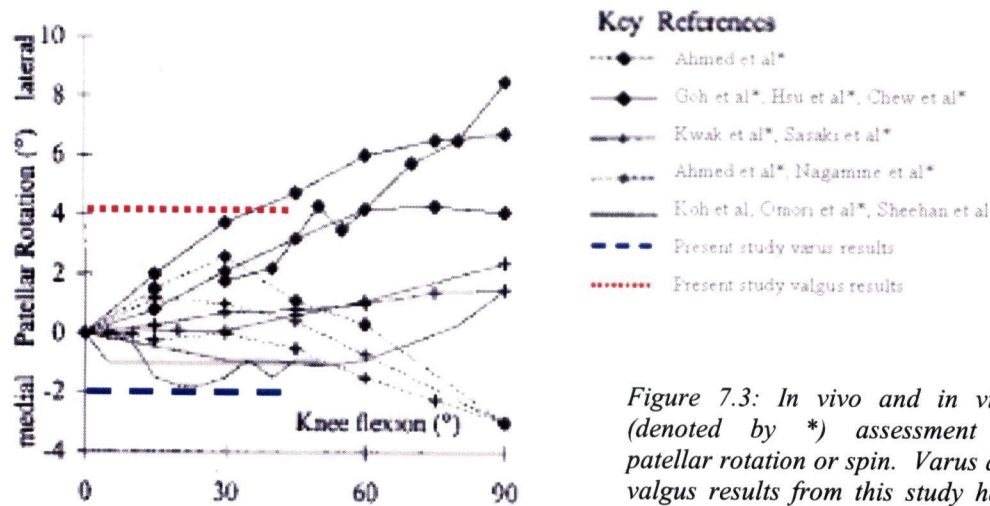


Figure 7.3: In vivo and in vitro (denoted by *) assessment of patellar rotation or spin. Varus and valgus results from this study have been added to the graph. Original graph: Katchburian 2003

7.2.5.4 Patellar Flexion, Proximal Translation and Anterior Translation

Our finding of patellar flexion and distal translations with tibiofemoral flexion is consistent with the literature. The rate of patellar flexion was slightly lower than that of tibiofemoral flexion and the rate of distal translation was approximately 5 mm per 10° of knee flexion. These results are consistent with those reported in the literature^{135,148}, however most groups do not measure this parameter. No other groups have presented results regarding anterior translation. However previous results from our lab have shown a relatively constant anterior position at 25 mm which is consistent with the valgus group results. The varus group's patellae are positioned more anteriorly than seen previously.

7.2.5.5 Patellar Kinematics in OA

Our results for lateral translation and patellar tilt of the varus group were similar to those reported in a study examining patellar kinematics in varus knees in early OA⁹². This study assessed only these two three-dimensional kinematic parameters and did so at 0°, 30° and 90° only. No difference in mediolateral translation at 0° and 30° was found

and the patella was centred in the trochlear groove. The healthy volunteers in this study showed a significant increase in medial shift from 0.1 mm at 0° of flexion to 1.6 mm at 30° of flexion⁹². Both our varus and valgus groups displayed a constant magnitude of translation and the mean value of translation was approximately 0 mm (centred in the trochlear groove). In the other study, the varus group displayed no difference in tilt at 0° or 30° with a constant tilt of approximately 9°. The normal group in this study showed a significant increase medial tilt of 2.7° between 0° and 30° of knee flexion⁹². In our study the varus group displayed a constant medial tilt at approximately 10° and the valgus group displayed an increasing medial tilt at a rate of approximately 2° per 10° of tibiofemoral flexion. The results for the varus group were similar to those of our varus group and the results of the normal group were slightly lower than those of our valgus group.

7.3 Analysis of the Results

7.3.1 Input Device Study

The input device study was designed to determine whether new interactive computer technology improves speed and resegmentation precision (reproducibility) of qMRI. These input devices had not previously been evaluated in the context of cartilage segmentation. Segmenting using the interactive touch-sensitive screen reduced manual segmentation times by approximately 15%. All input devices produced consistent results (no systematic bias) and similar precision errors. This suggests that using different input devices within one study (due to the preferences of different users, to reduce fatigue of the user by changing position, to increase user comfort) will not produce a systematic bias in the results. The consistency between segmentation input devices suggests that qMRI results depend on how the user views the image and defines the cartilage volume, and that this process is not influenced substantially by a particular input device for segmentation. The differences seen between input devices are small enough to not adversely affect study results.

7.3.2 Cartilage Morphology and Varus/Valgus Alignment

Results suggest that cartilage degeneration is in a slightly more advanced in the valgus group. It was not surprising that there was a difference in surface area and volume between the varus and valgus groups because the distribution of gender was not equal between groups. A larger surface area and volume was found in the varus group which was 80% male. The mean cartilage thickness and normalized cartilage volume were also significantly greater for the varus group, however this finding is likely an

indication that the valgus group is in a slightly more advanced stage of cartilage degeneration because these parameters are independent of joint size. It was surprising that no difference was seen for bone/cartilage interface at the patella because this is an indicator of joint size and we would assume a difference in this parameter due to the gender distribution. No difference in percentage cartilage coverage was observed likely because of the large standard deviation observed in the valgus group. The differences in cartilage morphology between groups may be attributed to a few individuals with more advanced OA. The apparent difference in stage of OA according to the amount of cartilage degeneration is not consistent with our assessment of the clinical/symptomatic progression of the disease using the WOMAC questionnaire.

This study did not reveal a compartment specific degeneration of cartilage in the varus or valgus groups. This may be due to the insufficient power of the study (Section 7.2.4.2) or because we were studying a group of individuals with early knee osteoarthritis. In later stages of OA this relationship may become more apparent. We assessed differences in cartilage morphology which is different from previous groups who assessed radiographic OA^{31,61}. The assessment of cartilage in radiographic OA is done indirectly by measuring the space that the cartilage is assumed to fill. Previous studies have not assessed the relationship between alignment and cartilage morphology and therefore it is possible that this relationship does not exist.

7.3.3 Three-dimensional Patellar Kinematics and Varus/Valgus Alignment

The pattern of patellar tracking in individuals with varus and valgus alignment appears to be different from those seen in other *in vivo* imaging based studies. The

differences seen may be due to the state of the osteoarthritic cartilage, as compared to normal, healthy cartilage. The change in lubrication of the joint surfaces may create friction that restricts the patella from travelling along a normal path.

We expected to observe a medial translation the varus group and a lateral translation in the valgus group. Instead we saw no medial or lateral translation in either group. The lateral force may not be large enough to overcome the friction on the surface causing us to see the pattern of constant position of the patella in this plane through the range of knee flexion. The malalignment may also cause changes in contact area. For varus malalignment an increase in medial contact area may be observed, again this would reduce the lateral force thereby reducing possible lateral translation.

We had expected varus alignment to cause medial tilt and valgus alignment to cause lateral tilt. We did not see this pattern. If the distribution of contact pressure shifted to one compartment we would expect to see a tilt in the direction of the excess force. The malalignment in this study may not have been severe enough to produce a measurable effect, especially in the valgus group. Alignment may play a greater role in tilt in deeper angles of knee flexion where the contact pressures are greater but we were unable to study these angles due to the size of the MRI bore.

Our finding of internal spin in the varus group and external spin in the valgus group was consistent with our expectations. The varus and valgus alignment is likely causing the patella to rotate in the direction of the malalignment in order to maintain its position in the trochlear groove. This is a logical finding that has not previously been assessed *in vivo*.

As expected, we saw patellar flexion and distal translation through the range of tibiofemoral flexion. We did however observe a difference between groups. The valgus group presented with what can be interpreted as patella alta. The starting position affects the remainder of the pattern of patellar flexion; therefore it is important to measure this parameter. This finding may be caused by tibiofemoral joint thinning, however we did not measure this parameter. This finding may also be due to changes in the material properties of the patellar ligament. Particularly in women as tensile strength of ligaments may be related to oestrogen¹¹⁷.

We expected the patella to remain in a constant anterior position through the range of flexion. The varus group, however, displayed a more anterior position. Some of the difference in anteriorposterior position can be described by the greater cartilage thickness observed in the varus group, however this accounted for only a small portion of the difference. In the varus group the patella was tilting medially which would also cause an anterior translation of the origin of the patella, as we defined it. Another possible explanation is that anterior translation is a function of patellar and femoral bone geometry which may be independent of alignment and cartilage health altogether.

7.3.4 Three-dimensional Patellar Kinematics and Cartilage Morphology

The relationship between the rate of change of patellar tilt and the proportion of medial to lateral patellar bone/cartilage interface area implies that patellar tilt may be related to the shape of the patella. Bone/cartilage interface describes bone surface area (not to be confused with cartilage surface area). Specifically, we saw that the patella tilted medially at a greater rate if the lateral patellar compartment was proportionally

larger. When the compartmental difference was small enough (the lateral compartment being only slightly larger) we observed a pattern of lateral patellar tilt. This relationship suggests that patellar type influences how the patella tracks. There are 3 types of patella: in type I both compartments are concave and of equal size (10% of population), in type II the medial compartment is smaller and the lateral compartment is concave (65% of population), and in type III the medial compartment is distinctly smaller (25%)¹⁸⁶. This relationship is likely due to the differences in area available for load transferred in each compartment. One possible outcome of this finding is the development of patella type specific treatment strategies for OA.

There appeared to be a moderate relationship between the rate of change of medial tilt and proportion of patellar surface area ($R^2=39\%$) and mean thickness ($R^2=33\%$). The surface area relationship was likely also related to patella type. The mean thickness relationship showed a small increase in rate of lateral tilt with a proportionally greater lateral compartment mean thickness and a small increase in rate of medial tilt with a proportionally greater medial compartment mean thickness. It is to be expected that thinner cartilage in one compartment is related an increased tilt towards that compartment but the relationship to rate of change would require a more detailed analysis of change in mean thickness across the cartilage plate itself.

We found that most individuals showed no change in rate in mediolateral patellar translation when there were very small differences in normalized volume, mean thickness and percentage cartilage coverage between the medial and lateral patellar compartments. The order of fit of the polynomials was increased for these parameters. We found that the R^2 values increased with higher order polynomials. Although we observed what

could be considered a statistically significant relationship with the higher order polynomials the results were in fact influenced by the data points of two individuals and therefore we cannot conclude that a relationship in fact exists. The two individuals that did not follow this pattern showed change in translation through the range of knee flexion. Individual 1 displayed an increasing shift laterally of 0.25 mm per degree of flexion and individual 2 an increasing shift medially of 0.32 mm per degree of flexion. Individual 1 had more significantly more cartilage in the medial compartment which suggests that perhaps lateral compartment degeneration causes an increased rate of lateral translation. Individual 2 had slightly more cartilage in the medial compartment therefore another factor such as bone geometry or joint contact area may be causing the increased rate of medial translation. Given the results of this pilot study we cannot conclude that the rate of change of lateral patellar translation is related to compartmental differences in cartilage morphology.

7.4 Strengths and Limitations

7.4.1 Strengths

One strength of our study is that we used a novel method for assessing three-dimensional patellar kinematics *in vivo*. Our method has been validated for accuracy using a cadaver model. Other patellar kinematic methods have assessed accuracy with a phantom or not at all^{92,135,148}. The intra-subject variability and inter-experimenter repeatability has also been assessed. Other studies have relied heavily on radiography to carry out OA assessment and measurement of lateral patellar translation and tilt from a two-dimensional view. Our method gives a true three-dimensional assessment of joint kinematics.

Using qMRI provides a more complete representation of cartilage degeneration at the patellofemoral joint. qMRI has been validated for accuracy and precision in both healthy and osteoarthritic knees. The analysis identifies regions of cartilage degeneration and it differentiates between the patellar and femoral cartilage. Radiography does not have this ability. By isolating the cartilage of the medial and lateral compartments we were able to relate cartilage degeneration to kinematics. This is different from previous studies that have related compartmental radiographic OA to alignment^{31,61}.

By combining *in vivo* three-dimensional patellar kinematics and qMRI analysis of cartilage morphology we were able to isolate cartilage degeneration from alignment and relate it to patellar kinematics. No other group has studied this relationship to date. Understanding the relationship between patellar movement and cartilage distribution and health is essential in developing treatment strategies for OA.

7.4.2 Limitations

7.4.2.1 Group differences

The gender distribution in this study was unequal between the varus and valgus groups. We have, however, minimized the group related differences by using normalized parameters and ratios. It is common in OA studies to see more women than men and we noted that the mean age of the men was significantly higher than the mean age of the women. This finding is consistent with the demographic of OA sufferers. The valgus group was 100% female and the varus group was 20% female, which has the potential to influence results. Cartilage volume in particular has been shown to be associated with gender; males tend to have more cartilage than females. This relationship has been shown both to be related⁶⁴ and unrelated to height and weight³³. To take into consideration the relationship of volume to joint size, the volume parameter is normalized to bone/cartilage interface. Also, mean cartilage thickness and percentage cartilage coverage are not influenced by joint size. No groups have assessed gender differences in patellar kinematics *in vivo* but it is not unreasonable to assume that bone geometry and joint loading patterns are not different between men and women. Alignment is more likely to affect patellar kinematics than gender. When studying the relationship between cartilage morphology and patellar kinematics we used the ratio of the cartilage parameters to eliminate differences due to size.

In future, full scale studies we will attempt to have an equal gender distribution between the varus and valgus groups. One option is to carry out the study with equal number of men and women in each group. A second option would be to carry out the

study with entirely men or entirely women. By adding a gender component to subject recruitment criteria, gender will no longer be a confounding variable.

7.4.2.2 Three-Dimensional Patellar Kinematics

Loading condition and range of tibiofemoral flexion are key limitations to the method used to assess three-dimensional patellar kinematics. The load applied in this study was only about 10% of what would be expected carrying out an activity such as walking. Also, it was applied while the subject lay supine, therefore the gravitational forces were different than those experienced in a standing position. The loading task was static and most activities that individuals carry out during a normal day, such as walking or climbing stairs, are dynamic. It has been shown that there are differences in three-dimensional patellar kinematics between static and dynamic activities²². The range of tibiofemoral flexion assessed is limited by the size of the MRI bore. Angles of tibiofemoral flexion about approximately 40° could not be assessed. There were also accuracy and precision (repeatability) errors associated with the patellar tracking method which were measured previously⁶⁵. The inter-experimenter error is not of concern in the present study because one experimenter analyzed all datasets. The intra-subject positioning error and the accuracy can be combined using a root mean square calculation to assess the combined error in the method which was less than 2.8° for rotations and less than 1.1 mm for translations.

7.4.2.3 qMRI

Patellar and femoral cartilage morphology was limited by the in-plane resolution and the field of view of the MR scans. The cardiac coil was used to obtain the MR images due to its flexible nature. It allowed us to position the subject's knee at 30° in order to visualize the femoral cartilage however it did not have the capability to collect the data at an in-plane resolution of 0.31 mm. The data was collected at 0.625 mm and interpolated to 0.31 mm. The knee coil is most commonly used in qMRI as it has the ability to collect data at 0.31 mm but does not allow for knee flexion. Also, the field of view limited the amount of femoral cartilage we could assess.

The medial and lateral patellar and femoral compartments were divided in the sagittal plane. This direction is not necessarily normal to the bone/cartilage interface. The division was therefore dependent on the orientation of the acquired image. Another possible method of identifying the medial and lateral compartments would be to create the division normal to the bone/cartilage interface. This method would be consistent with the cartilage morphology algorithms. A small study assessing the most appropriate method of dividing compartments should be carried out.

It would also be advantageous to carry out a principal components analysis to determine if any of the qMRI parameters are associated with one another. In this analysis the key parameters would be identified and expressed as a single factor. This would make the statistical computation less complex.

7.4.2.4 Statistics

We used a linear random effects model to interpret our patellar kinematics data. Because this is a pilot study, we felt that using a linear model was sufficient to assess initial differences between the varus and valgus groups. A higher order random effects model may be used in a larger scale study if it better represents the pattern of tracking.

The study was not powered sufficiently to observe statistically significant differences between compartmental cartilage morphology (medial and lateral) between the varus and valgus groups. We observed a 15% difference between medial and lateral compartments for percentage cartilage coverage. For this size difference to be statistically significant, 30 individuals would be required for each group. Future, full scale studies looking at compartmental cartilage differences should contain this number of subjects per group.

In order to carry out a linear regression we summarized the patellar kinematic parameters and the cartilage morphologic parameters. It was not practical to compare the mean kinematic parameters between individuals due to the large differences in the mean tibiofemoral angle between individuals, therefore it was not used. In our study we examined the rate of change of the kinematic parameter only by comparing the cartilage ratio to each individual's slope. This does not provide any information about the position or orientation of the patella, just the rate at which it is changing. Also, by calculating the ratio of medial to lateral compartment for the mean and rate of change of kinematic parameters we do not obtain any information with regards to the state of cartilage degeneration. Only relative cartilage degeneration can be obtained. Individuals with severe cartilage degeneration are not differentiated from those with minimal

degeneration. A grading system should be implemented into analysis in future studies in order to identify the amount of degeneration that has occurred for each individual.

7.4.2.5 Study Design

The small sample size, early stage of OA and cross-sectional nature of this pilot study were key limitations. Although we only had a small sample we were able to detect differences in some parameters. We could also determine effect size from the pilot data we obtained. Therefore we can ensure to power future full scale studies sufficiently. All of the individuals in our study were in early stages of patellofemoral OA. This was perhaps one reason that we did not see a compartmental difference in cartilage morphology between the varus and valgus groups. Also, we were not able to determine conclusively if compartmental differences in cartilage morphology were related to patellar kinematics. If we'd had subjects with a range of cartilage degeneration this relationship may have been clearer. Our foremost limitation is the cross-sectional nature of this study. We were therefore not able to study any cause and effect relationship related to our research questions. Only associations between parameters could be determined. Longitudinal studies are preferable in OA research due to the often slow progression of the disease. The cause and effect relationship is important when developing OA treatment strategies.

7.5 Contributions and Future Work

7.5.1 Relevance of the Work

We found differences in three-dimensional patellar kinematics between individuals with varus and valgus alignment and knee OA. Previous studies have associated alignment to OA, but alignment is not a measure of relative movement of the bones or loading patterns at the joint^{31,61}. By assessing differences in three-dimensional patellar kinematics with our validated method we are one step closer to understanding the effect of alignment on the local biomechanical environment.

We did not see a compartment difference in cartilage morphology between the varus and valgus groups. Previous studies have focussed on the relationship between radiographic OA and alignment^{31,61}. Joint space narrowing, a surrogate measure of cartilage degeneration, is only one portion of the radiographic definition of OA. In this study we, examined the relationship between cartilage morphology and alignment. It is possible that a relationship between cartilage morphology and alignment does not exist.

To our knowledge, this study is the first to examine the relationship between cartilage morphology and three-dimensional patellar kinematics. We found patellar type, proportional differences in medial and lateral compartment in particular, may influence the rate at which the patella tilts with tibiofemoral flexion. Other possible relationship, such as that between rate of lateral patellar translation and normalized, volume mean thickness and percentage cartilage coverage require further study.

7.5.2 Future Work

Improvements could be made to our patellar kinematic method by attempting to control the angles of tibiofemoral flexion measured. One possible method of doing this is by making markings on the subject's knee that identify the joint centre and the anatomical axes of the femur and the tibia. The goniometer would be consistently positioned for each angle of flexion. The result of this would be a more consistent difference between measured angles of flexion. A more accurate regression fit would be obtained to describe each individual's pattern of patellar kinematics. Also, the mean kinematic value for each measurement would be more similar between individuals and could be used to assess the relationship between the mean magnitude of patellar kinematic parameters and cartilage morphology.

We have shown that patterns of patellar tracking are different between the varus and valgus groups however we do not know which, if any, of these patterns are associated with knee OA. Patellar kinematics of normal, healthy, age-matched individuals should be assessed using our method and a database assembled. We could then establish if the individuals with malalignment show significantly different patterns of patellar tracking than normal individuals. Further, the relationship between alignment and OA could be assessed by comparing the patterns of patellar kinematics of individuals with varus or valgus alignment, with and without OA.

Our study did not find a compartment specific relationship between cartilage morphology and alignment however a sufficiently powered study might. A study containing 30 individuals in each group with an equal gender distribution has the potential to display a compartmental difference in percentage cartilage coverage if in fact

this relationship exists. The relationship between compartmental cartilage morphology and alignment would be better assessed in a longitudinal study because isolated compartmental changes in cartilage could be isolated. Also, by collecting the MRI scans of cartilage at an in-plane resolution of 0.31 mm the edges of the cartilage would be more defined and more accurate results could be obtained.

To further understand the relationship between cartilage morphology and patellar kinematics, a comprehensive study of healthy individuals and individuals with various stages of OA should be carried out. The majority of the group we studied was at comparable stages of cartilage degeneration and showed comparable results in terms of compartmental distribution of cartilage. This was not the ideal group to study this relationship in. By studying both normal individuals and individuals in various stages of cartilage degeneration with and without malalignment a more representative sample of the population would be assessed and possible trends identified.

Results from this pilot study have raised new questions with regards to the cause and effect relationship between patellar kinematics and knee OA. It would be interesting to determine if patellar kinematics change as cartilage degenerates by carrying out a longitudinal study. Our patellar kinematics method is well suited for longitudinal studies because the original anatomical axes can be used at each measurement point so it is sensitive to changes. We also found that patella type was associated with the rate of change of patellar tilt. This raises the question: Are individuals with a certain type of patella more likely to have compartment specific cartilage degeneration? This study would ideally be carried out longitudinally grouping individuals according to patella type in order to assess the progression of cartilage degeneration.

Other aspects of patellofemoral mechanics, such as contact areas, must also be studied *in vivo* to gain understating of the effect of the local biomechanical environment on OA progression. We propose that by adding a contact area assessment to the patellar kinematics method we would be able to establish which features of patellar tracking cause changes in loading patterns. It is likely that abnormal loading patterns lead to OA. Also, it would be beneficial to assess patellar kinematics and contact areas through a larger range of knee flexion. This could be done using an open MRI system. By gaining understanding of the mechanics of the joint better treatment strategies to arrest the onset and progression of OA can be developed.

Chapter 8: Conclusion

In this pilot study, we assessed three-dimensional patellar kinematics and cartilage morphology in individuals with varus/valgus malalignment and early knee OA.

We were able to answer our research questions and our findings are summarized below:

Question 1: Which features of three-dimensional patellar kinematics are associated with valgus alignment and which features are associated with varus alignment?

We found that three-dimensional patellar kinematics were different between the varus and valgus groups.

- The varus group displayed a constant medial patellar tilt of approximately 10° and the valgus group displayed an increasing medial patellar tilt, beginning at approximately 6° of medial tilt, through the range of tibiofemoral flexion.
- Both the varus and valgus groups displayed a constant spin through the range of tibiofemoral flexion, but the patellae of the varus group displayed an internal spin of approximately 2° and the patellae of the valgus group displayed an external spin of approximately 4.5° .
- The patellae of both groups flexed and translated distally at the same rate with increasing tibiofemoral flexion. The patellae of the valgus groups were initially positioned approximately 10 mm more proximal than those of the varus group.
- The valgus group displayed a constant anterior position through the range of tibiofemoral flexion at approximately 25 mm. The varus group displayed a small amount of anterior translation, beginning at approximately 31 mm.

- There was no difference in lateral translation between the varus and valgus groups and the mean amount of translation was approximately 0 mm.

Our findings for the varus group for tilt and lateral translation were consistent with what was found previously⁹². The results for spin were as we expected but the results for lateral translation were not. By identifying abnormal patterns of patellar tracking, treatment strategies aimed at correcting these patterns, such as physiotherapy programs and orthotics, can be developed.

Question 2: Is local, compartmental patellofemoral cartilage morphology associated with varus or valgus alignment?

We did not find local, compartmental cartilage morphology to be associated with varus or valgus alignment. We had expected varus alignment to be associated with a reduced amount of cartilage in the medial compartment and valgus alignment to be associated with a reduced amount of cartilage in the lateral compartment. After carrying out a power analysis we determined that each group would have to contain 30 individuals to find a significant difference. There are two other possible reasons to explain why this relationship was not seen. First, the osteoarthritis was not advanced enough for isolated compartmental cartilage degeneration to have occurred. Second, cartilage degeneration is not associated with alignment. Previous studies have shown that alignment may be associated with OA progression³¹ but this was assessed radiographically and joint space narrowing, a surrogate for cartilage degeneration, is only one component in this definition of OA progression.

Question 3: Are specific patterns of three-dimensional patellar kinematics associated with local, compartmental patellar cartilage morphology?

We have shown that the rate of medial patellar tilt was greater in individual's proportionately larger lateral compartment bone/cartilage interface area. A relationship may exist between the rate of change in lateral patellar translation and normalized volume, mean thickness and percentage cartilage coverage. However this relationship was influenced by a small number of data points. This relationship requires further study in a more diverse sample which includes healthy and OA knees and varying degrees of malalignment. There may also be value in examining the relationship between mean kinematic parameters and cartilage morphology in the future.

In this pilot study we found differences in patellar kinematics between the varus and valgus groups, some of which were unexpected. We found these differences despite the relatively small samples size for each group which suggests that the differences in patterns of patellar kinematics between groups was quite strong. We expected lateral translation to be related to valgus alignment and medial translation to be related to varus alignment. This was not the case. The pattern of patellar spin was as we expected. Treatment strategies are currently implemented on the basis that the patterns of patellar kinematics are as we would expect them to be. The expected patterns are based on assumptions made with regards to how the patella will likely move and not on measured values. Our results may influence treatment interventions that aim to correct abnormal patterns of patellar tracking.

We also assessed the relationship between compartmental cartilage morphology and alignment, which is different from previous studies that most often assess the relationship between radiographic OA and alignment. Mean cartilage thickness and percentage cartilage coverage are a more accurate measure of cartilage degeneration in the joint than joint space narrowing measurement from radiography. However, cartilage degeneration is just one component of OA progression. It is possible that alignment may be associated with other OA indicators, such as the presence of osteophytes, and not cartilage degeneration. We also related compartmental cartilage morphology and rates of change patellar kinematics but no clear associations were found. If a relationship were to exist it would likely be between tilt and/or lateral translation and compartmental mean thickness and/or percentage cartilage coverage as these are more direct measures of cartilage degeneration.

In conclusion, the common aim in answering our three research questions was to provide information that will improve treatment strategies to arrest the onset and progression of patellofemoral OA. By gaining a better understanding of the local biomechanical environment at the patellofemoral joint and its relationship to cartilage degeneration, pathological features can be identified and interventions to correct the abnormalities carried out. Better treatment strategies are needed to improve the quality of life of individuals suffering from this debilitating disease.

References

1. Aglietti P, Insall JN, Cerulli G. Patellar pain and incongruence. I: Measurements of incongruence. *Clin Orthop* 1983; 217-24.
2. Ahmed AM, Burke DL, Hyder A. Force analysis of the patellar mechanism. *J Orthop Res* 1987; 5:69-85.
3. Ahmed AM, Burke DL, Yu A. In-vitro measurement of static pressure distribution in synovial joints--Part II: Retropatellar surface. *J Biomech Eng* 1983; 105:226-36.
4. Arroll B, Goodyear-Smith F. Corticosteroid injections for osteoarthritis of the knee: meta-analysis. *BMJ* 2004; 328:869
5. Asano T, Akagi M, Koike K, Nakamura T. In vivo three-dimensional patellar tracking on the femur. *Clin Orthop* 2003; 222-32.
6. Ateshian GA, Soslowky LJ, Mow VC. Quantitation of articular surface topography and cartilage thickness in knee joints using stereophotogrammetry. *J Biomech* 1991; 24:761-76.
7. Badley EM. The economic burden of musculoskeletal disorders in Canada is similar to that for cancer, and may be higher. *J Rheumatol* 1995; 22:204-6.
8. Badley EM, Wang PP. Arthritis and the aging population: projections of arthritis prevalence in Canada 1991 to 2031. *J Rheumatol* 1998; 25:138-44.
9. Baici A, Bradamante P. Interaction between human leukocyte elastase and chondroitin sulfate. *Chem Biol Interact* 1984; 51:1-11.
10. Baici A, Salgam P, Fehr K, Boni A. Inhibition of human elastase from polymorphonuclear leucocytes by a glycosaminoglycan polysulfate (Arteparon). *Biochem Pharmacol* 1980; 29:1723-7.
11. Baker KR, Xu L, Zhang Y, Nevitt M, Niu J, Aliabadi P, et al. Quadriceps weakness and its relationship to tibiofemoral and patellofemoral knee osteoarthritis in Chinese: the Beijing osteoarthritis study. *Arthritis Rheum* 2004; 50:1815-21.
12. Bellamy N, Buchanan WW, Goldsmith CH, Campbell J, Stitt LW. Validation study of WOMAC: a health status instrument for measuring clinically important patient relevant outcomes to antirheumatic drug therapy in patients with osteoarthritis of the hip or knee. *J Rheumatol* 1988; 15:1833-40.
13. Bellamy N, Campbell J, Stevens J, Pilch L, Stewart C, Mahmood Z. Validation study of a computerized version of the Western Ontario and McMaster Universities VA3.0 Osteoarthritis Index. *J Rheumatol* 1997; 24:2413-5.
14. Berman BM, Lao L, Greene M, Anderson RW, Wong RH, Langenberg P, et al. Efficacy of traditional Chinese acupuncture in the treatment of symptomatic knee osteoarthritis: a pilot study. *Osteoarthritis Cartilage* 1995; 3:139-42.
15. Berman BM, Singh BB, Lao L, Langenberg P, Li H, Hadhazy V, et al. A randomized trial of acupuncture as an adjunctive therapy in osteoarthritis of the knee. *Rheumatology (Oxford)* 1999; 38:346-54.

16. Besl P. J., McKay ND. A method for registration of 3-D shapes. *IEEE Transaction on Pattern Analysis and Machine Intelligence* 1992; 14:239-255.
17. Boegard T, Rudling O, Petersson IF, Sanfridsson J, Saxne T, Svensson B, et al. Joint-space width in the axial view of the patello-femoral joint. Definitions and comparison with MR imaging. *Acta Radiol* 1998; 39:24-31.
18. Borgefors G. Distance transformations in digital images. *Compu Vision Graphics Image Processing* 1986; 34:344-71.
19. Brandt KD, Doherty M, Lohmander S. *Osteoarthritis*. 2nd ed ed. Oxford ;, New York : Oxford University Press, 2003.
Notes: LC Control Number: 2003272260
Includes bibliographical references and index
20. Bremander AB, Petersson IF, Roos EM. Validation of the Rheumatoid and Arthritis Outcome Score (RAOS) for the lower extremity. *Health Qual Life Outcomes* 2003; 1:55
21. Brooks LO; Rolfe MI, Cheras PA, Myers SP. The comprehensive osteoarthritis test: a simple index for measurement of treatment effects in clinical trials. *J Rheumatol* 2004; 31:1180-6.
22. Brossmann J, Muhle C, Bull CC, Schroder C, Melchert UH, Zieplies J, et al. Evaluation of patellar tracking in patients with suspected patellar malalignment: cine MR imaging vs arthroscopy. *AJR Am J Roentgenol* 1994; 162:361-7.
23. Brossmann J, Muhle C, Schroder C, Melchert UH, Bull CC, Spielmann RP, et al. Patellar tracking patterns during active and passive knee extension: evaluation with motion-triggered cine MR imaging. *Radiology* 1993; 187:205-12.
24. Buckland-Wright C. Protocols for precise radio-anatomical positioning of the tibiofemoral and patellofemoral compartments of the knee. *Osteoarthritis Cartilage* 1995; 3 Suppl A:71-80.
25. Buckwalter JA, Mankin HJ. Articular cartilage: degeneration and osteoarthritis, repair, regeneration, and transplantation. *Instr Course Lect* 1998; 47:487-504.
26. Bull AM, Katchburian MV, Shih YF, Amis AA. Standardisation of the description of patellofemoral motion and comparison between different techniques. *Knee Surg Sports Traumatol Arthrosc* 2002; 10:184-93.
27. Burgkart R, Glaser C, Hyhlik-Durr A, Englmeier KH, Reiser M, Eckstein F. Magnetic resonance imaging-based assessment of cartilage loss in severe osteoarthritis: accuracy, precision, and diagnostic value. *Arthritis Rheum* 2001; 44:2072-7.
28. Burgkart R, Glaser C, Hyhlik-Durr A, Englmeier KH, Reiser M, Eckstein F. Magnetic resonance imaging-based assessment of cartilage loss in severe osteoarthritis: accuracy, precision, and diagnostic value. *Arthritis Rheum* 2001; 44:2072-7.
29. Burstein D, Velyvis J, Scott KT, Stock KW, Kim YJ, Jaramillo D, et al. Protocol issues for delayed Gd(DTPA)(2-)-enhanced MRI (dGEMRIC) for clinical evaluation of articular cartilage. *Magn Reson Med* 2001; 45:36-41.
30. Cahue S, Dunlop D, Hayes K, Song J, Torres L, Sharma L. Varus-valgus alignment in the progression of patellofemoral osteoarthritis. *Arthritis Rheum* 2004; 50:2184-90.

31. Cahue S, Dunlop D, Hayes K, Song J, Torres L, Sharma L. Varus-valgus alignment in the progression of patellofemoral osteoarthritis. *Arthritis Rheum* 2004; 50:2184-90.
32. Cicuttini F, Forbes A, Asbeutah A, Morris K, Stuckey S. Comparison and reproducibility of fast and conventional spoiled gradient-echo magnetic resonance sequences in the determination of knee cartilage volume. *J Orthop Res* 2000; 18:580-4.
33. Cicuttini F, Forbes A, Morris K, Darling S, Bailey M, Stuckey S. Gender differences in knee cartilage volume as measured by magnetic resonance imaging. *Osteoarthritis Cartilage* 1999; 7:265-71.
34. Cicuttini F, Wluka A, Hankin J, Wang Y. Longitudinal study of the relationship between knee angle and tibiofemoral cartilage volume in subjects with knee osteoarthritis. *Rheumatology (Oxford)* 2004; 43:321-4.
35. Cicuttini FM, Wluka AE, Stuckey SL. Tibial and femoral cartilage changes in knee osteoarthritis. *Ann Rheum Dis* 2001; 60:977-80.
36. Cicuttini FM, Wluka AE, Wang Y, Stuckey SL. Longitudinal study of changes in tibial and femoral cartilage in knee osteoarthritis. *Arthritis Rheum* 2004; 50:94-7.
37. Coggon D, Reading I, Croft P, McLaren M, Barrett D, Cooper C. Knee osteoarthritis and obesity. *Int J Obes Relat Metab Disord* 2001; 25:622-7.
38. Cohen ZA, McCarthy DM, Kwak SD, Legrand P, Fogarasi F, Ciaccio EJ, et al. Knee cartilage topography, thickness, and contact areas from MRI: in-vitro calibration and in-vivo measurements. *Osteoarthritis Cartilage* 1999; 7:95-109.
39. Cohen ZA, Mow VC, Henry JH, Levine WN, Ateshian GA. Templates of the cartilage layers of the patellofemoral joint and their use in the assessment of osteoarthritic cartilage damage. *Osteoarthritis Cartilage* 2003; 11:569-79.
40. Cohen ZA, Mow VC, Henry JH, Levine WN, Ateshian GA. Templates of the cartilage layers of the patellofemoral joint and their use in the assessment of osteoarthritic cartilage damage. *Osteoarthritis Cartilage* 2003; 11:569-79.
41. Cole GK, Nigg BM, Ronsky JL, Yeadon MR. Application of the joint coordinate system to three-dimensional joint attitude and movement representation: a standardization proposal. *J Biomech Eng* 1993; 115:344-9.
42. Cooke TD, Li J, Scudamore RA. Radiographic assessment of bony contributions to knee deformity. *Orthop Clin North Am* 1994; 25:387-93.
43. Cooper C, McAlindon T, Snow S, Vines K, Young P, Kirwan J, et al. Mechanical and constitutional risk factors for symptomatic knee osteoarthritis: differences between medial tibiofemoral and patellofemoral disease. *J Rheumatol* 1994; 21:307-13.
44. Cushnaghan J, McCarthy C, Dieppe P. Taping the patella medially: a new treatment for osteoarthritis of the knee joint? *BMJ* 1994; 308:753-5.
45. D'Agata SD, Pearsall AW 4th, Reider B, Draganich LF. An in vitro analysis of patellofemoral contact areas and pressures following procurement of the central one-third patellar tendon. *Am J Sports Med* 1993; 21:212-9.

46. Danielsson P.E. Euclidean distance mapping. *Computer Graphics and Image Processing* 1980; 14:227-48.
47. Deal CL, Schnitzer TJ, Lipstein E, Seibold JR, Stevens RM, Levy MD, et al. Treatment of arthritis with topical capsaicin: a double-blind trial. *Clin Ther* 1991; 13:383-95.
48. Derek T, Cooke V, Kelly BP, Harrison L, Mohamed G, Khan B. Radiographic grading for knee osteoarthritis. A revised scheme that relates to alignment and deformity. *J Rheumatol* 1999; 26:641-4.
49. Duffy GP, Trousdale RT, Stuart MJ. Total knee arthroplasty in patients 55 years old or younger. 10- to 17-year results. *Clin Orthop* 1998; 22-7.
50. Eckstein F, Buck RJ, Charles HC, Hudelmaier M, Wirth W, Kraus V, et al. IMPROVED PRECISION OF QUANTITATIVE CARTILAGE MEASUREMENTS WITH MAGNETIC RESONANCE IMAGING AT 3 TESLA. *Osteoarthritis and Cartilage* in press; Abstract.
51. Eckstein F, Gavazzeni A, Sittek H, Haubner M, Losch A, Milz S, et al. Determination of knee joint cartilage thickness using three-dimensional magnetic resonance chondro-crassometry (3D MR-CCM). *Magn Reson Med* 1996; 36:256-65.
52. Eckstein F, Gavazzeni A, Sittek H, Haubner M, Losch A, Milz S, et al. Determination of knee joint cartilage thickness using three-dimensional magnetic resonance chondro-crassometry (3D MR-CCM). *Magn Reson Med* 1996; 36:256-65.
53. Eckstein F, Heudorfer L, Faber SC, Burgkart R, Englmeier KH, Reiser M. Long-term and resegmentation precision of quantitative cartilage MR imaging (qMRI). *Osteoarthritis Cartilage* 2002; 10:922-8.
54. Eckstein F, Heudorfer L, Faber SC, Burgkart R, Englmeier KH, Reiser M. Long-term and resegmentation precision of quantitative cartilage MR imaging (qMRI). *Osteoarthritis Cartilage* 2002; 10:922-8.
55. Eckstein F, Lemberger B, Stammberger T, Englmeier KH, Reiser M. Patellar cartilage deformation in vivo after static versus dynamic loading. *J Biomech* 2000; 33:819-25.
56. Eckstein F, Schnier M, Haubner M, Priebsch J, Glaser C, Englmeier KH, et al. Accuracy of cartilage volume and thickness measurements with magnetic resonance imaging. *Clin Orthop* 1998; 137-48.
57. Eckstein F, Stammberger T, Priebsch J, Englmeier KH, Reiser M. Effect of gradient and section orientation on quantitative analysis of knee joint cartilage. *J Magn Reson Imaging* 2000; 11:161-7.
58. Eckstein F, Tieschky M, Faber SC, Haubner M, Kolem H, Englmeier KH, et al. Effect of physical exercise on cartilage volume and thickness in vivo: MR imaging study. *Radiology* 1998; 207:243-8.
59. Eckstein F, Westhoff J, Sittek H, Maag KP, Haubner M, Faber S, et al. In vivo reproducibility of three-dimensional cartilage volume and thickness measurements with MR imaging. *AJR Am J Roentgenol* 1998; 170:593-7.
60. Elahi S, Cahue S, Felson DT, Engelman L, Sharma L. The association between varus-valgus alignment and patellofemoral osteoarthritis. *Arthritis Rheum* 2000; 43:1874-80.

61. Elahi S, Cahue S, Felson DT, Engelman L, Sharma L. The association between varus-valgus alignment and patellofemoral osteoarthritis. *Arthritis Rheum* 2000; 43:1874-80.
62. Ernst E. Acupuncture as a symptomatic treatment of osteoarthritis. A systematic review. *Scand J Rheumatol* 1997; 26:444-7.
63. Ettinger WH Jr, Burns R, Messier SP, Applegate W, Rejeski WJ, Morgan T, et al. A randomized trial comparing aerobic exercise and resistance exercise with a health education program in older adults with knee osteoarthritis. The Fitness Arthritis and Seniors Trial (FAST). *JAMA* 1997; 277:25-31.
64. Faber SC, Eckstein F, Lukasz S, Muhlbauer R, Hohe J, Englmeier KH, et al. Gender differences in knee joint cartilage thickness, volume and articular surface areas: assessment with quantitative three-dimensional MR imaging. *Skeletal Radiol* 2001; 30:144-50.
65. Fellows, R. A. Magnetic Resonance Imaging for In Vivo Assessment of Three-Dimensional Patellar Tracking: A Study on the Accuracy and Repeatability of a Novel Measurement Protocol. Master's Thesis 2003
66. Fellows RA, Hill NA, Gill HS, MacIntyre NJ, Harrison MM, Ellis RE, et al. Magnetic resonance imaging for *in vivo* assessment of three-dimensional patellar tracking: the repeatability of a new measurement technique. *Journal of Magnetic Resonance Imaging* accepted;
67. Fellows RA, Hill NA, Gill HS, MacIntyre NJ, Harrison MM, Ellis RE, et al. Magnetic Resonance Imaging for *In Vivo* Assessment of Three-Dimensional Patellar Tracking. *Journal of Biomechanics* In Press;
68. Felson DT, Anderson JJ, Naimark A, Walker AM, Meenan RF. Obesity and knee osteoarthritis. The Framingham Study. *Ann Intern Med* 1988; 109:18-24.
69. Felson DT, Lawrence RC, Dieppe PA, Hirsch R, Helmick CG, Jordan JM, et al. Osteoarthritis: new insights. Part 1: the disease and its risk factors. *Ann Intern Med* 2000; 133:635-46.
70. Felson DT, Lawrence RC, Hochberg MC, McAlindon T, Dieppe PA, Minor MA, et al. Osteoarthritis: new insights. Part 2: treatment approaches. *Ann Intern Med* 2000; 133:726-37.
71. Felson DT, Radin EL. What causes knee osteoarthrosis: are different compartments susceptible to different risk factors? *J Rheumatol* 1994; 21:181-3.
72. Felson DT, Zhang Y. An update on the epidemiology of knee and hip osteoarthritis with a view to prevention. *Arthritis Rheum* 1998; 41:1343-55.
73. Felson DT, Zhang Y, Anthony JM, Naimark A, Anderson JJ. Weight loss reduces the risk for symptomatic knee osteoarthritis in women. The Framingham Study. *Ann Intern Med* 1992; 116:535-9.
74. Ficat P, Ficat C, Bailleux A. [External hypertension syndrome of the patella. Its significance in the recognition of arthrosis]. *Rev Chir Orthop Reparatrice Appar Mot* 1975; 61:39-59.
75. Fisher NM, Pendergast DR, Gresham GE, Calkins E. Muscle rehabilitation: its effect on muscular and functional performance of patients with knee osteoarthritis. *Arch Phys Med Rehabil* 1991; 72:367-74.

76. Fries JF, Carey C, McShane DJ. Patient education in arthritis: randomized controlled trial of a mail-delivered program. *J Rheumatol* 1997; 24:1378-83.
77. Gilmore J. Body Mass Index and Health. *Statistics Canada* 1999; 11:31-43.
78. Glaser C, Burgkart R, Kutschera A, Englmeier KH, Reiser M, Eckstein F. Femoro-tibial cartilage metrics from coronal MR image data: Technique, test-retest reproducibility, and findings in osteoarthritis. *Magn Reson Med* 2003; 50:1229-36.
79. Glaser C, Faber S, Eckstein F, Fischer H, Springer V, Heudorfer L, et al. Optimization and validation of a rapid high-resolution T1-w 3D FLASH water excitation MRI sequence for the quantitative assessment of articular cartilage volume and thickness. *Magn Reson Imaging* 2001; 19:177-85.
80. Gluer CC, Blake G, Lu Y, Blunt BA, Jergas M, Genant HK. Accurate assessment of precision errors: how to measure the reproducibility of bone densitometry techniques. *Osteoporos Int* 1995; 5:262-70.
81. Goodfellow J, Hungerford DS, Zindel M. Patello-femoral joint mechanics and pathology. 1. Functional anatomy of the patello-femoral joint. *J Bone Joint Surg Br* 1976; 58:287-90.
82. Graichen H, Springer V, Flaman T, Stammberger T, Glaser C, Englmeier KH, et al. Validation of high-resolution water-excitation magnetic resonance imaging for quantitative assessment of thin cartilage layers. *Osteoarthritis Cartilage* 2000; 8:106-14.
83. Graichen H, von Eisenhart-Rothe R, Vogl T, Englmeier KH, Eckstein F. Quantitative assessment of cartilage status in osteoarthritis by quantitative magnetic resonance imaging: technical validation for use in analysis of cartilage volume and further morphologic parameters. *Arthritis Rheum* 2004; 50:811-6.
84. Graichen H, von Eisenhart-Rothe R, Vogl T, Englmeier KH, Eckstein F. Quantitative assessment of cartilage status in osteoarthritis by quantitative magnetic resonance imaging: technical validation for use in analysis of cartilage volume and further morphologic parameters. *Arthritis Rheum* 2004; 50:811-6.
85. Graichen H, von Eisenhart-Rothe R, Vogl T, Englmeier KH, Eckstein F. Quantitative assessment of cartilage status in osteoarthritis by quantitative magnetic resonance imaging: technical validation for use in analysis of cartilage volume and further morphologic parameters. *Arthritis Rheum* 2004; 50:811-6.
86. Grelsamer RP, Weinstein CH. Applied biomechanics of the patella. *Clin Orthop* 2001; 9-14.
87. Grood ES, Suntay WJ. A joint coordinate system for the clinical description of three-dimensional motions: application to the knee. *J Biomech Eng* 1983; 105:136-44.
88. Haubner M, Eckstein F, Schnier M, Losch A, Sittek H, Becker C, et al. A non-invasive technique for 3-dimensional assessment of articular cartilage thickness based on MRI. Part 2: Validation using CT arthrography. *Magn Reson Imaging* 1997; 15:805-13.
89. Health Canada. Policy Research Division: Economic Burden of Illness in Canada 1998
90. Hill, N. A. Magnetic Resonance Imaging for In Vivo Assessment of Three-Dimensional Patellar Tracking: A Study of the Effect of High Tibial Osteotomy on Patellar Tracking. Master's Thesis 2003.

91. Hill, N. A., Fellows, R. A., MacIntyre, N. J., Harrison, M. M., Ellis, R. E., and Wilson, D. R.. The effect of high tibial osteotomy on three-dimensional tibiofemoral and patellofemoral kinematics: an in vivo study using magnetic resonance imaging. Meeting of the Orthopaedic Research Society 2005
92. Hinterwimmer S, von Eisenhart-Rothe R, Siebert M, Welsch F, Vogl T, Graichen H. Patella kinematics and patello-femoral contact areas in patients with genu varum and mild osteoarthritis. *Clin Biomech (Bristol, Avon)* 2004; 19:704-10.
93. Hochberg MC, Altman RD, Brandt KD, Clark BM, Dieppe PA, Griffin MR, et al. Guidelines for the medical management of osteoarthritis. Part II. Osteoarthritis of the knee. American College of Rheumatology. *Arthritis Rheum* 1995; 38:1541-6.
94. Hohe J, Ateshian G, Reiser M, Englmeier KH, Eckstein F. Surface size, curvature analysis, and assessment of knee joint incongruity with MRI in vivo. *Magn Reson Med* 2002; 47:554-61.
95. Hohe J, Ateshian G, Reiser M, Englmeier KH, Eckstein F. Surface size, curvature analysis, and assessment of knee joint incongruity with MRI in vivo. *Magn Reson Med* 2002; 47:554-61.
96. Hohe J, Faber S, Stammberger T, Reiser M, Englmeier KH, Eckstein F. A technique for 3D in vivo quantification of proton density and magnetization transfer coefficients of knee joint cartilage. *Osteoarthritis Cartilage* 2000; 8:426-33.
97. Huberti HH, Hayes WC. Patellofemoral contact pressures. The influence of q-angle and tendofemoral contact. *J Bone Joint Surg Am* 1984; 66:715-24.
98. Huberti HH, Hayes WC, Stone JL, Shybut GT. Force ratios in the quadriceps tendon and ligamentum patellae. *J Orthop Res* 1984; 2:49-54.
99. Hudelmaier M, Glaser C, Englmeier KH, Reiser M, Putz R, Eckstein F. Correlation of knee-joint cartilage morphology with muscle cross-sectional areas vs. anthropometric variables. *Anat Rec* 2003; 270A:175-84.
100. Hungerford DS, Barry M. Biomechanics of the patellofemoral joint. *Clin Orthop* 1979; 9-15.
101. Hyhlik-Durr A, Faber S, Burgkart R, Stammberger T, Maag KP, Englmeier KH, et al. Precision of tibial cartilage morphometry with a coronal water-excitation MR sequence. *Eur Radiol* 2000; 10:297-303.
102. Ivarsson I, Myrner R, Gillquist J. High tibial osteotomy for medial osteoarthritis of the knee. A 5 to 7 and 11 year follow-up. *J Bone Joint Surg Br* 1990; 72:238-44.
103. Iwano T, Kurosawa H, Tokuyama H, Hoshikawa Y. Roentgenographic and clinical findings of patellofemoral osteoarthrosis. With special reference to its relationship to femorotibial osteoarthrosis and etiologic factors. *Clin Orthop* 1990; 190-7.
104. Johnson F, Leitz S, Waugh W. The distribution of load across the knee. A comparison of static and dynamic measurements. *J Bone Joint Surg Br* 1980; 62:346-9.
105. Katchburian MV, Bull AM, Shih YF, Heatley FW, Amis AA. Measurement of patellar tracking: assessment and analysis of the literature. *Clin Orthop* 2003; 241-59.

106. Kauffmann C, Gravel P, Godbout B, Gravel A, Beaudoin G, Raynauld JP, et al. Computer-aided method for quantification of cartilage thickness and volume changes using MRI: validation study using a synthetic model. *IEEE Trans Biomed Eng* 2003; 50:978-88.
107. Keating EM, Faris PM, Ritter MA, Kane J. Use of lateral heel and sole wedges in the treatment of medial osteoarthritis of the knee. *Orthop Rev* 1993; 22:921-4.
108. Kellgren JH, Lawrence JS. *Atlas of Standard Radiographs: The Epidemiology of Chronic Rheumatism*. Oxford: Blackwell, 1963.
109. KELLGREN JH, LAWRENCE JS. Radiological assessment of osteo-arthritis. *Ann Rheum Dis* 1957; 16:494-502.
110. Kirschner S, Walther M, Bohm D, Matzer M, Heesen T, Faller H, et al. German short musculoskeletal function assessment questionnaire (SMFA-D): comparison with the SF-36 and WOMAC in a prospective evaluation in patients with primary osteoarthritis undergoing total knee arthroplasty. *Rheumatol Int* 2003; 23:15-20.
111. Koh TJ, Grabiner MD, De Swart RJ. In vivo tracking of the human patella. *J Biomech* 1992; 25:637-43.
112. Konig A, Walther M, Matzer M, Heesen T, Kirschner S, Faller H. [II. Validity and sensitivity to change of the Musculoskeletal Functional Assessment Questionnaire in primary gonarthrosis and total endoprosthetic joint replacement]. *Z Orthop Ihre Grenzgeb* 2000; 138:302-5.
113. Kshirsagar AA, Watson PJ, Tyler JA, Hall LD. Measurement of localized cartilage volume and thickness of human knee joints by computer analysis of three-dimensional magnetic resonance images. *Invest Radiol* 1998; 33:289-99.
114. Lafortune MA, Cavanagh PR, Sommer HJ 3rd, Kalenak A. Three-dimensional kinematics of the human knee during walking. *J Biomech* 1992; 25:347-57.
115. Lane NE, Kremer LB. Radiographic indices for osteoarthritis. *Rheum Dis Clin North Am* 1995; 21:379-94.
116. Lavernia CJ, Guzman JF, Gachupin-Garcia A. Cost effectiveness and quality of life in knee arthroplasty. *Clin Orthop* 1997; 134-9.
117. Lee CY, Smith CL, Zhang X, Hsu HC, Wang DY, Luo ZP. Tensile forces attenuate estrogen-stimulated collagen synthesis in the ACL. *Biochem Biophys Res Commun* 2004; 317:1221-5.
118. Lerner AL, Tamez-Pena JG, Houck JR, Yao J, Harmon HL, Salo AD, et al. The use of sequential MR image sets for determining tibiofemoral motion: reliability of coordinate systems and accuracy of motion tracking algorithm. *J Biomech Eng* 2003; 125:246-53.
119. Lin F, Makhous M, Chang AH, Hendrix RW, Zhang LQ. In vivo and noninvasive six degrees of freedom patellar tracking during voluntary knee movement. *Clin Biomech (Bristol, Avon)* 2003; 18:401-9.

120. Lin F, Wang G, Koh JL, Hendrix RW, Zhang LQ. In vivo and noninvasive three-dimensional patellar tracking induced by individual heads of quadriceps. *Med Sci Sports Exerc* 2004; 36:93-101.
121. Lorig K, Lubeck D, Kraines RG, Seleznick M, Holman HR. Outcomes of self-help education for patients with arthritis. *Arthritis Rheum* 1985; 28:680-5.
122. Marder WD, Meenan RF, Felson DT, Reichlin M, Birnbaum NS, Croft JD, et al. The present and future adequacy of rheumatology manpower. A study of health care needs and physician supply. *Arthritis Rheum* 1991; 34:1209-17.
123. McAlindon T, Zhang Y, Hannan M, Naimark A, Weissman B, Castelli W, et al. Are risk factors for patellofemoral and tibiofemoral knee osteoarthritis different? *J Rheumatol* 1996; 23:332-7.
124. McAlindon TE, LaValley MP, Gulin JP, Felson DT. Glucosamine and chondroitin for treatment of osteoarthritis: a systematic quality assessment and meta-analysis. *JAMA* 2000; 283:1469-75.
125. McAlindon TE, Snow S, Cooper C, Dieppe PA. Radiographic patterns of osteoarthritis of the knee joint in the community: the importance of the patellofemoral joint. *Ann Rheum Dis* 1992; 51:844-9.
126. McWalter EJ, Wilson DR. Effect of X-ray Tube Position on Joint Space Measurement at the Patellofemoral Joint. *Osteoarthritis and Cartilage* 2003; 11: Abstract.
127. McWalter EJ, Wirth W, Siebert M, von Eisenhart-Rothe R, Hudelmaier M, Wilson DR, et al. Use of novel interactive input devices for segmentation of articular cartilage from magnetic resonance images. *Osteoarthritis Cartilage* In Press;
128. Merchant AC. Patellofemoral imaging. *Clin Orthop* 2001; 15-21.
129. Merchant AC, Mercer RL, Jacobsen RH, Cool CR. Roentgenographic analysis of patellofemoral congruence. *J Bone Joint Surg Am* 1974; 56:1391-6.
130. Minor MA, Hewett JE, Webel RR, Anderson SK, Kay DR. Efficacy of physical conditioning exercise in patients with rheumatoid arthritis and osteoarthritis. *Arthritis Rheum* 1989; 32:1396-405.
131. Moreland JR, Bassett LW, Hanker GJ. Radiographic analysis of the axial alignment of the lower extremity. *J Bone Joint Surg Am* 1987; 69:745-9.
132. Moreland JR, Bassett LW, Hanker GJ. Radiographic analysis of the axial alignment of the lower extremity. *J Bone Joint Surg Am* 1987; 69:745-9.
133. Mow VC, Hayes WC. Basic orthopaedic biomechanics. 2nd ed ed. Philadelphia : Lippincott-Raven, 1997.
Notes: LC Control Number: 97001336
Includes bibliographical references and index
134. Nagaosa Y, Mateus M, Hassan B, Lanyon P, Doherty M. Development of a logically devised line drawing atlas for grading of knee osteoarthritis. *Ann Rheum Dis* 2000; 59:587-95.
135. Patel VV, Hall K, Ries M, Lindsey C, Ozhinsky E, Lu Y, et al. Magnetic resonance imaging of patellofemoral kinematics with weight-bearing. *J Bone Joint Surg Am* 2003; 85-A:2419-24.

136. Patel VV, Hall K, Ries M, Lotz J, Ozhinsky E, Lindsey C, et al. A three-dimensional MRI analysis of knee kinematics. *J Orthop Res* 2004; 22:283-92.
137. Perla R, Frank C, Fick G. The effect of elastic bandages on human knee proprioception in the uninjured population. *Am J Sports Med* 1995; 23:251-5.
138. Peterfy CG, van Dijke CF, Janzen DL, Gluer CC, Namba R, Majumdar S, et al. Quantification of articular cartilage in the knee with pulsed saturation transfer subtraction and fat-suppressed MR imaging: optimization and validation. *Radiology* 1994; 192:485-91.
139. Peterfy CG, van Dijke CF, Janzen DL, Gluer CC, Namba R, Majumdar S, et al. Quantification of articular cartilage in the knee with pulsed saturation transfer subtraction and fat-suppressed MR imaging: optimization and validation. *Radiology* 1994; 192:485-91.
140. Piplani MA, Disler DG, McCauley TR, Holmes TJ, Cousins JP. Articular cartilage volume in the knee: semiautomated determination from three-dimensional reformations of MR images. *Radiology* 1996; 198:855-9.
141. Pollo FE. Clinical gait analysis in biomechanics. *IEEE Eng Med Biol Mag* 1998; 17:32-3.
142. Pollo FE. Bracing and heel wedging for unicompartmental osteoarthritis of the knee. *Am J Knee Surg* 1998; 11:47-50.
143. Radin EL, Rose RM. Role of subchondral bone in the initiation and progression of cartilage damage. *Clin Orthop* 1986; 34-40.
144. Ranawat CS, Flynn WF Jr, Saddler S, Hansraj KK, Maynard MJ. Long-term results of the total condylar knee arthroplasty. A 15-year survivorship study. *Clin Orthop* 1993; 94-102.
145. Ravaud P, Moulinier L, Giraudeau B, Ayrat X, Guerin C, Noel E, et al. Effects of joint lavage and steroid injection in patients with osteoarthritis of the knee: results of a multicenter, randomized, controlled trial. *Arthritis Rheum* 1999; 42:475-82.
146. Raya SP, Udupa JK. Shape-Based Interpolation of Multidimensional Objects. *IEEE Transactions on Medical Imaging* 1990; 9:32-42.
147. Raynauld JP, Kauffmann C, Beaudoin G, Berthiaume MJ, de Guise JA, Bloch DA, et al. Reliability of a quantification imaging system using magnetic resonance images to measure cartilage thickness and volume in human normal and osteoarthritic knees. *Osteoarthritis Cartilage* 2003; 11:351-60.
148. Rebmann AJ, Sheehan FT. Precise 3D skeletal kinematics using fast phase contrast magnetic resonance imaging. *J Magn Reson Imaging* 2003; 17:206-13.
149. Ritter MA, Herbst SA, Keating EM, Faris PM, Meding JB. Long-term survival analysis of a posterior cruciate-retaining total condylar total knee arthroplasty. *Clin Orthop* 1994; 136-45.
150. Roos EM, Lohmander LS. The Knee injury and Osteoarthritis Outcome Score (KOOS): from joint injury to osteoarthritis. *Health Qual Life Outcomes* 2003; 1:64
151. Roos EM, Toksvig-Larsen S. Knee injury and Osteoarthritis Outcome Score (KOOS) - validation and comparison to the WOMAC in total knee replacement. *Health Qual Life Outcomes* 2003; 1:17

152. Sanfridsson J, Svahn G, Jonsson K, Ryd L. Computed radiography for characterisation of the weight-bearing knee. *Acta Radiol* 1997; 38:514-9.
153. Sasaki T, Yasuda K. Clinical evaluation of the treatment of osteoarthritic knees using a newly designed wedged insole. *Clin Orthop* 1987; 181-7.
154. Schipplein OD, Andriacchi TP. Interaction between active and passive knee stabilizers during level walking. *J Orthop Res* 1991; 9:113-9.
155. Scott WW Jr, Lethbridge-Cejku M, Reichle R, Wigley FM, Tobin JD, Hochberg MC. Reliability of grading scales for individual radiographic features of osteoarthritis of the knee. The Baltimore longitudinal study of aging atlas of knee osteoarthritis. *Invest Radiol* 1993; 28:497-501.
156. Sharma L, Cahue S, Song J, Hayes K, Pai YC, Dunlop D. Physical functioning over three years in knee osteoarthritis: role of psychosocial, local mechanical, and neuromuscular factors. *Arthritis Rheum* 2003; 48:3359-70.
157. Sharma L, Lou C, Cahue S, Dunlop DD. The mechanism of the effect of obesity in knee osteoarthritis: the mediating role of malalignment. *Arthritis Rheum* 2000; 43:568-75.
158. Sharma L, Song J, Felson DT, Cahue S, Shamiyeh E, Dunlop DD. The role of knee alignment in disease progression and functional decline in knee osteoarthritis. *JAMA* 2001; 286:188-95.
159. Sharma L, Song J, Felson DT, Cahue S, Shamiyeh E, Dunlop DD. The role of knee alignment in disease progression and functional decline in knee osteoarthritis. *JAMA* 2001; 286:188-95.
160. Sheehan FT, Zajac FE, Drace JE. Using cine phase contrast magnetic resonance imaging to non-invasively study in vivo knee dynamics. *J Biomech* 1998; 31:21-6.
161. Sheehan FT, Zajac FE, Drace JE. Using cine phase contrast magnetic resonance imaging to non-invasively study in vivo knee dynamics. *J Biomech* 1998; 31:21-6.
162. Sheehan FT, Zajac FE, Drace JE. In vivo tracking of the human patella using cine phase contrast magnetic resonance imaging. *J Biomech Eng* 1999; 121:650-6.
163. Shih YF, Bull AM, McGregor AH, Humphries K, Amis AA. A technique for the measurement of patellar tracking during weight-bearing activities using ultrasound. *Proc Inst Mech Eng [H]* 2003; 217:449-57.
164. Simon SR, Radin EL, Paul IL, Rose RM. The response of joints to impact loading. II. In vivo behavior of subchondral bone. *J Biomech* 1972; 5:267-72.
165. Slemenda C, Brandt KD, Heilman DK, Mazzuca S, Braunstein EM, Katz BP, et al. Quadriceps weakness and osteoarthritis of the knee. *Ann Intern Med* 1997; 127:97-104.
166. Smith MD, Wetherall M, Darby T, Esterman A, Slavotinek J, Roberts-Thomson P, et al. A randomized placebo-controlled trial of arthroscopic lavage versus lavage plus intra-articular corticosteroids in the management of symptomatic osteoarthritis of the knee. *Rheumatology (Oxford)* 2003; 42:1477-85.

167. Solloway S, Hutchinson CE, Waterton JC, Taylor CJ. The use of active shape models for making thickness measurements of articular cartilage from MR images. *Magn Reson Med* 1997; 37:943-52.
168. Spector TD, Cooper C, Cushnaghan J, Hart DJ, Dieppe PA. *A Radiographic Atlas of Knee Osteoarthritis*. London: Springer Verlag, 1992.
169. Spector TD, Hart DJ, Byrne J, Harris PA, Dacre JE, Doyle DV. Definition of osteoarthritis of the knee for epidemiological studies. *Ann Rheum Dis* 1993; 52:790-4.
170. Stammberger T, Eckstein F, Englmeier KH, Reiser M. Determination of 3D cartilage thickness data from MR imaging: computational method and reproducibility in the living. *Magn Reson Med* 1999; 41:529-36.
171. Stammberger T, Eckstein F, Englmeier KH, Reiser M. Determination of 3D cartilage thickness data from MR imaging: computational method and reproducibility in the living. *Magn Reson Med* 1999; 41:529-36.
172. Stammberger T, Eckstein F, Michaelis M, Englmeier KH, Reiser M. Interobserver reproducibility of quantitative cartilage measurements: comparison of B-spline snakes and manual segmentation. *Magn Reson Imaging* 1999; 17:1033-42.
173. Stammberger T, Eckstein F, Michaelis M, Englmeier KH, Reiser M. Interobserver reproducibility of quantitative cartilage measurements: comparison of B-spline snakes and manual segmentation. *Magn Reson Imaging* 1999; 17:1033-42.
174. Sun Y, Gunther KP, Brenner H. Reliability of radiographic grading of osteoarthritis of the hip and knee. *Scand J Rheumatol* 1997; 26:155-65.
175. Superio-Cabuslay E, Ward MM, Lorig KR. Patient education interventions in osteoarthritis and rheumatoid arthritis: a meta-analytic comparison with nonsteroidal antiinflammatory drug treatment. *Arthritis Care Res* 1996; 9:292-301.
176. Tennant S, Williams A, Vedi V, Kinmont C, Gedroyc W, Hunt DM. Patello-femoral tracking in the weight-bearing knee: a study of asymptomatic volunteers utilising dynamic magnetic resonance imaging: a preliminary report. *Knee Surg Sports Traumatol Arthrosc* 2001; 9:155-62.
177. Vacha J, Pesakova V, Krajickova J, Adam M. Effect of glycosaminoglycan polysulphate on the metabolism of cartilage ribonucleic acid. *Arzneimittelforschung* 1984; 34:607-9.
178. van Baar ME, Assendelft WJ, Dekker J, Oostendorp RA, Bijlsma JW. Effectiveness of exercise therapy in patients with osteoarthritis of the hip or knee: a systematic review of randomized clinical trials. *Arthritis Rheum* 1999; 42:1361-9.
179. Vanwanseele B, Eckstein F, Knecht H, Spaepen A, Stussi E. Longitudinal analysis of cartilage atrophy in the knees of patients with spinal cord injury. *Arthritis Rheum* 2003; 48:3377-81.
180. Veldpaus FE, Woltring HJ, Dortmans LJ. A least-squares algorithm for the equiform transformation from spatial marker co-ordinates. *J Biomech* 1988; 21:45-54.
181. Veress SA, Lippert FG, Hou MC, Takamoto T. Patellar tracking patterns measurement by analytical x-ray photogrammetry. *J Biomech* 1979; 12:639-50.

182. von Eisenhart-Rothe R, Siebert M, Bringmann C, Vogl T, Englmeier KH, Graichen H. A new in vivo technique for determination of 3D kinematics and contact areas of the patello-femoral and tibio-femoral joint. *J Biomech* 2004; 37:927-34.
183. Ware JE Jr, Keller SD, Hatoum HT, Kong SX. The SF-36 Arthritis-Specific Health Index (ASHI): I. Development and cross-validation of scoring algorithms. *Med Care* 1999; 37:MS40-50.
184. Weinberger M. Telephone-based interventions in outpatient care. *Ann Rheum Dis* 1998; 57:196-7.
185. Weinberger M, Tierney WM, Booher P, Katz BP. Can the provision of information to patients with osteoarthritis improve functional status? A randomized, controlled trial. *Arthritis Rheum* 1989; 32:1577-83.
186. Wiberg G. Roentgenographic and anatomic studies on the femoropatellar joint, with special reference to chondromalacia patellae. *Acta Orthop Scand* 1941; 12:319-340.
187. Wirth W, Hudelmaier M, Eckstein F. A software suite dedicated to quality controlled cartilage analysis for drug development trials. *Osteoarthritis and Cartilage* 2003; 11:S 61 Abstract.
188. Wluka AE, Davis SR, Bailey M, Stuckey SL, Cicuttini FM. Users of oestrogen replacement therapy have more knee cartilage than non-users. *Ann Rheum Dis* 2001; 60:332-6.
189. Yamada K, Healey R, Amiel D, Lotz M, Coutts R. Subchondral bone of the human knee joint in aging and osteoarthritis. *Osteoarthritis Cartilage* 2002; 10:360-9.
190. Yasuda K, Sasaki T. The mechanics of treatment of the osteoarthritic knee with a wedged insole. *Clin Orthop* 1987; 162-72.

Appendix A: WOMAC Questionnaire

WOMAC® Osteoarthritis Index LK3.1

INSTRUCTIONS TO PATIENTS

In Sections A, B and C, questions will be asked in the following format. You should give your answers by putting an "X" in one of the boxes.

EXAMPLES:

1. If you put your "X" in the left-hand box, i.e.

None	Mild	Moderate	Severe	Extreme
<input checked="" type="checkbox"/>	<input type="checkbox"/>	<input type="checkbox"/>	<input type="checkbox"/>	<input type="checkbox"/>

Then you are indicating that you have **no** pain.

2. If you put your "X" in the right-hand box, i.e.

None	Mild	Moderate	Severe	Extreme
<input type="checkbox"/>	<input type="checkbox"/>	<input type="checkbox"/>	<input type="checkbox"/>	<input checked="" type="checkbox"/>

Then you are indicating that your pain is **extreme**.

3. Please note:

- that the further to the right you place your "X" the **more** pain you are experiencing.
- that the further to the left you place your "X" the **less** pain you are experiencing.
- please do not** place your "X" **outside the box**.

You will be asked to indicate on this type of scale the amount of pain, stiffness or disability you have experienced in the last 48 hours.

Think about your _____ (study joint) when answering the questionnaire. Indicate the severity of your pain, stiffness and physical disability that you feel is caused by arthritis in your _____ (study joint).

Your study joint has been identified for you by your health care professional. If you are unsure which joint is your study joint, please ask before completing the questionnaire.

WOMAC® Osteoarthritis Index LK3.1

Section A

PAIN

Think about the pain you felt in your _____ (study joint) due to your arthritis during the last 48 hours.

(Please mark your answers with an "X".)

QUESTION: How much pain do you have?	Study Coordinator Use Only
1. Walking on a flat surface. None <input type="checkbox"/> Mild <input type="checkbox"/> Moderate <input type="checkbox"/> Severe <input type="checkbox"/> Extreme <input type="checkbox"/>	PAIN1 _____
2. Going up or down stairs. None <input type="checkbox"/> Mild <input type="checkbox"/> Moderate <input type="checkbox"/> Severe <input type="checkbox"/> Extreme <input type="checkbox"/>	PAIN2 _____
3. At night while in bed, i.e., pain that disturbs your sleep. None <input type="checkbox"/> Mild <input type="checkbox"/> Moderate <input type="checkbox"/> Severe <input type="checkbox"/> Extreme <input type="checkbox"/>	PAIN3 _____
4. Sitting or lying. None <input type="checkbox"/> Mild <input type="checkbox"/> Moderate <input type="checkbox"/> Severe <input type="checkbox"/> Extreme <input type="checkbox"/>	PAIN4 _____
5. Standing upright. None <input type="checkbox"/> Mild <input type="checkbox"/> Moderate <input type="checkbox"/> Severe <input type="checkbox"/> Extreme <input type="checkbox"/>	PAIN5 _____

WOMAC® Osteoarthritis Index LK3.1

Section B

STIFFNESS

Think about the stiffness (not pain) you felt in your _____ (study joint) due to your arthritis during the last 48 hours.

Stiffness is a sensation of **decreased** ease in moving your joint.

(Please mark your answers with an "X".)

<p>6. How severe is your stiffness after first awakening in the morning?</p> <p>None Mild Moderate Severe Extreme</p> <p><input type="checkbox"/> <input type="checkbox"/> <input type="checkbox"/> <input type="checkbox"/> <input type="checkbox"/></p>	<p>Study Coordinator Use Only</p> <p>STIFF6 _____</p>
<p>7. How severe is your stiffness after sitting, lying or resting later in the day?</p> <p>None Mild Moderate Severe Extreme</p> <p><input type="checkbox"/> <input type="checkbox"/> <input type="checkbox"/> <input type="checkbox"/> <input type="checkbox"/></p>	<p>STIFF7 _____</p>

WOMAC® Osteoarthritis Index LK3.1

Section C

DIFFICULTY PERFORMING DAILY ACTIVITIES

Think about the difficulty you had in doing the following daily physical activities due to arthritis in your _____ (study joint) during the last 48 hours. By this we mean **your ability to move around and to look after yourself**.

(Please mark your answers with an " X ".)

QUESTION: What degree of difficulty do you have?	Study Coordinator Use Only
8. Descending stairs. None Mild Moderate Severe Extreme <input type="checkbox"/> <input type="checkbox"/> <input type="checkbox"/> <input type="checkbox"/> <input type="checkbox"/>	PFTN8 _____
9. Ascending stairs. None Mild Moderate Severe Extreme <input type="checkbox"/> <input type="checkbox"/> <input type="checkbox"/> <input type="checkbox"/> <input type="checkbox"/>	PFTN9 _____
10. Rising from sitting. None Mild Moderate Severe Extreme <input type="checkbox"/> <input type="checkbox"/> <input type="checkbox"/> <input type="checkbox"/> <input type="checkbox"/>	PFTN10 _____
11. Standing. None Mild Moderate Severe Extreme <input type="checkbox"/> <input type="checkbox"/> <input type="checkbox"/> <input type="checkbox"/> <input type="checkbox"/>	PFTN11 _____
12. Bending to the floor. None Mild Moderate Severe Extreme <input type="checkbox"/> <input type="checkbox"/> <input type="checkbox"/> <input type="checkbox"/> <input type="checkbox"/>	PFTN12 _____
13. Walking on a flat surface. None Mild Moderate Severe Extreme <input type="checkbox"/> <input type="checkbox"/> <input type="checkbox"/> <input type="checkbox"/> <input type="checkbox"/>	PFTN13 _____

WOMAC® Osteoarthritis Index LK3.1

Section C

DIFFICULTY PERFORMING DAILY ACTIVITIES

Think about the difficulty you had in doing the following daily physical activities due to arthritis in your _____ (study joint) during the last 48 hours. By this we mean **your ability to move around and to look after yourself**.

(Please mark your answers with an "X".)

QUESTION: What degree of difficulty do you have?	Study Coordinator Use Only
14. Getting in or out of a car, or getting on or off a bus. None Mild Moderate Severe Extreme <input type="checkbox"/> <input type="checkbox"/> <input type="checkbox"/> <input type="checkbox"/> <input type="checkbox"/>	PFTN14 _____
15. Going shopping. None Mild Moderate Severe Extreme <input type="checkbox"/> <input type="checkbox"/> <input type="checkbox"/> <input type="checkbox"/> <input type="checkbox"/>	PFTN15 _____
16. Putting on your socks or stockings. None Mild Moderate Severe Extreme <input type="checkbox"/> <input type="checkbox"/> <input type="checkbox"/> <input type="checkbox"/> <input type="checkbox"/>	PFTN16 _____
17. Rising from bed. None Mild Moderate Severe Extreme <input type="checkbox"/> <input type="checkbox"/> <input type="checkbox"/> <input type="checkbox"/> <input type="checkbox"/>	PFTN17 _____
18. Taking off your socks or stockings. None Mild Moderate Severe Extreme <input type="checkbox"/> <input type="checkbox"/> <input type="checkbox"/> <input type="checkbox"/> <input type="checkbox"/>	PFTN18 _____
19. Lying in bed. None Mild Moderate Severe Extreme <input type="checkbox"/> <input type="checkbox"/> <input type="checkbox"/> <input type="checkbox"/> <input type="checkbox"/>	PFTN19 _____

WOMAC® Osteoarthritis Index LK3.1

Section C

DIFFICULTY PERFORMING DAILY ACTIVITIES

Think about the difficulty you had in doing the following daily physical activities due to arthritis in your _____ (study joint) during the last 48 hours. By this we mean **your ability to move around and to look after yourself**.

(Please mark your answers with an "X".)

QUESTION: What degree of difficulty do you have?	Study Coordinator Use Only
20. Getting in or out of the bath. None Mild Moderate Severe Extreme <input type="checkbox"/> <input type="checkbox"/> <input type="checkbox"/> <input type="checkbox"/> <input type="checkbox"/>	PFTN20 _____
21. Sitting. None Mild Moderate Severe Extreme <input type="checkbox"/> <input type="checkbox"/> <input type="checkbox"/> <input type="checkbox"/> <input type="checkbox"/>	PFTN21 _____
22. Getting on or off the toilet. None Mild Moderate Severe Extreme <input type="checkbox"/> <input type="checkbox"/> <input type="checkbox"/> <input type="checkbox"/> <input type="checkbox"/>	PFTN22 _____
23. Performing heavy domestic duties. None Mild Moderate Severe Extreme <input type="checkbox"/> <input type="checkbox"/> <input type="checkbox"/> <input type="checkbox"/> <input type="checkbox"/>	PFTN23 _____
24. Performing light domestic duties. None Mild Moderate Severe Extreme <input type="checkbox"/> <input type="checkbox"/> <input type="checkbox"/> <input type="checkbox"/> <input type="checkbox"/>	PFTN24 _____

Appendix B: Anatomical Axes Assignment

I. Femoral Axes Assignment

To create the femoral coordinate system four anatomical landmarks were identified.

1. The most posterior aspect of the lateral femoral condyle (f1)
2. The most posterior aspect of the medial femoral condyle (f2)
3. The most superior aspect of the intercondylar notch (f3)
4. The centroid of the superior femoral shaft (f4)

f1 and f2, the posterior lateral and medial femoral condylar points, were identified from the last axial slice in which the most superior aspect of the intercondylar notch was visible (Figure B.1).

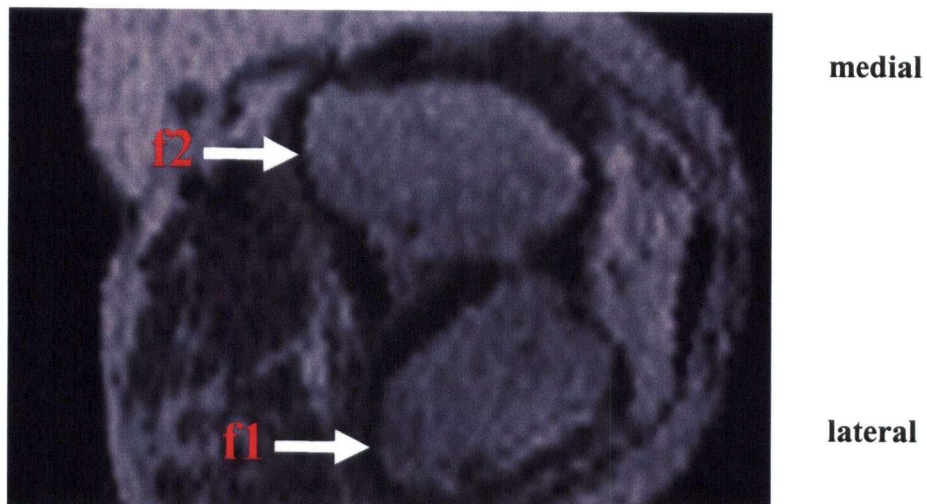


Figure B.1: The lower arrow indicates the lateral posterior femoral point (f1) and the upper arrow indicates the medial posterior point of the femur (f2). These points are identified on the last axial slice containing a bridge between femoral condyles.

Next the sagittal slice containing the most superior aspect of the intercondylar notch was identified and the most inferior point of femoral bone was recorded as f3 (Figure B.2).

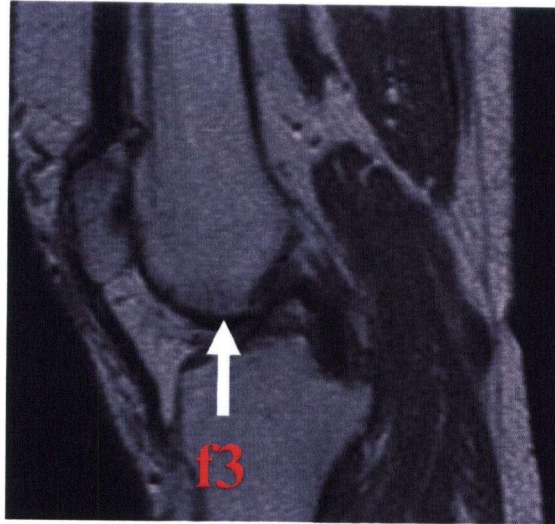


Figure B.2: Point f_3 identifies the most distal point on the femur. This point is identified on the sagittal slice containing the most superior point of the intercondylar notch.

The centroid of the superior femoral shaft was calculated from the geometric model of the femur created from the high resolution image. The superior axial slice of the femur was identified and the geometric mean of all of the points in this slice was determined and recorded as f_4 .

To determine the coordinate axes for the femur the following unit vectors were found:

1. $f_1 \times f_2$ (posterior aspects of the medial and lateral condyles)

$$\overrightarrow{PosteriorCondyles} = \frac{\overline{f_1 f_2}}{\|f_1 f_2\|}$$

2. $f_3 \times f_4$ (superior aspect of the intercondylar notch and the centroid of the superior shaft). This vector defines the superior/inferior femoral axis (SIaxis) where superior is the positive direction.

$$\overrightarrow{SIaxis} = \frac{\overline{f_3 f_4}}{\|f_3 f_4\|}$$

The cross-product of these two unit vectors was then determined to define the anterior/posterior femoral axis (APAxis) where anterior is the positive direction.

$$\overrightarrow{APAxis} = \overrightarrow{SIAxis} \times \overrightarrow{PosteriorCondyles}$$

Finally, the cross-product of the APAxis vector and the SIAxis vector was found to determine the medial/lateral axis vector (MLaxis).

$$\overrightarrow{MLAxis} = \overrightarrow{APAxis} \times \overrightarrow{SIaxis}$$

The origin of this coordinate system (Figure B.3) is f3, the superior aspect of the intercondylar notch.

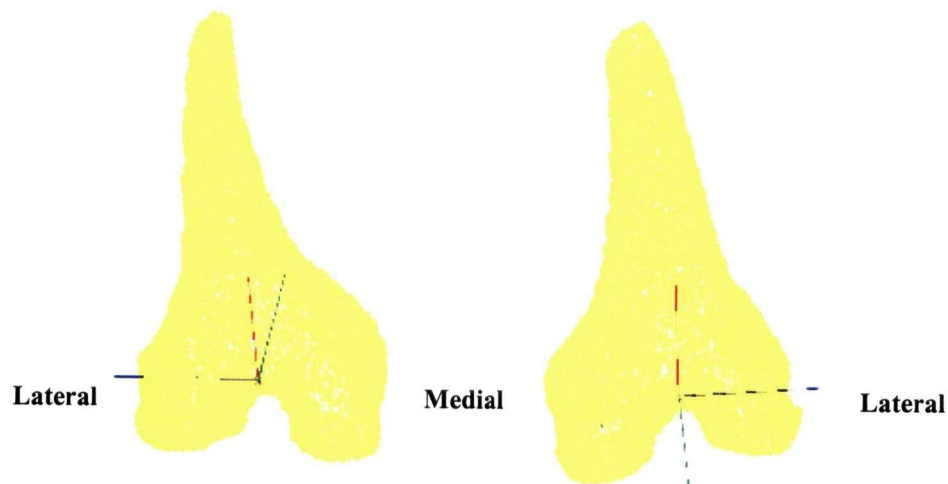


Figure B.3: Femoral coordinate system. Left: left knee (anterioposterior view), Right: right knee (anterioposterior view)

II. Tibial Axes Assignment

The anatomical landmarks required to define the tibial coordinate system are as follows:

1. The superior aspect of the fibula (t1)
2. The most posterior aspect of the lateral tibial plateau (t2)
3. The most posterior aspect of the medial tibial plateau (t3)
4. The superior medial tibial eminence (t4)
5. The centroid of the inferior tibia (t5)

t1 was found on the sagittal slice showing the most proximal part of the fibula (Figure B.4).

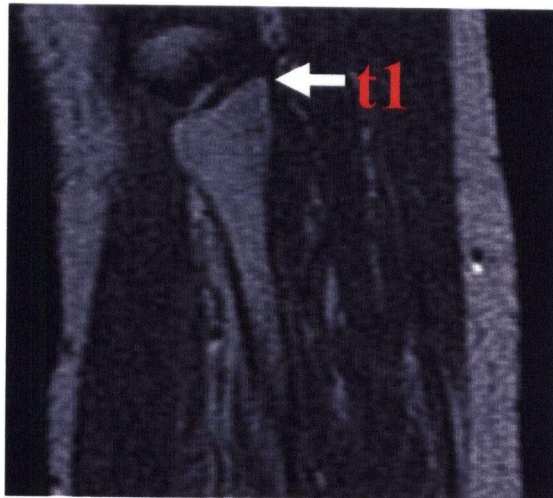


Figure B.4: Point t1 is the most superior point of the fibula identified on a sagittal slice.

The axial coordinate of t1 was used to find the axial slice in which t2 and t3 will be defined. Once the axial slice was located a check can be carried out to ensure that the fibula does in fact disappear in the next most superior slice. t2 and t3, the posterior lateral and medial tibial plateau was then identified (Figure B.5).

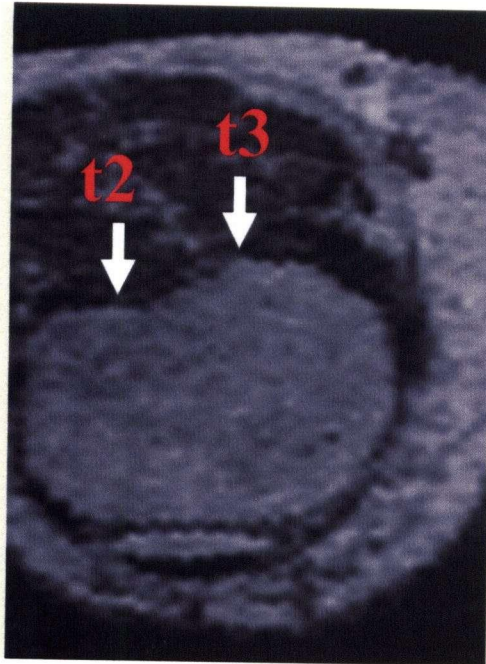


Figure B.5: The axial slice containing the most superior point of the fibula. t2 and t3 are identified as the most posterior lateral and medial aspects of the tibial plateau.

t4, the superior medial tibial eminence, was found in the sagittal slice with the most proximal point of the eminence (Figure B.6).

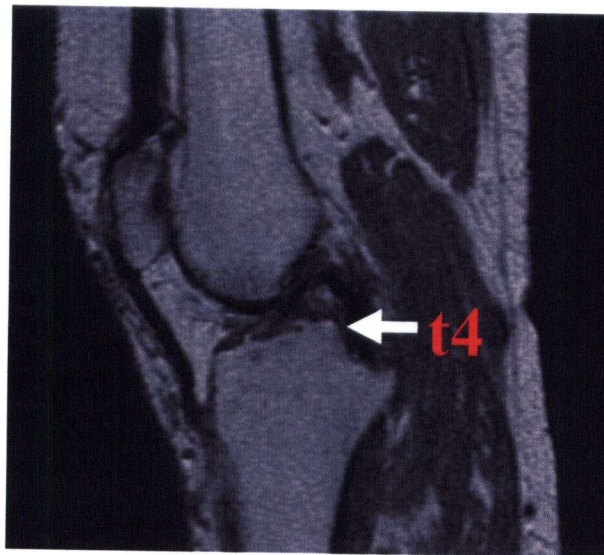


Figure B.6: Most superior point of the medial tibial eminence found on a sagittal slice.

Finally, f5, the centroid of the inferior tibia was determined using the same method as outlined for finding the centroid of the superior femur.

To determine the coordinate axes for the femur the following unit vectors were found:

1. $t_2 \times t_3$ (posterior aspects of the medial and lateral tibial plateau)

$$\overrightarrow{PosteriorPlateau} = \frac{\overrightarrow{t_2 t_3}}{\| \overrightarrow{t_2 t_3} \|}$$

2. $t_4 \times t_5$ (superior aspect of the medial tibial eminence and the centroid of the inferior tibia). This vector defines the superior/inferior tibial axis (SIaxis).

$$\overrightarrow{SIAxis} = \frac{\overrightarrow{t_4 t_5}}{\| \overrightarrow{t_4 t_5} \|}$$

The cross-product of these two unit vectors was then determined to define the anterior/posterior tibial axis (APAxis).

$$\overrightarrow{APAxis} = \overrightarrow{SIAxis} \times \overrightarrow{PosteriorPlateau}$$

Finally the cross product of the anterior/posterior axis (APAxis) vector and the superior/inferior axis (SIAxis) vector was found to determine the medial/lateral axis vector (MLaxis).

$$\overrightarrow{MLAxis} = \overrightarrow{APAxis} \times \overrightarrow{SIaxis}$$

The origin of this coordinate system (Figure B.7) is t_4 , the superior aspect of the medial tibial eminence.

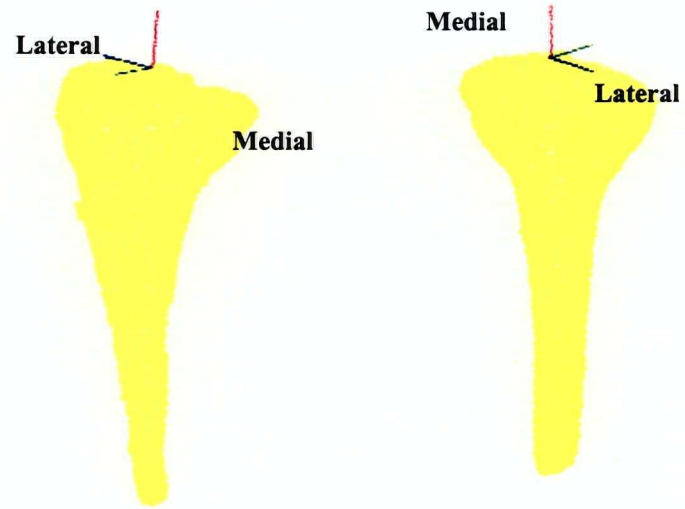


*Figure B.7: Tibial coordinate system. Left: left knee (oblique view),
Right: right knee (oblique view)*

III. Patellar Axes Assignment

Four landmarks on the patella were identified in order to assign the patellar coordinate system. They were:

1. The posterior point of the mid axial patellar slice (p1)
2. The lateral point of the mid axial patellar slice (p2)
3. The superior point of the mid sagittal patellar slice (p3)
4. the inferior point of the mid sagittal patellar slice (p4)

To determine the mid axial patellar slice the first and last axial slices in which the patella was visible were identified and the slice midway between these two was identified. If there are two mid slices, that in which the posterior patellar point is more posterior was chosen. P1 and p2 are found on the mid slice as seen in Figure B.8.

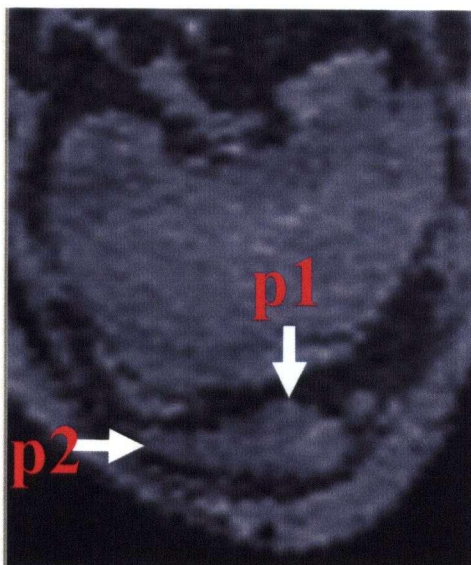


Figure B.8: The most posterior point (p1) and lateral point (p2) on the axial midslice of the patella.

The sagittal patellar mid slice was determined in the same manner as the axial patellar mid slice and p3 and p4, the superior and inferior points on the patella, were recorded as seen in Figure B.9.

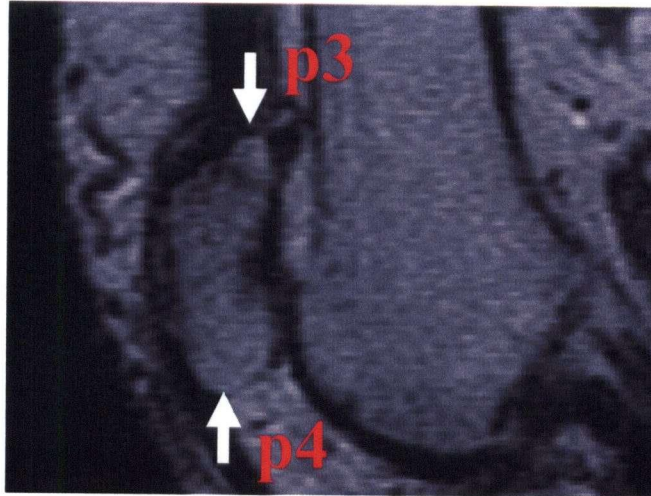


Figure B.9: The superior ($p3$) and inferior ($p4$) points on the sagittal midslice of the patella.

To calculate the coordinate axes for the patella the following unit vectors were found:

1. $p1 \times p2$ (posterior and lateral mid axial points)

$$\overrightarrow{PosteriorLateralVector} = \frac{\overrightarrow{p1p2}}{\| \overrightarrow{p1p2} \|}$$

2. $p3 \times p4$ (superior and inferior mid sagittal points). This vector defines the superior/inferior patellar axis (SIaxis).

$$\overrightarrow{SIAxis} = \frac{\overrightarrow{p3p4}}{\| \overrightarrow{p3p4} \|}$$

The anterior/posterior patellar axis (APAxis) was defined as the cross-product of the superior/inferior axis (SIaxis) and the posterior-lateral vector.

$$\overrightarrow{APAxis} = \overrightarrow{SIAxis} \times \overrightarrow{PosteriorLateralVector}$$

And finally, the medial/lateral patellar axis (MLAxis) is the cross-product of the APAxis and the SIAxis.

$$\overrightarrow{MLAxis} = \overrightarrow{APAxis} \times \overrightarrow{SIaxis}$$

The origin of the patellar coordinate system (Figure B.10) is p1, the most posterior point of the mid axial slice.

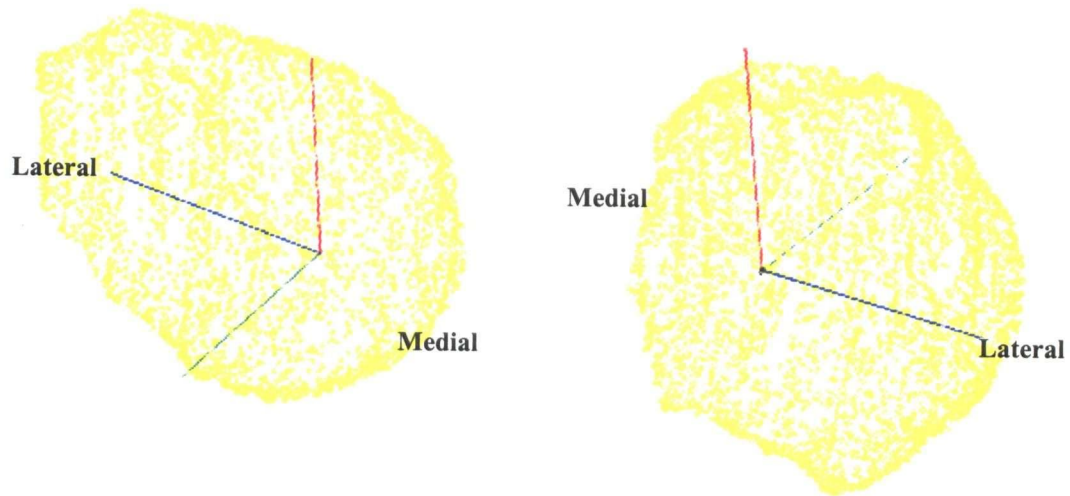


Figure B.10: Patellar coordinate system. Left: left knee (oblique view), Right: right knee (oblique view)

Appendix C: Participant Consent Form

Principal Investigator:	Dr. David R. Wilson, Ph.D (604) 875 4428 Department of Orthopaedics Division of Orthopaedic Engineering Research Vancouver General Hospital
Co-Investigators:	Dr. Jolanda Cibere, M.D., Ph.D Department of Health Care and Epidemiology, VGH Arthritis Centre Dr. Savvas Nicolaou, M.D. Department of Radiology, VGH Dr. Alex MacKay, Ph.D Department of Radiology, VGH Department of Physics, UBC Emily McWalter, B.Sc. Mechanical Engineering Division of Orthopaedic Engineering Research, VGH Department of Mechanical Engineering, UBC
Contact:	Emily McWalter, B.Sc. Mechanical Engineering (604) 875 4111 ext. 66314 In case of Emergency call (24 hours a day) (604) 875 4111 ext. 55056 Division of Orthopaedic Engineering Research, VGH Department of Mechanical Engineering, UBC

Title: Image Guided Assessment of Patellar Tracking and Planning of Patellar Realignment

Purpose:

The purpose of this study is to examine the relationship between varus and valgus malalignment (bow-legs and knock-knees), patellar mechanics (how your knee-cap moves when you bend your knee) and cartilage thickness in the patellofemoral joint (the joint between your knee-cap and your thigh bone). We, the investigators, are interested in examining a possible relationship between these items and patellofemoral osteoarthritis (the degeneration or break-down of cartilage).

Invitation:

You have been asked to participate in this research study as you have participated in previous research studies through the Mary Pack Arthritis Centre at Vancouver General Hospital and have expressed an interest in participating in further research studies. You also display varus or valgus knee alignment (bow-legs or knock-knees) which is an area of particular interest to the investigators of this study. Finally, you also have some knee pain which may be associated with possible osteoarthritis in your patellofemoral joint (the break down of cartilage in the space between your knee-cap and your thigh bone).

Treatment Alternatives:

This study is a research study. It is **not** an alternative to the normal treatments available for knee osteoarthritis. You should continue with the treatment regime suggested to you by your primary care giver and any specialists you have consulted.

Sponsor:

This study is funded by the Canadian Institute of Health Research (CIHR) who is the major federal funding agency of health research in Canada.

Study Procedures:

The study will take place during a morning or afternoon of your choosing. You will be asked to commit four or five hours of your time to the study. This amount of time is outside your normal health care and is strictly voluntary. Your normal health care regime will continue as usual.

By participating in this study you will be asked to fill out the following questionnaire:

1. Western Ontario and McMaster University Osteoarthritis Index –WOMAC questionnaire. This questionnaire will take approximately 15 minutes to complete. You will be asked questions regarding your knee pain, stiffness and function. This questionnaire will help the investigators to classify possible osteoarthritis.

By participating in this study you will be asked to undergo the following imaging sessions:

1. One full lower limb standing X-ray (from hip to ankle). This will take approximately 15 minutes to complete. This X-ray is used to determine the angle of varus or valgus at your knee joint (bow-leg or knock-knee).
2. Assessment of patellar tracking using an MRI machine. One high-resolution MRI scan will be taken, this will last about 15 minutes. Six low-resolution MRI scans will be taken, each one lasting about 40 seconds. During the quick, low-resolution scans you will be asked to press on a pedal with your knee bent at

different angles. You will spend about one hour in the MRI suite, this accounts for scanning time and leg positioning time. This process allows the investigators to study how your patella (knee-cap) moves as you bend your knee.

3. To measure cartilage thickness at the patellofemoral joint you will be randomly selected to undergo one of the following imaging sessions:
 - a. One skyline X-ray of the patellofemoral joint (the X-ray is taken from above, looking down on your joint). This will take approximately half an hour including positioning and the actual X-ray. The X-ray image itself is instantaneous. From this X-ray the investigators can measure the distance between the knee-cap and the thigh bone.
 - or
 - b. One CT scan of the knee. This will take approximately half an hour including positioning and the actual CT imaging. The scan itself will last approximately 30 seconds. Cartilage is visible on CT images therefore from this scan the investigators will measure the cartilage thickness.
 - or
 - c. One MRI scan of the knee. This will take approximately half an hour including positioning and the actual MRI scan. The MRI scan itself takes approximately 8 minutes. From the MRI scan obtained the investigators will be able to measure cartilage thickness, volume and surface area.

Special Note: A small group of participants will be asked to undergo all three methods of measuring cartilage thickness so that the investigators can compare the three methods. If you are interested in undergoing all three methods of measurement you will be volunteering five hours of your time as opposed to four. Please sign the extra section at the very end of this consent form if you wish to participate in the two extra scanning sessions. Please read the risk section carefully before making your decision.

If you have any questions regarding the procedure or do not understand any of the steps please do not hesitate to contact Emily McWalter at 604 875 1111 x 66314, she will be more than happy to respond to all of your questions and concerns.

Subject Eligibility:

In order to participate in the study all of the following four statements must be true:

1. You must have varus or valgus malalignment
2. You must be over the age of 50
3. You must display osteophytes, which are small bony growths on the surface of the joint, in one or more knee compartments
4. You must experience some knee pain when carrying out knee intensive activities

Exclusion Criteria:

You may not participate in the study if you have any of the following conditions: injection in either knee to relieve pain within the last 3 months, minor knee surgery within the last 6 months (incision less than 1 inch), major knee surgery within the last year (incision greater than 1 inch), a total knee replacement in either knee, history of chronic inflammation of the knee, rheumatoid arthritis, systemic inflammatory arthritis (for example lupus), a bone fracture at the knee joint, Paget's disease, villonodular synovitis (swelling of the lining of your joint), joint infections, ochronosis (blue/black discolouration of bone, cartilage or skin), neuropathic arthropathy (loss of sensation at the joint), acromegaly (abnormal bony enlargement of hands or feet), hemochromatosis (over absorption of iron), Wilson's disease (over absorption of copper), osteochondromatosis (fragments of lining in the joint), gout (crystals in or around the joint space), recurrent pseudogout (calcium crystal build up in the joint), osteopetrosis (overly dense bones from birth).

Risks:

There is some risk associated with having X-rays and CT scans taken. In both X-rays and CT scans you will be exposed to a small amount of radiation. The maximum radiation you will be exposed to is 1.4 mSv, this is equal the radiation you would be exposed to if you flew in an airplane for 140 hours. However, if you choose to participate in all three methods of cartilage thickness measurement will be exposed to a maximum of 1.6 mSv of radiation (equivalent to 160 hours of flying time). To put these numbers in perspective, all individuals are exposed to 2 mSv of background radiation per year. Background radiation is the radiation we are all exposed to from sources such as the sun, the earth and other substances in our environment. The total radiation you will be exposed to by participating in this study is less than one year's worth of background radiation. Radiation can damage body cells, however at this small dose this is unlikely. Side effects due to this amount of exposure are highly unlikely. There is no known risk to your physical health associated with MRI scans, however there is a risk of claustrophobia. During the scan you will be lying down on a bed and the bed will be moved into a tunnel-like environment. If you feel uncomfortable at any point during the scan you will be able to tell the operator and he or she will help you leave the MRI scanning area.

Confidentiality:

Your confidentiality will be respected. No information that discloses your identity will be released or published without your specific consent to the disclosure. However, research records and medical records identifying you may be inspected in the presence of the Investigator or his or her designate by representatives of (name the sponsoring company if relevant), Health Canada, (the U.S. Food and Drug Administration, if relevant), and the UBC Research Ethics Board for the purpose of monitoring the research. However, no records which identify you by name or initials will be allowed to leave the Investigators' offices.

All of the data collected in this study is strictly confidential. Access to data is restricted to the investigators reported at the opening of this document only. Your name and

contact information will not appear in any data files, a number assigned to you will be the only means of identification. This identification number will be associated with your name and contact information in a separate file to which only Dr. David Wilson (lead investigator) and Emily McWalter (co-investigator) will have access.

Refusal or Withdrawal from Study:

This study is strictly voluntary; it is your choice as to whether or not you wish to participate. You may decline to enter, or withdraw from the study at any time without consequence. Refusing to participate in this study at any time **will not** compromise your medical care now or at any point in the future. Any information related to your continuing participating will be disclosed to me in a timely manner.

Further Participation:

We will disclose to you, in a timely manner, any information regarding your further participation in the present study. For example, you may be asked to participate in a sub-study or an extension of the current study. If so, your participation is again strictly voluntary and your participation in the present study by no means requires to you participate in any further research studies.

Remuneration/Compensation:

All travel expenses will be covered. For example, if you travel from your home to and from Vancouver General Hospital by taxi the fare will be paid for by the study. If you live within Vancouver you will be reimbursed up to a maximum of \$50 and if you live outside of Vancouver you will be reimbursed up to a maximum of \$250. Receipts for travel expenses are required.

Concerns or Comments:

If you have any concerns regarding your treatment or rights as a participant in the present research study please do not hesitate to contact the Director of the Office of Research Services at the University of British Columbia at 604-822-8598.

Consent:

I have read and understood all of the statements above. I understand that participation in this study is strictly voluntary and all of the measurements are in addition to my normal health care. I realize that I am not waiving my legal rights by signing this consent form. I have received a copy of this document for my personal records.

I consent to participate in this study.

Appendix D: Higher order regression results for cartilage surface area, normalized volume, mean thickness and percentage coverage and lateral patellar translation.

D.1: Surface Area

Slope of Lateral Translation vs. Ratio of Surface Area
2nd order polynomial fit

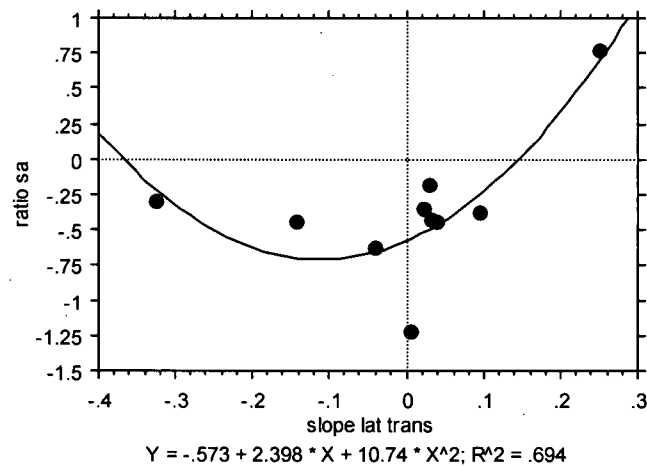


Figure D.1: 2nd order polynomial regression fit of the ratio of medial to lateral surface area to the slope of lateral patellar translation. The regression equation and the R^2 values are shown.

Slope of Lateral Translation vs. Ratio of Surface Area
3rd order polynomial fit

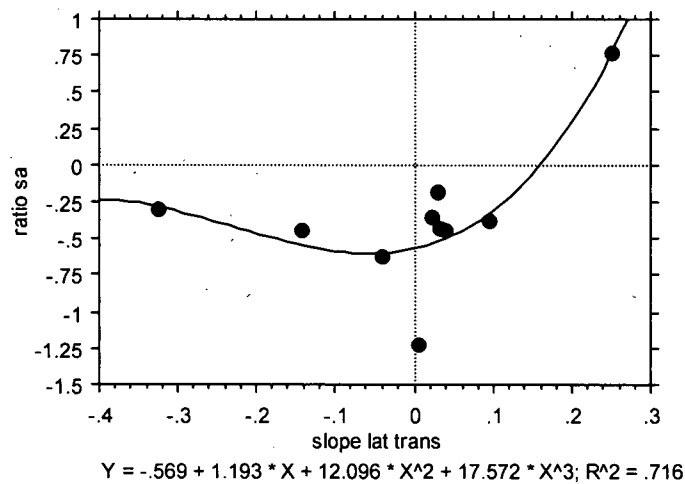


Figure D.2: 3rd order polynomial regression fit of the ratio of medial to lateral surface area to the slope of lateral patellar translation. The regression equation and the R^2 values are shown.

D.2: Mean Thickness

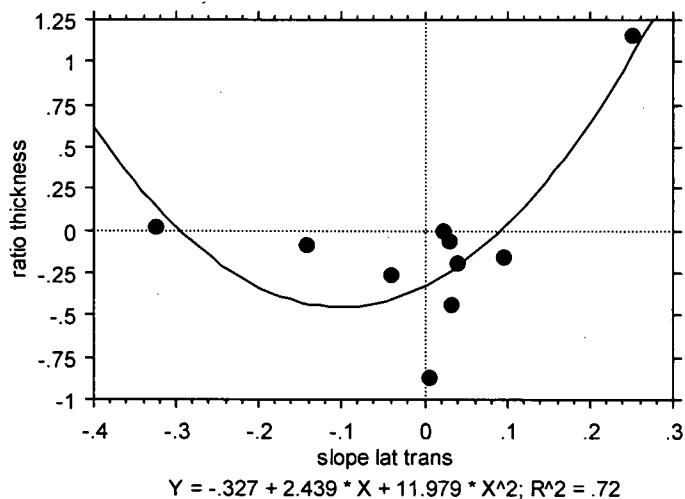
Slope of Lateral Translation vs. Ratio of Mean Thickness
2nd order polynomial fit

Figure D.3: 2nd order polynomial regression fit of the ratio of medial to lateral mean thickness to the slope of lateral patellar translation. The regression equation and the R^2 values are shown.

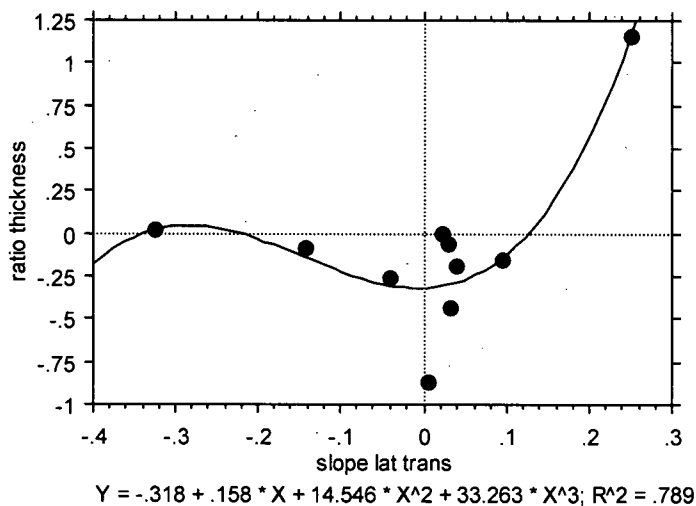
Slope of Lateral Translation vs. Ratio of Mean Thickness
3rd order polynomial fit

Figure D.4: 3rd order polynomial regression fit of the ratio of medial to lateral mean thickness to the slope of lateral patellar translation. The regression equation and the R^2 values are shown.

D.3: Normalized Volume

Slope of Lateral Translation vs. Ratio of Normalized Volume
2nd order polynomial fit

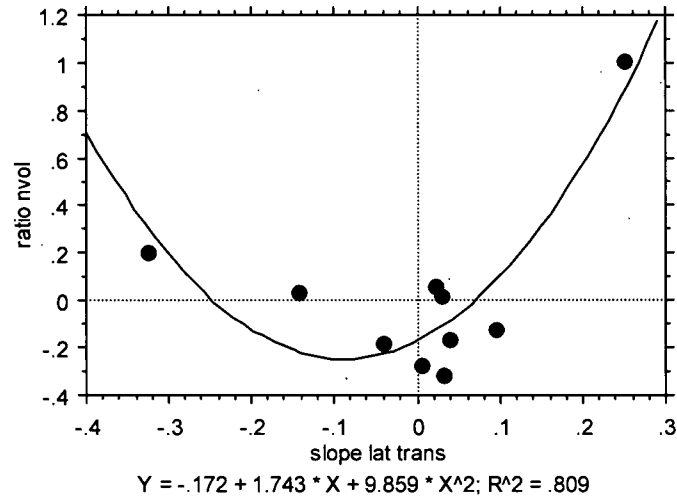


Figure D.5: 2nd order polynomial regression fit of the ratio of medial to lateral normalized volume to the slope of lateral patellar translation. The regression equation and the R² values are shown.

Slope of Lateral Translation vs. Ratio of Normalized Volume
3rd order polynomial fit

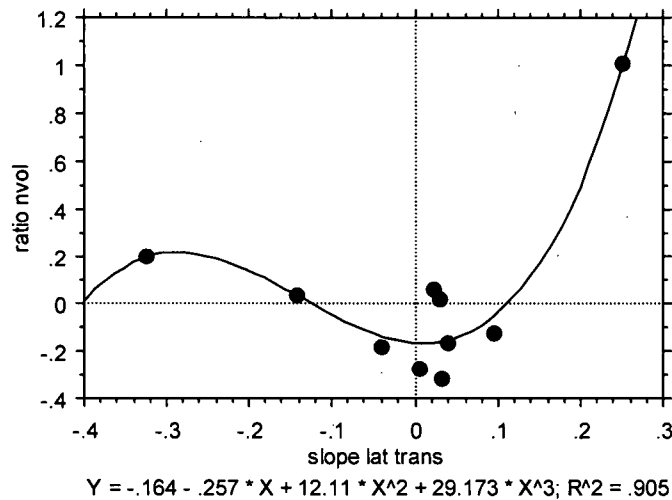


Figure D.6: 3rd order polynomial regression fit of the ratio of medial to lateral normalized volume to the slope of lateral patellar translation. The regression equation and the R^2 values are shown.

Slope of Lateral Translation vs. Ratio of Normalized Volume
4th order polynomial fit

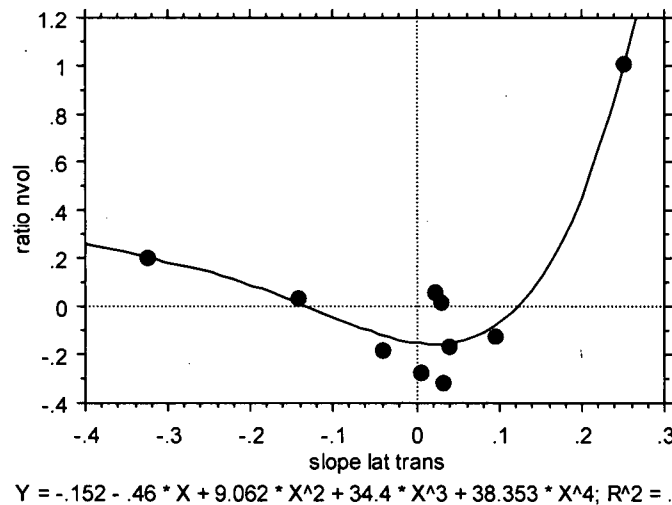
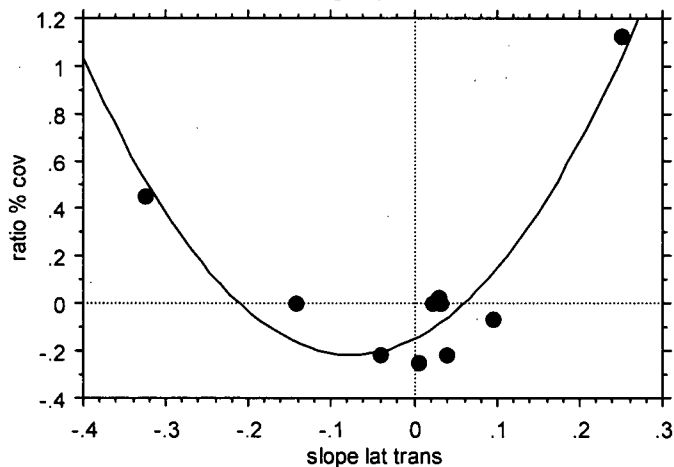


Figure D.7: 4th order polynomial regression fit of the ratio of medial to lateral normalized volume to the slope of lateral patellar translation. The regression equation and the R^2 values are shown.

6.7.5 Percentage Cartilage Coverage

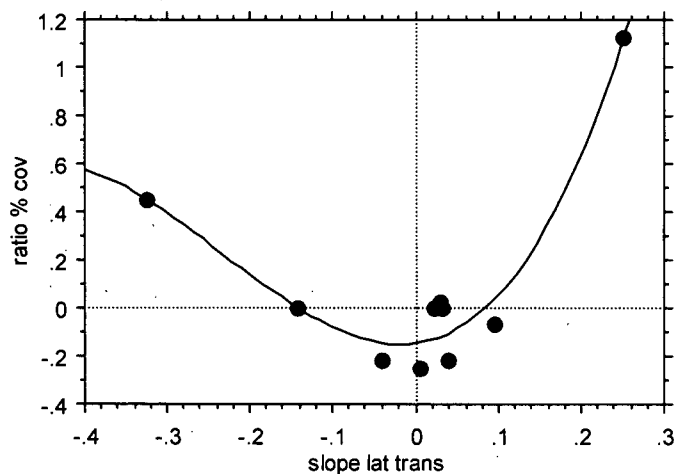
Slope of Lateral Translation vs. Ratio of Percentage Cartilage Coverage
2nd order polynomial fit



$$Y = -.151 + 1.786 * X + 11.844 * X^2; R^2 = .907$$

Figure D.8: 2nd order polynomial regression fit of the ratio of medial to lateral percentage cartilage coverage to the slope of lateral patellar translation. The regression equation and the R^2 values are shown.

Slope of Lateral Translation vs. Ratio of Percentage Cartilage Coverage
3rd order polynomial fit



$$Y = -.146 + .48 * X + 13.314 * X^2 + 19.054 * X^3; R^2 = .941$$

Figure D.9: 3rd order polynomial regression fit of the ratio of medial to lateral percentage cartilage coverage to the slope of lateral patellar translation. The regression equation and the R^2 values are shown.